

UNIVERSITY OF OKLAHOMA

GRADUATE COLLEGE

OIL POTENTIAL OF THE ASQUITH MARKER, LEWIS SHALE, GREATER  
GREEN RIVER BASIN, WYOMING.

A THESIS

SUBMITTED TO THE GRADUATE FACULTY

in partial fulfillment of the requirements for the

Degree of

MASTER OF SCIENCE

By

LIGIA CAROLINA MAYORGA-GONZALEZ

Norman, Oklahoma

2016

OIL POTENTIAL OF THE ASQUITH MARKER, LEWIS SHALE, GREATER  
GREEN RIVER BASIN, WYOMING.

A THESIS APPROVED FOR THE  
CONOCOPHILLIPS SCHOOL OF GEOLOGY AND GEOPHYSICS

BY

---

Dr. Roger Slatt, Chair

---

Dr. Paul Philp

---

Dr. Matthew Pranter

© Copyright by LIGIA CAROLINA MAYORGA-GONZALEZ 2016  
All Rights Reserved.

*To Javier, Gizmo, and my parents for keeping me down to earth*



## **Acknowledgements**

I would like to first thank Dr. Slatt for always being available for questions and discussions, for providing the funding for this research, and for giving me excellent academic and life advice. Secondly, I want to thank my family, especially my mom and dad who made uncountable sacrifices and provided me with the tools so that I could pursue my own path. This has been an amazing experience from which I have learned and gained knowledge, friendships, and professional opportunities. Thanks to the University of Oklahoma for giving me the opportunity to experience this amazing university and its people. Thanks to all my friends: the ones that I brought with me and the ones that I have gained here. I would not have made it without your visits and coffees. Finally, to my family here, Javier Tellez, thank you for keeping me down to earth, for teaching me, for helping me through this process, and for making me a stronger person.

## Table of Contents

Acknowledgements .....	iv
List of Tables .....	vii
List of Figures .....	viii
Abstract.....	xiv
Chapter 1: Introduction.....	1
Location of the Study Area .....	1
Research Objectives .....	1
Well logs correlations and maps.....	2
Potential to generate oil .....	2
Petroleum System.....	3
Research Methods .....	6
Outcrop Data .....	8
Subsurface Data.....	9
Interpretation .....	11
Chapter 2: Geological Setting.....	14
Regional Geology.....	14
Local Geology.....	18
Depositional Environment .....	24
Chapter 3: Maps and Correlations .....	26
Mapping .....	32
Outcrop Data .....	35

Chapter 4: Geochemical Analyses .....	49
Chapter 5: Identification of Potential Areas of Oil Accumulation .....	92
Chapter 6: Conclusions.....	94
Recommendations .....	96
References.....	97
Appendix 1: Wells used in correlations .....	104
Appendix 2: Overpressure Analysis.....	111
Appendix 3: Pyrograms .....	118
Appendix 4: XRD Analyses for other intervals.....	148

## List of Tables

Table 1. Samples used for the geochemical analyses.....	10
Table 2. TOC content in shales based on early oil window maturity (Jarvie, 1991)...	51
Table 3. List of the entire suite of samples including those that does not correspond to the Asquith Marker. It also shows their potential to generate hydrocarbons based on the parameters introduced by Jarvie, 1991. ....	52
Table 4. TOC present and TOC original calculated with the formula introduced by Jarvie 2003.....	57
Table 5. Source rock potential associated with the S1 and S2 peaks. Modified from Peters (1986).....	64
Table 6. List of samples from the Asquith Marker by depth with TOC values obtained from LECO TOC and S1, S2 and S3 values obtained from Rock-Eval. S1 and S2 peaks are associated with their potential to generate hydrocarbons based on table 5..	64
Table 7. Type of hydrocarbon generated based on HI and S2/S3 values from the pyrolysis. Modified from Peters (1986) .....	71
Table 8. Samples from the Organic rich facies of the Lewis Shale. ....	73
Table 9. List of well used for the analysis, ratios used to measure maturity and other parameters and the result of the maturity analysis. ....	83
Table 10. List of constraints used to define potential areas.....	92

## List of Figures

Figure 1. Location of the study area. Figure A shows the entire Greater Green River Basin. Figure B shows the area in which this study is focused. ....	5
Figure 2. Flow diagram illustrating the different steps used to characterize unconventional resource shales. The two main methods used in this thesis are highlighted in red (From Slatt et al., 2012). ....	7
Figure 3. Gamma ray well log from Amoco Champlin 276 D-1 well. Top of the Asquith Marker formation is marked in purple, base of the Asquith Marker is marked in dark grey and top of the Almond formation is marked in yellow. ....	13
Figure 4. Sub-basins in the Greater Green River basin. ....	16
Figure 5. Location of the Embayment during the Late Cretaceous. Black arrows mark the systems that drained into the embayment. It also shows the submarine fan sediments that were deposited in the center of the embayment. From Pyles (2000). ..	17
Figure 6. Approximate location of the interior seaway during the late Cretaceous in the Greater Green River Basin. Red dot corresponds to the location of the Rawlins outcrop. Red lines correspond to the major faults present in the area. Modified from Blakey, 2011. ....	19
Figure 7. Stratigraphic cross section from East to West from the Greater Green River Basin. The Lewis Shale is highlighted in orange (From USGS, 2005). ....	21
Figure 8. Stratigraphic chart of the Greater Green River Basin. Modified after Schell (1973) in Pyles (2000). ....	23

Figure 9. Paleogeographic map showing the different directions of sediment transport and the various depositional environments during the deposition of the Lewis shale. Hachures show where the different environments overlap making the geology of the area more complex. From U.S. Geological Survey Digital Data Series DDS-69-D. ...25

Figure 10. Wells used in the basin for cross sections and mapping purposes. Amoco Champlin 276 D-1 well was used as a referenced well and is highlighted in orange on the map. ....27

Figure 11. SW-NE Cross section (A-A' in the map) from the Washakie Basin to the Great Divide Basin showing the geometry of the Basin. The Grey interval represents the sandier sections from the middle and upper Lewis Shale. The Asquith Marker is represented in purple. ....30

Figure 12. East-West cross section (B-B'). The shale facies thins towards the Rock Springs uplift where the depositional environment was shallower at the time of deposition. The grey interval represents the sandier sections from the middle and upper Lewis Shale. The Asquith Marker is represented in purple and the black shale is the lower section of the lower member of the Lewis Shale.....31

Figure 13. Structural map at the top of the Asquith Marker. Wells are highlighted in red. Names are omitted for clustering effect. The orange star shows the location of the Rawlins outcrop and the Amoco Champlin 276 D-1 well.....33

Figure 14. Isochore map of the Asquith Marker. Wells are highlighted in red. Dashed red line marks the limits of the depocenter. Names are omitted for clustering effect. The orange star shows the location of the Amoco Champlin D-1 well. ....34

Figure 15. Location of the Asquith Marker's outcrop named the Rawlins Outcrop by Pyles (2000) .....	37
Figure 16. Gamma ray plot from the Asquith Marker outcrop. The orange point corresponds to a limestone bed. ....	38
Figure 17. Picture of the extension of the outcrop. Trenches were dug on the right side of the mound every 2 stratigraphic ft. Numbers indicate these points.....	39
Figure 18. Broken fossil from point 1. ....	40
Figure 19. Organic matter and fossil from point 5.....	40
Figure 20. Possible correlation of the Rawlins Outcrop and Red Rim-1 well. ....	41
Figure 21. Plot of sonic log versus depth. The straight lines on the log represent the trend. The place where the line does not follow the trend is the top of the overpressure zone. This is the methodology proposed by Surdam (2005) to detect an overpressure zone. ....	44
Figure 22. Overpressure analysis for two wells showing the change in the trend of the sonic log marked by the green line. The top of this green line represents the top of the overpressure zone.....	45
Figure 23. Cross section showing the wells used for the overpressure analysis. Green line represents the top of the overpressure zone. ....	46
Figure 24. X-ray diffraction analyses for two samples from the Amoco Champlin D-1 well at 8138ft. and 8152ft. depth. ....	48
Figure 25. Proportion of Organic Carbon in a rock sample and each one of its different constituents. Modified from Jarvie, (1991). ....	50

Figure 26. Plot of TOC vs. Depth based on the TOC potential shown in table 2. From LECO TOC analysis.....54

Figure 27. Cross section of the wells with TOC measurements showing a decrease in TOC content with depth. ....56

Figure 28. Figure showing the TOC curve and GR curve used to make a correlation and extrapolate to the other wells. The other points are measurements taken by others and analyzed by different labs. From Pasternack, 2005.....59

Figure 29. TOC Curves obtained from the correlation obtained by plotting the GR vs. TOC data from core from Pasternack (2005) on the left. Black dots represent the location of the samples taken for TOC analysis, used as a check point for the TOC curves obtained. The TOC points and the curve match in some points but not for all the wells..... 60

Figure 30. TOC curve (black line on the right) obtained using the methodology proposed by Passey et al., (1990). The red point represents the TOC measured from core sample. ....61

Figure 31. Typical pyrogram showing the three peaks (S1, S2 and S3) and the Tmax associated with the S2 peak. Modified from Hart and Steen, 2015. .... 63

Figure 32. Pyrogram from Amoco Bog Field well. This is one of the wells with a low S2 peak, which makes the Tmax difficult to determine. ....68

Figure 33. Pyrogram from Stage Stop Unit 2 well. There is a small S1 and S2 peak. 69

Figure 34. Pyrogram from Amoco Champlin 276 D-1 Well. It shows a high S2 peak meaning a high potential to generate hydrocarbons. This is one of the samples obtained



from core that was not affected by caving or handling as was the case of the cutting samples. ....70

Figure 35. Plot of Hydrogen Index (HI) vs. Depth and the type of hydrocarbon it can generate.....72

Figure 36. S2 vs. TOC diagram from the Amoco Champlin 276 D-1 well. ....76

Figure 37. Thermal maturity from Vitrinite reflectance. From Tissot and Welte, 1984. ....79

Figure 38. Tasmanites (Ts) picture from Creston Unit 1 well.....80

Figure 39. Vitrinite Reflectance values map overlaid by the structural map (grey lines) from the Mesaverde Group and some values from the Lewis Shale in the basin. According to Figure 37, the boundary between immature and oil-condensate is not very definitive and varies depending upon the type of organic matter present in the rock (Tissot and Welte 1981). The general trend of the map shows an increase in thermal maturity (increase in vitrinite reflectance) towards the North and South which also corresponds to the deeper trends in the basin. Vitrinite values decrease towards the center of the map that corresponds to the shallower area in the basin. ....81

Figure 40. Amoco Champlin 276 D-1 GC chromatogram for the Amoco Champlin 276 D-1 well at 8138ft. depth. It shows the location for C17, C18, Pr and Ph n-alkanes. ....86

Figure 41. Amoco Champlin 276 D-1 GCMS from the m/z 191 ion showing the oleanane, C35 hopanes, and the C30 hopanes. ....86

Figure 42. Amoco Champlin 276 D-1 well GCMS from the m/z 217 ion, it shows the high abundance of diasteranes and the presence of C30. ....87

Figure 43. Amoco Champlin 276 E-1 well GCMS from the m/z 191 ion. The ratio of Ts/Tm suggests the sample is very immature. The S/R ratio suggests is early mature. The presence of C29 moretane indicates that this rock is highly immature since they are highly unstable and tend to disappear with increasing maturity. ....90

Figure 44. Amoco Champlin 276 E-1 well GCMS m/z 217, showing the high abundance of diasteranes that as stated before indicate a shale rich rock and marine environment. ....90

Figure 45. Stage Stop Unit 2 well GCMS from m/z 191 ion showing the C30 hopane, moretane, gammacerane, oleanane and the C32, C33, C34 and C35 triplets, which indicate that the sample is highly immature, from stratified waters, with higher plant material input. ....91

Figure 46. Stage Stop Unit 2 well GCMS from m/z 217 ion showing the C27, C28, C29 and C30 steranes, which indicate a shale. ....91

Figure 47. Map showing the resulted potential area. Thickness, Ro, depth and were used as constraints to define the potential areas. ....93

## Abstract

Large volumes of gas and some oil have been produced from the Cretaceous Lewis Shale, and it is often considered a regional source of gas in the Greater Green River Basin. However, the Lewis Shale has never been studied as a potential oil-prone source or reservoir rock despite the fact that there is a small Lewis oil field on the western part of the Wamsutter arch: the Stage Stop field.

In this thesis, I evaluated the potential of the Asquith Marker as an oil-prone source rock. The Asquith Marker, in the lower Lewis Shale, is a relatively organic-rich shale easily recognizable on the gamma ray log as an anomalously high API. It is a third order condensed section that has a maximum thickness of 100ft. and covers a large area of the Greater Green River Basin.

Based upon limited subsurface data, I have evaluated samples from one cored well that penetrated the Asquith as well as samples from six other Lewis Shale cores above the Asquith Marker, five well cuttings and eight outcrop samples from the Asquith Marker. Structure and stratigraphic maps have been compiled and used to identify the areas where the Asquith Marker is thickest and deep enough to generate oil. Analyses included Rock-Eval, XRD, vitrinite reflectance, and biomarker geochemistry, from which the composition, maturity, oil potential and kerogen type were determined.

Rock-Eval analysis showed some pitfalls associated with sample type (cutting and outcrop sample vs. core sample). Core samples showed high potential to generate oil from Type II kerogen. Lower TOC from cutting and outcrop samples was caused by caving, weathering and handling of the samples during the storage of the cutting

samples. This low TOC also affected the parameters obtained from the Rock-Eval as HI, Tmax, OI and the S1, S2, S3 and S4 peaks from the pyrograms. Vitrinite reflectance from other intervals close to the Asquith Marker suggested the Asquith Marker interval is within the oil window or early oil window. Biomarker analysis was performed on three samples: one sample from the Amoco Champlin 276 D-1 well, one sample from the Amoco Champlin E- 1 well and one sample from Stage Stop Unit 2 well. This analysis suggested the samples are within the oil window or early oil window from marine, hypersaline stratified waters with high clay content. There was also evidence of some higher plant material input.

The general sparseness of data has hindered a more robust analysis, but several indicators suggest the Asquith Marker might be oil-prone as an unconventional resource shale. In order to define potential areas for unconventional development thickness, depth, vitrinite reflectance and biomarker maturity data were used as constraint. According to Jarvie (2005), the lower the TOC the thicker the shale interval must be in order to be economically viable for extraction. Depth was chosen based upon maturity and potential to generate hydrocarbons from TOC, biomarkers and vitrinite reflectance. A depth between 1400-(-6600) ft. depth (TVDSS) was used as constraint. The total area obtained from these constraints is close to  $2.5 \times 10^7$  acres; a map shows the aerial extent of the oil-prone Asquith Marker.

New information about two oil producing wells that were drilled as horizontal wells through the Asquith Marker (Rush Unit 4-1 and Spirit of Ratio 7-1H) is used as proof of concept. They have a total oil production of 26775 Bbls. and 14350 Bbls.

respectively but the decline rate characteristics of unconventional wells led to the abandonment of the Rush Unit 4-1H well on 2016.

# **Chapter 1: Introduction**

## **Location of the Study Area**

Most of the Greater Green River Basin is located in Wyoming but it also occurs in Utah and Colorado (Roehler, 1992). This thesis focuses in the area within Wyoming encompassing the Uinta, Sweetwater, Lincoln, Sublette, Teton, Fremont and Carbon counties (Figure 1A). According to Roehler (1992), the Greater Green River basin has an area of approximately 19,700 mi<sup>2</sup>. Towards the north the Wind River Mountains and Sweetwater Arch (Granite Mountain) bound the basin with the Uinta Mountains to the south, the Sierra Madre uplift, Rawlins uplift and the Wyoming thrust belt towards the east. The Lewis Shale transitioned to a more proximal facies towards the eastern section of the basin, towards the Rock Springs uplift (it becomes the Fox Hills sandstones) during the time of deposition. Since the main objective of this study is to map and evaluate the Lewis Shale all wells used for correlations are located at the east of the uplift in Carbon and Sweetwater counties (Figure 1B).

## **Research Objectives**

This present work focuses on shales and mudstones within the stratigraphic section of the Lower Lewis Shale and its potential for generating oil as an unconventional resource shale. Analysis of core samples from Amoco Champlin 276 Amoco D 1 well located towards the eastern part of the basin reveal the potential for oil generation with a TOC between 2 and 4 wt.%. Samples obtained from the organic rich facies of the Lower member of the Lewis shale, including the Asquith Marker in wells throughout the basin, as well as outcrop samples used to perform Rock-Eval, XRD mineralogy, vitrinite reflectance, and biomarker geochemistry analyses.

This thesis focuses on two main objectives. The first objective is to develop correlations from well logs and maps made to identify areas with a higher potential to generate and produce oil. The second objective is to analyze the organic rich facies of the Lewis Shale, particularly the Asquith Marker, for their potential to generate oil. Analysis were performed on well cuttings, core and outcrop samples. The evaluation and analysis of the samples are summarized on the following pages.

#### *Well logs correlations and maps*

Many previous studies have used the Asquith Marker (Winn et al., 1987, Pyles, 2000) as a regional marker due to its easily identified log pattern of high gamma-ray API and low resistivity. Correlations were conducted using raster logs from the Wyoming Oil and Gas Conservation Commission data base. In some areas, the gamma ray log was not clear or available, so it was necessary to use another suite of logs like Spontaneous Potential, Deep Resistivity, Neutron, Density and Sonic logs in order to provide better coverage of the basin. Correlations provided maps in which the changes in thickness and distribution of the formation were visualized to identify prospective areas.

#### *Potential to generate oil*

Analysis of core samples from Amoco Champlin 276 Amoco D 1 well reveals the potential for oil generation with a TOC between 2 and 4 wt. % from a Type II kerogen.

Rock-Eval, vitrinite reflectance, XRD mineralogy and biomarker geochemistry from samples obtained from the organic rich facies of the Lower member of the Lewis

shale, including the Asquith Marker, in conjunction with outcrop samples throughout the basin, confirm a good potential to generate liquid hydrocarbons.

### *Petroleum System*

The Lewis Shale, also known as the Lewis Total Petroleum System (Hettinger, 2005), comprises source, reservoir and seal rock. Hettinger (2005) reports that between 600 and 675 billion cubic ft. (bcf) of gas with some oil have been produced from the formation since 1974.

The Lewis Shale is informally divided into three members. Each member contains variable amounts of shale, siltstone and very fine to medium grained sandstone. The lower member is dominated by black shale. The middle Dad Sandstone member is dominated by sandstones and siltstones. The upper member is dominated by dark gray to olive gray mudstone (Almon, 2002).

The lower member includes the organic rich interval informally named the Asquith Marker, which has a maximum thickness of 100ft., and is the focus of this study. The Asquith Marker has been used as a regional geological marker because it is a widespread third order condensed section in the Greater Green River basin (Pyles, 2000).

Structurally, the basin is heavily faulted and depths of the formations vary largely through the basin, allowing the study of the behavior of the rock at these different depths, ultimately to identify the “oil window” depth.

Law and Surdam (2005) have identified an overpressure regime within the basin affecting the chances of oil generation from the rock. This effect is associated with gas-bearing and low permeability formations. Depth at which this phenomenon takes



place also varies through the basin both vertically and horizontally, making it necessary to identify and delineate accurately these zones.

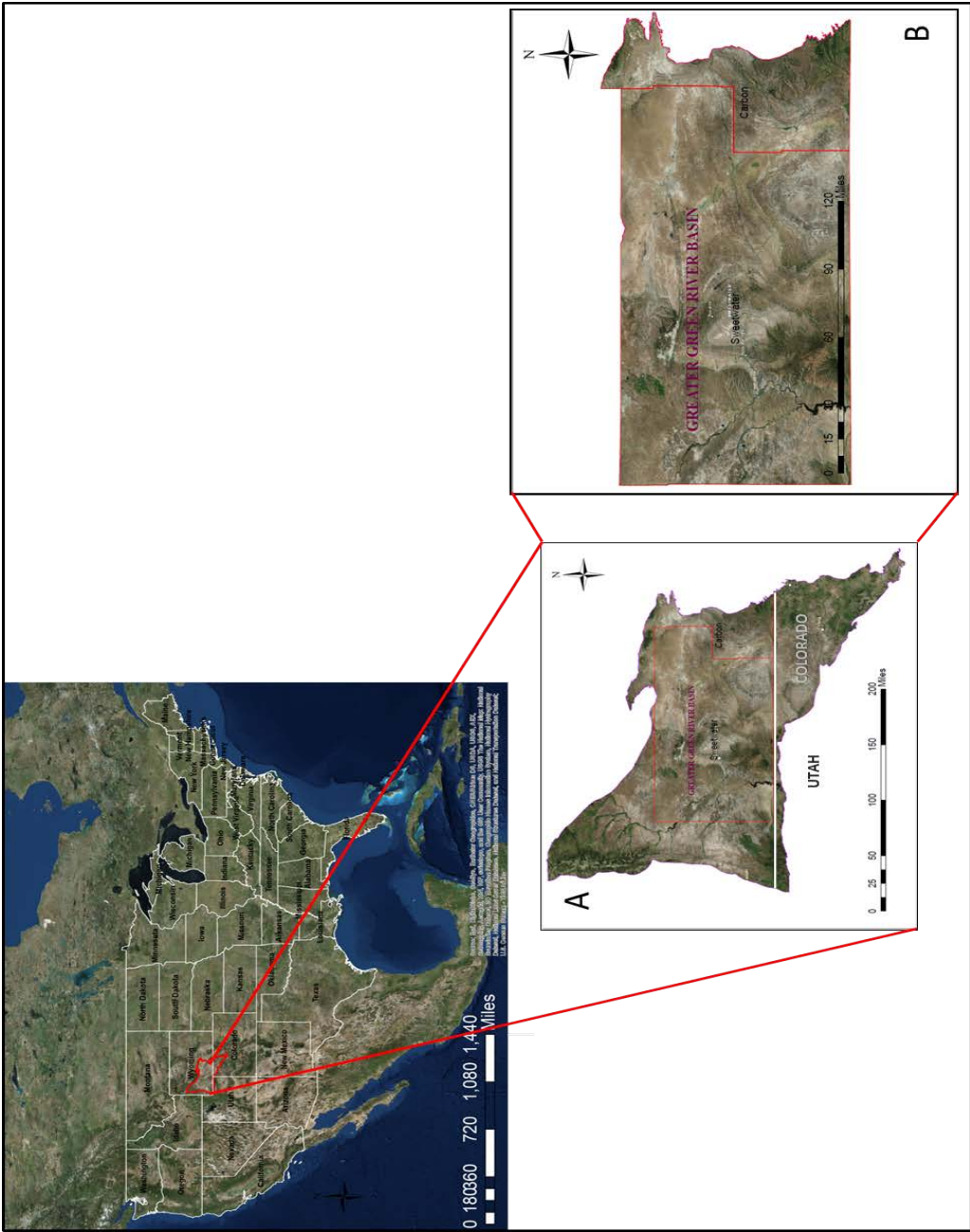


**Figure 1. Location of the study area. Figure A shows the entire Greater Green River Basin.**

## **Research Contributions**

Since all the work previously done concludes that the Lewis Shale is producing gas due to the overpressure and the maturity of the rocks (Roberts et al., 2005), the oil potential of the basin has never been examined despite the fact that there are some oil and gas fields producing from the Lewis Shale. One specifically located between the Wamsutter Arch and the Rock Springs uplift is named Stage Stop; it has produced 951,168 BBLS of oil from 1978 to 2014 from the Lewis shale (Hettinger, 2005).

The present thesis aims to define the potential of the basin to generate and produce oil from the Asquith Marker and some organic rich shales from the Lewis Shale.

It also will contribute with:

1. A regional understanding of the thickness distribution of the Asquith Marker throughout the basin;
2. Understand the depositional environment of the Asquith Marker;
3. A maturity study of the formation in the basin;
4. First oil potential study in the formation;
5. Address the uncertainty of the origin of the oil produced from the Lewis Shale reservoir.

## **Research Methods**

In general, the workflow of this thesis follows the one proposed by Slatt et al., (2012) to characterize unconventional shales (Figure 2).

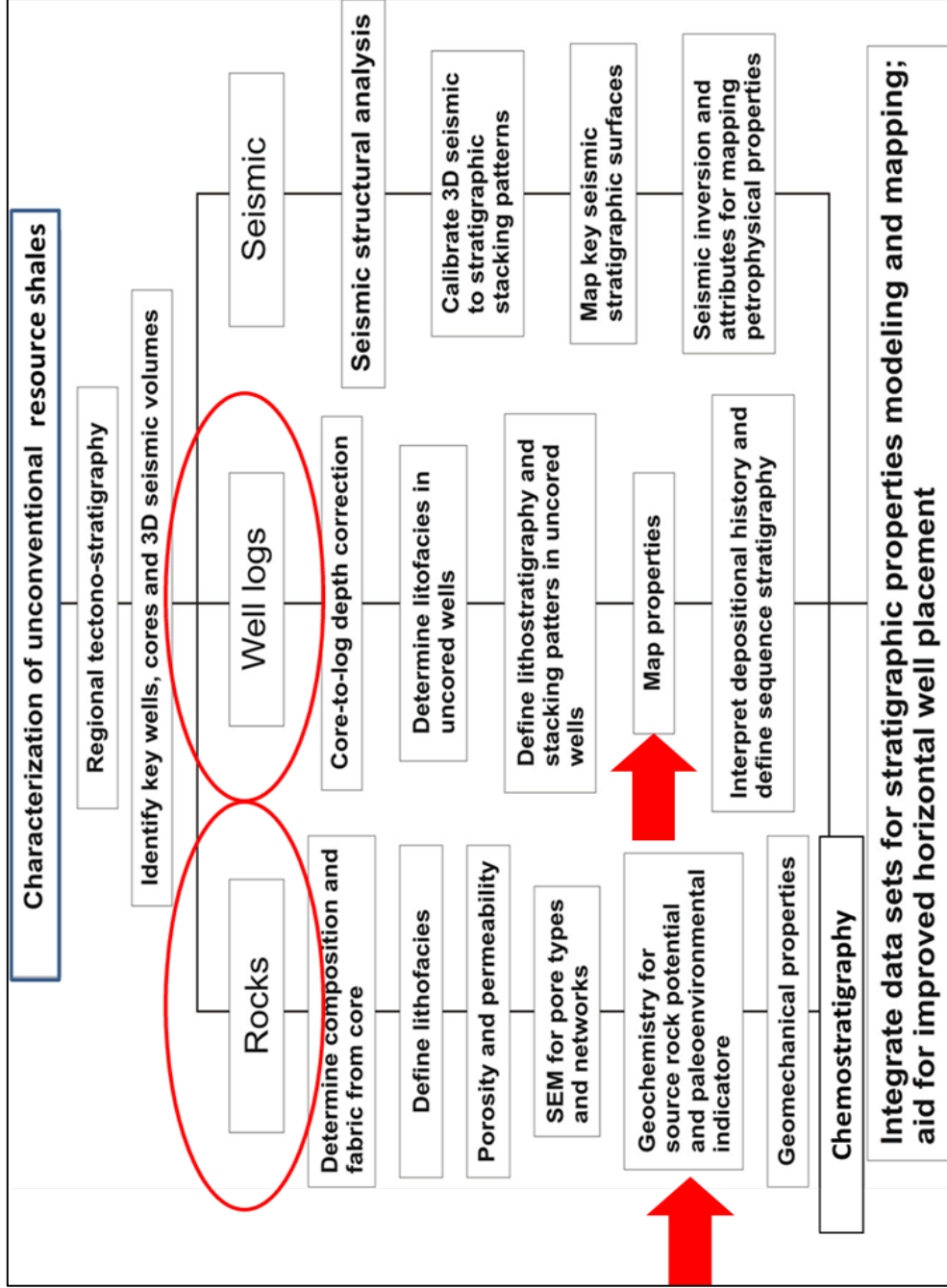


Figure 2. Flow diagram illustrating the different steps used to characterize unconventional resource shales. The two main methods used in this thesis are highlighted in red (From Slatt et al., 2012).

## **Data**

The types of data used in this study are outcrop data and subsurface data.

Outcrop data consists of a measured section from which gamma ray measurements and samples were taken in order to perform geochemical analysis. Subsurface data consists of well logs, core samples and well cuttings.

### *Outcrop Data*

The outcrop is located near the Rawlins uplift, Carbon County, Wyoming. Data includes a section in which gamma Ray was measured and samples were taken in order to perform the geochemical analysis. A gamma ray profile was constructed for the measured section to correlate the outcrop gamma ray responses with the subsurface responses.

Although the outcrop gamma ray is measured in cps (counts per second) and the gamma ray well logs are measured in API, the shapes of the curves are comparable. Therefore, it provides an idea of the response for radioactivity of the rock. Radioactivity is often correlated with organic rich facies, in which the more radioactive the shale, the more organic rich are the facies.

Measurements were taken at two stratigraphic ft. intervals. Five total gamma ray readings were taken from a hand held gamma ray scintillometer from which the highest and lowest values were discarded. Then, the average of the remaining three readings was calculated. Relationship between organic richness and high gamma ray counts is observed from depth versus gamma ray plots.

Samples from the Asquith Marker were taken each two ft. to perform the geochemical analysis. Trenches approximately forty inches deep were dug to reduce the chance of collecting weathered rock.

### *Subsurface Data*

Well logs were obtained from the Wyoming Oil and Gas Conservation Commission as raster images, which were then calibrated using the Petra software®. Correlations were primarily based on gamma ray log. This was due to a kick in the gamma ray response that is representative of the Asquith Marker. This kick is in mostly cases correlatable with amount of organic matter and TOC; where the richer in organic matter the higher the TOC and higher the gamma ray response will be (Figure 3).

Geochemical analyses were conducted on ten samples from five different cored wells, five well cuttings and seven outcrop samples. Samples were chosen based on the color of the rock, assuming that the darker the color the more organic rich the rock will be. Unfortunately only a small number of wells have cored the Asquith Marker or in some cases the information is not publicly available. The samples that were obtained were from shales above or below the Asquith Marker and not from the Asquith Marker per se. Just one cored well corresponds to the Asquith Marker, the Amoco Champlin 276 D-1 well.

The USGS has one of the largest core and cuttings library in the world that is available to the public, with wells from all over the United States. It was necessary to search wells that drilled past the Asquith Marker to obtain cuttings that could be used to conduct the geochemical analyses. A total of eight samples from five different wells were identified for this purpose (Table 1).

**Table 1. Samples used for the geochemical analyses.**

<b>Wells</b>	<b>Depths</b>	<b>Type of sample</b>
<b>Monument Lake Unit 2</b>	11430,11447,11467	Core
<b>Champlin 446 Amoco A-1</b>	14195,14205,14224	Core
<b>Desert Springs Unit 19</b>	5946	Core
<b>Horseshoe Creek 1</b>	4937	Core
<b>Creston Unit-1</b>	7482,7515	Core
<b>Stage Stop Unit 2</b>	5380-5390,5400-5410	Cutting
<b>Amoco Bog</b>	13320-13330,13330-13340	Cutting
<b>Champlin 448</b>	10560-10570	Cutting
<b>Champlin 276 Amoco D-1</b>	8138,8151,8152,8153,8154	Core
<b>Chorney</b>	11370-11380,11390-11400	Cutting
<b>Champlin 276 E-1</b>	8970-9000	Cutting
<b>Outcrop Samples</b>	Each two stratigraphic Feet	Outcrop sample

## *Interpretation*

### Correlations

Outcrops and wells were correlated using the gamma ray log obtained from outcrop and wells. Therefore, the stratigraphic position of the formation within the regional stratigraphic framework was well established. Boundaries between the formations are easy to pick on well logs due to the difference in lithology that gives a different response on the gamma ray log. The Asquith Marker corresponds with a higher gamma ray and the top of the Almond formation a contrasting lower gamma ray showing the characteristic response of sandstone in the gamma ray (Figure 3).

### Interpretation of Petroleum System

The petroleum system includes the reservoir rock, trap, source rock, and seal rock. In the present study the source rock also comprises trap and seal rock hence analyses were focused on TOC and Rock- Eval, vitrinite reflectance, XRD, and GC, GCMS for biomarker analysis.

The outputs from TOC and Rock Eval analyses are:

1. Total organic carbon (TOC) (wt. % carbon)
2. S1 (mg HC/g), S2 (mg HC/g) and S3 (mgCO<sub>2</sub>/g) peaks
3. Tmax (°C)
4. Oil production Index [transformation ratio (S1/(S1+S2))]
5. Hydrogen Index (S<sub>2</sub>\*100/TOC)
6. Oxygen Index (S<sub>3</sub>\*100/TOC)



TOC and Rock-Eval data was performed by Geomark research Ltd., located in Houston, Texas. The other geochemical analyses were performed at University of Oklahoma Organic Geochemistry Laboratories located in Norman, Oklahoma.

In order to perform the geochemical analysis it was necessary to crush the samples for the screening analysis and the soxhlet extraction. Weights for the samples varied depending upon the availability of it from the USGS core facility.

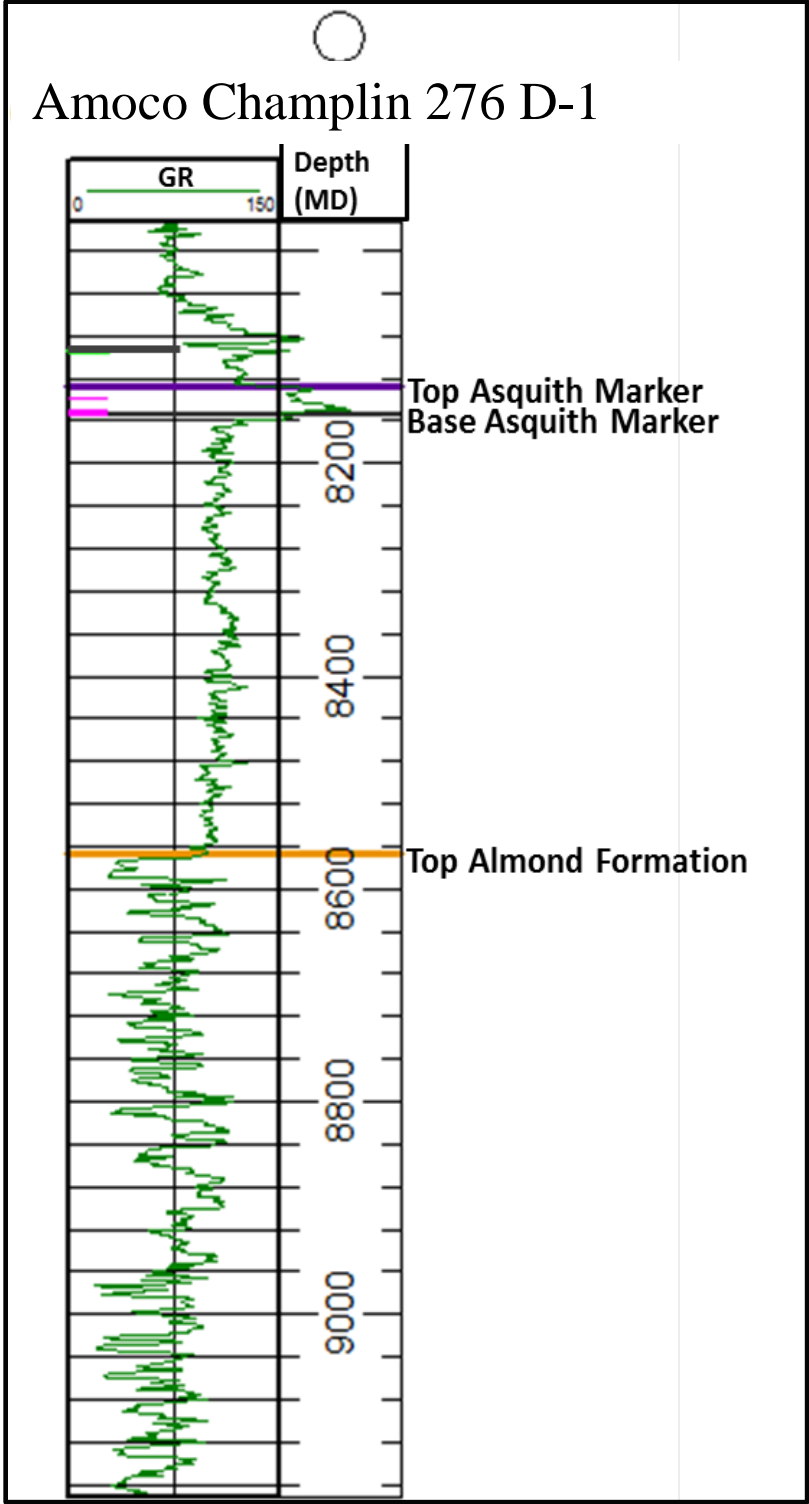


**Figure 3. Gamma ray well log from Amoco Champlin 276 D-1 well. Top of the Asquith Marker formation is marked in purple, base of the Asquith Marker is marked in dark grey and top of the Almond formation is marked in yellow.**

## **Chapter 2: Geological Setting**

### **Regional Geology**

The Greater Green River basin is structurally divided into four sub-basins by intrabasin anticlines. The Rock Springs uplift trends from north to south and separates the Greater Green River basin into two almost equal parts (Figure 4). This is a fore-land fold in front of the Cretaceous orogenic belt of central and northern Utah (Ritzma, 1955) that was a positive area during the deposition of the Lewis Shale and equivalent formations. The west boundary of the basin was bordered by the Cordilleran Highland that was the main source of sediment to the seaway.

The east part of the basin is subdivided into three sub-basins. From north to south, the Great Divide and Washakie basins are divided by the Wamsutter arch. To the south, the Sand Wash basin is bounded by an anticline of the same name. The west part is solely comprised by the Green River basin (Roehler, 1992).

This structural framework was developed during the Laramide orogeny, which uplifted the basement at the end of the Cretaceous at the Lost Soldier Anticline, Wind River Uplift and Granite Mountains. This uplifting caused the erosion of the sediments of the Mesaverde Group and the Lewis Shale that created an embayment in the seaway where the sediments continued to be deposited (Figure 5) (Pyles, 2000).

During the Laramide Orogeny, the mountains bordering the basin suffered uplifts and thrusting at the basin margin flank, local folding, normal faulting and subsidence at the depocenters of the basin (Roehler, 1992).

Sedimentation was continuous along the basin except during episodic periods of tectonism (Roehler, 1992). In Figure 5 the black arrows show two major systems

that drain into the embayment. In one of these tectonic episodes, towards the end of the Cretaceous the Wamsutter arch and Rock Springs uplift were subject to partial erosion of the Lance, Fox Hills and Lewis Formations. The Great Divide and Washakie basins were subject to subsidence at the end of the Cretaceous and continued to develop when the Wamsutter arch was uplifted during the Eocene.

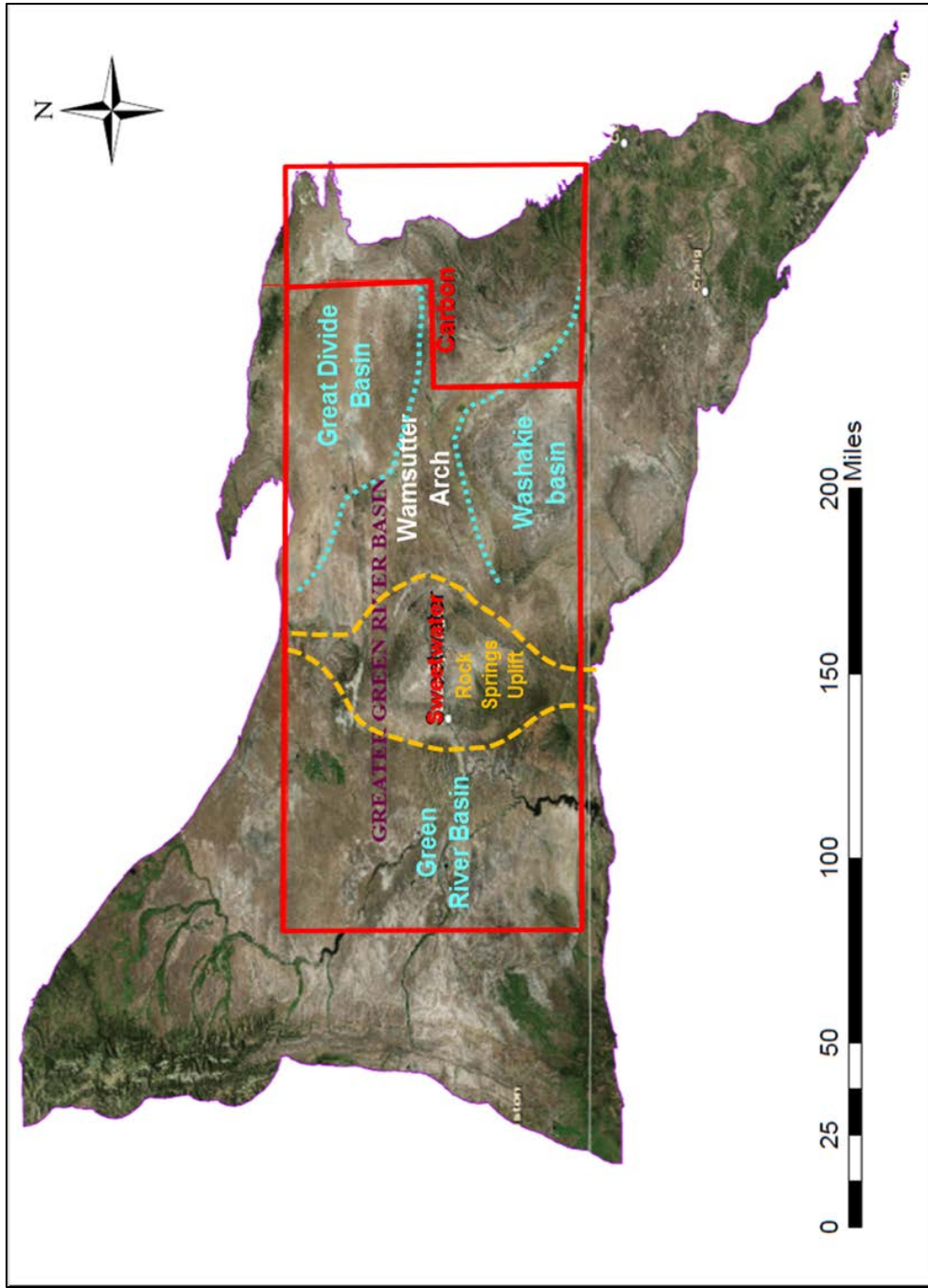
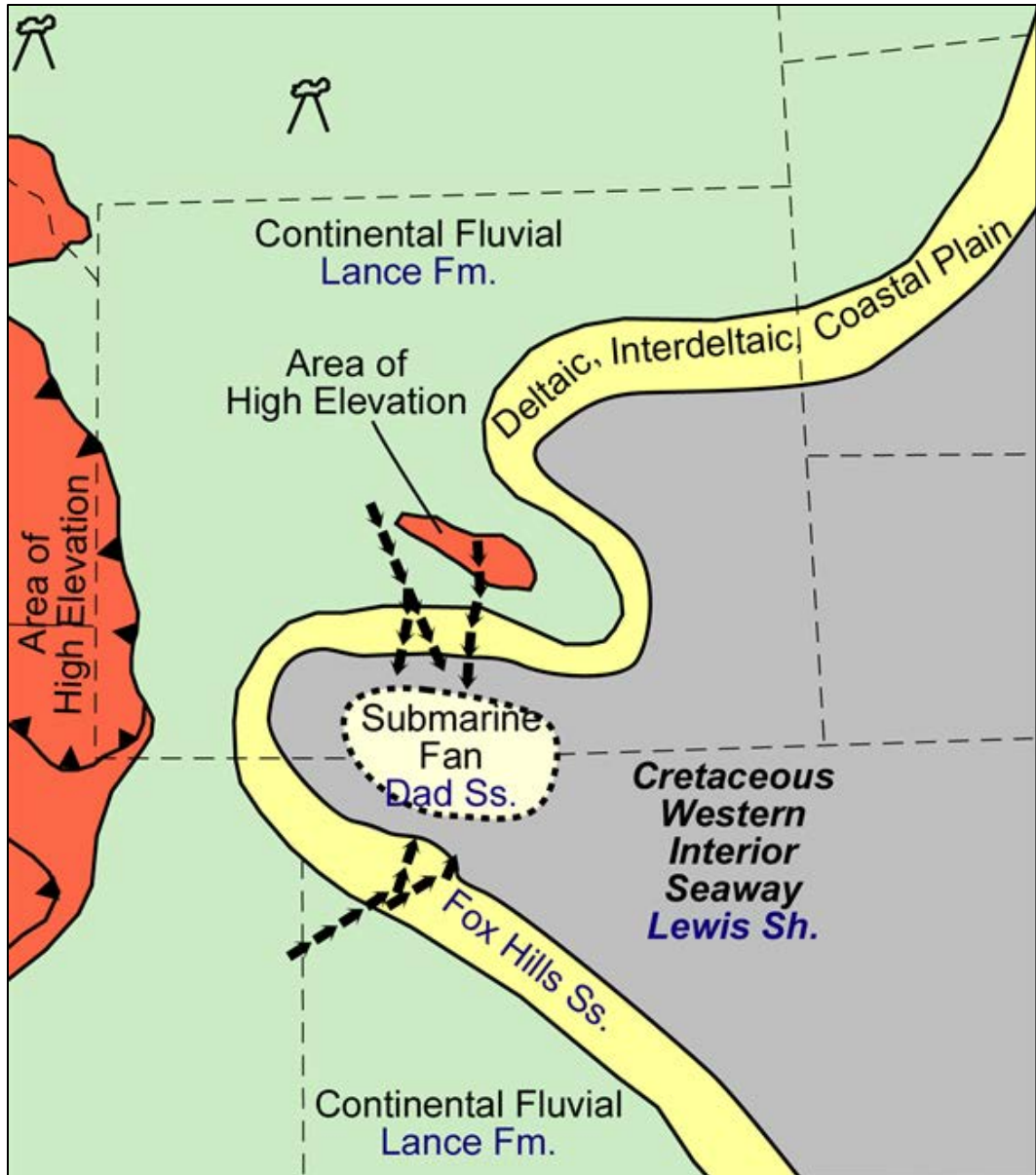


Figure 4. Sub-basins in the Greater Green River basin.



**Figure 5. Location of the Embayment during the Late Cretaceous. Black arrows mark the systems that drained into the embayment. It also shows the submarine fan sediments that were deposited in the center of the embayment. From Pyles (2000).**

## **Local Geology**

The Lewis Shale was deposited in the seaway during the final transgression that took place in the Lower Maastrichtian, covering approximately 2.2 Ma (Pyles and Slatt, 2007). The age of the Lewis Shale was dated based on ammonite extinction zones: *Baculites eliasi* (71.0 Ma extinction age), *Baculites baculus* (70.5 Ma extinction age), *Baculites grandis* (70.0 Ma extinction age) and *Baculus clinolobatus* (69.4 Ma extinction age) (Hettinger et al., 2005). Figure 6 shows the approximate position of the seaway during the deposition of the Lower Lewis Shale and equivalent formations.

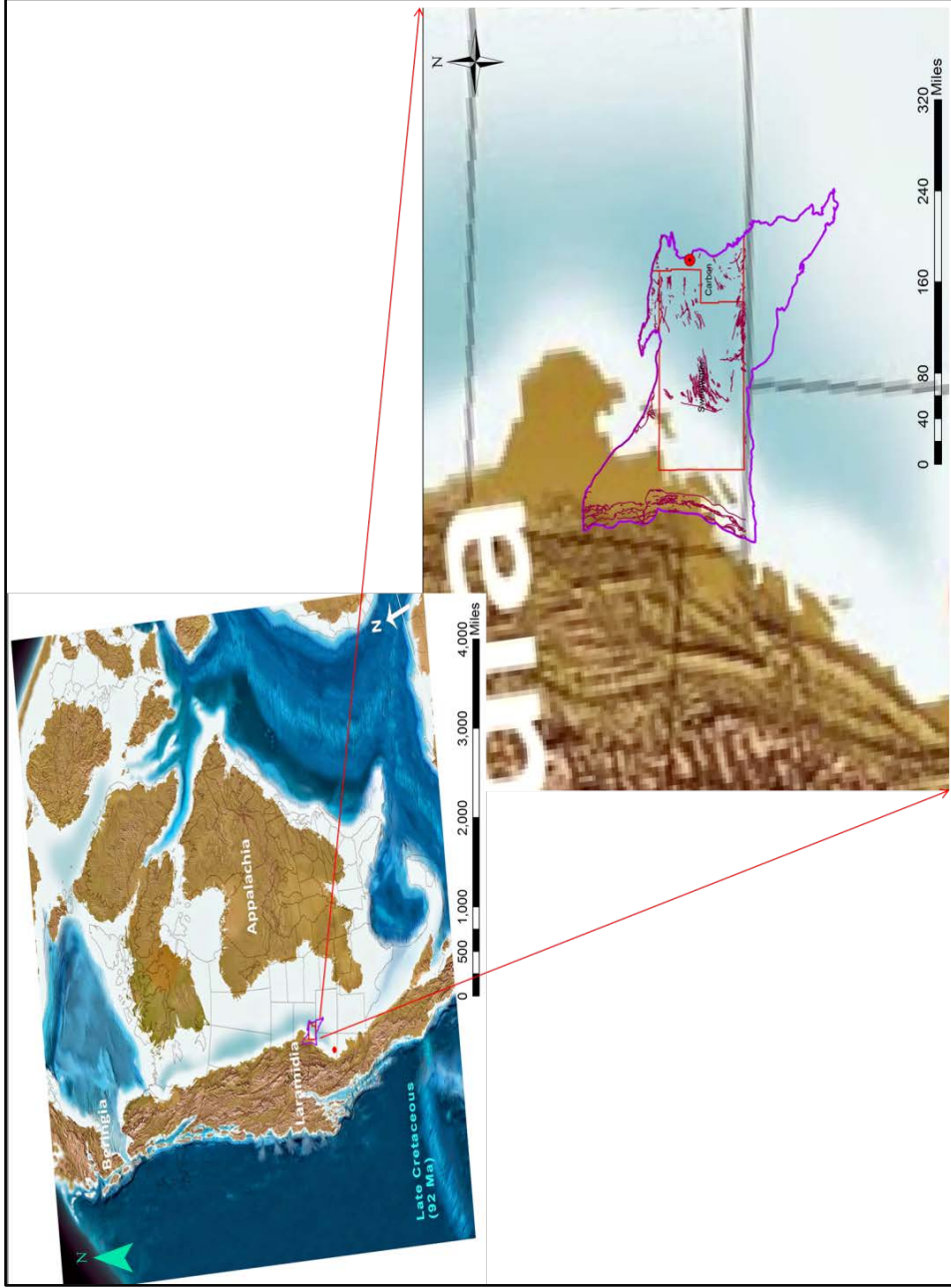


**Figure 6.** Approximate location of the interior seaway during the late Cretaceous in the Greater Green River Basin. Red dot corresponds to the location of the Rawlins outcrop. Red lines correspond to the major faults present in the area. Modified from Blakey, 2011.



The Lewis Shale was named by Cross and Spencer (1899) as the marine shale that is exposed near Fort Lewis in southwestern Colorado (Gill et al., 1970). Though it is not correlative with the Lewis Shale of South Central Wyoming (differs in age and composition) the name remained the same for both units (Hamilton, 2006).

The Lewis Shale is divided informally into three members: the Lower member is comprised mainly by black shale, the middle Dad member is comprised by sandstones and siltstones, and the Upper member is comprised by dark gray to olive gray mudstone (Almon et al., 2002). Total thickness ranges between 2,100 and 2,300ft. along the eastern margin of the Washakie and Great Divide basins. Towards the north and west, it pinches out near the Rock Springs and Granite Mountains uplifts (Figure 7).

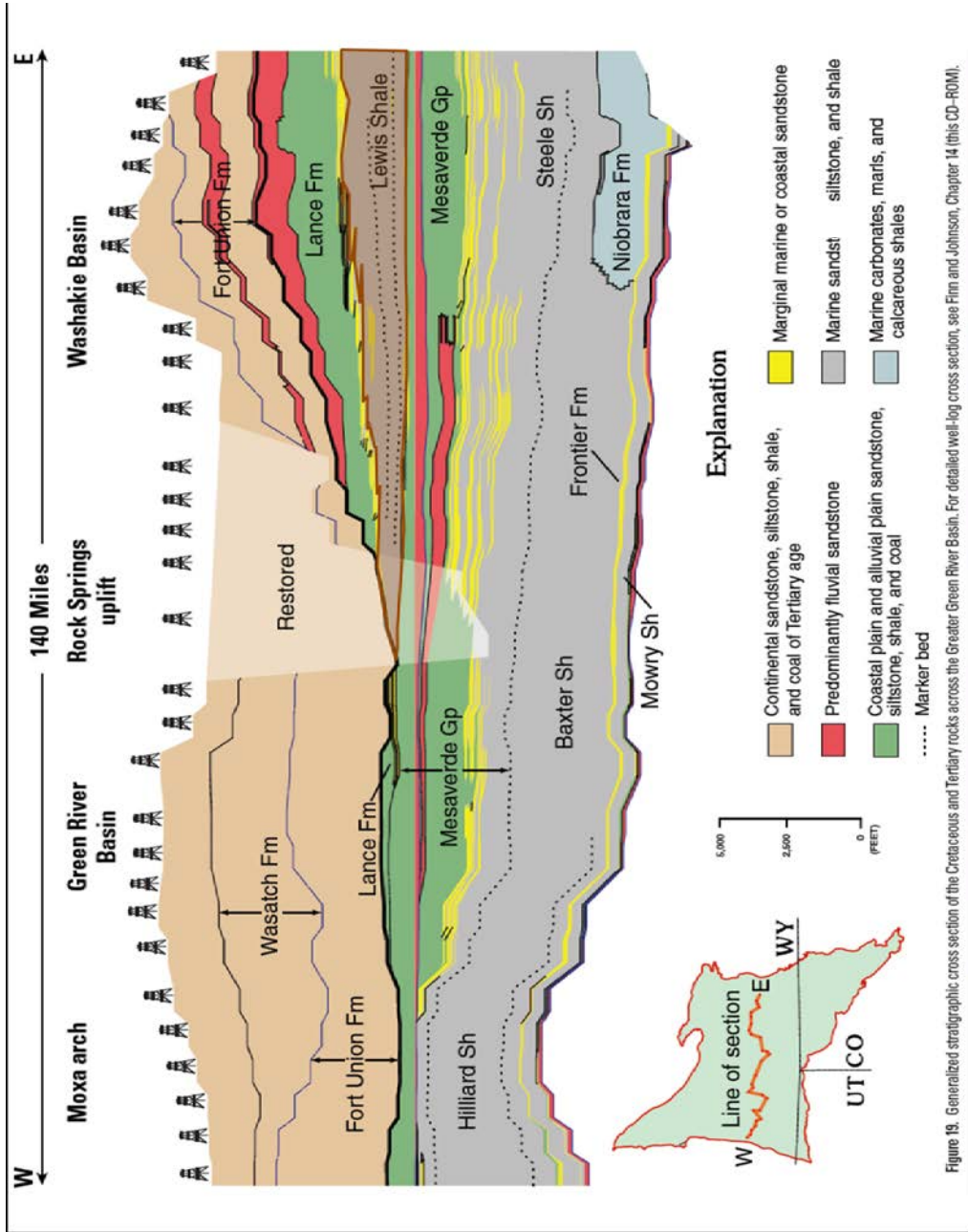


Figure 19. Generalized stratigraphic cross section of the Cretaceous and Tertiary rocks across the Greater Green River Basin. For detailed well-log cross section, see Firm and Johnson, Chapter 14 (this CD-ROM).

**Figure 7. Stratigraphic cross section from East to West from the Greater Green River Basin. The Lewis Shale is highlighted in orange (From USGS, 2005).**

The Lewis Shale conformably overlies the shallow-marine and non-marine Almond Formation in most of the basin (Pasternack, 2005). Towards the east flank of the Rock Springs Uplift there is an unconformable truncation of the Lower Lewis Shale and Middle Almond (Van Horn, 1979 in Pasternack, 2005). The Fox Hills Formation lies conformably above the Lewis Shale (Pasternack, 2005). Figure 8 shows the stratigraphic chart of the Greater Green River basin.

The Asquith Marker is located in the Lower member of the Lewis shale. It is a third order condensed section that is less than 100ft. thick (Pyles, 2000). The Asquith Marker is an organic rich shale easily recognizable on the GR log. It can be traced through the entire basin which makes it a suitable regional stratigraphic marker horizon (Pyles and Slatt, 2000).

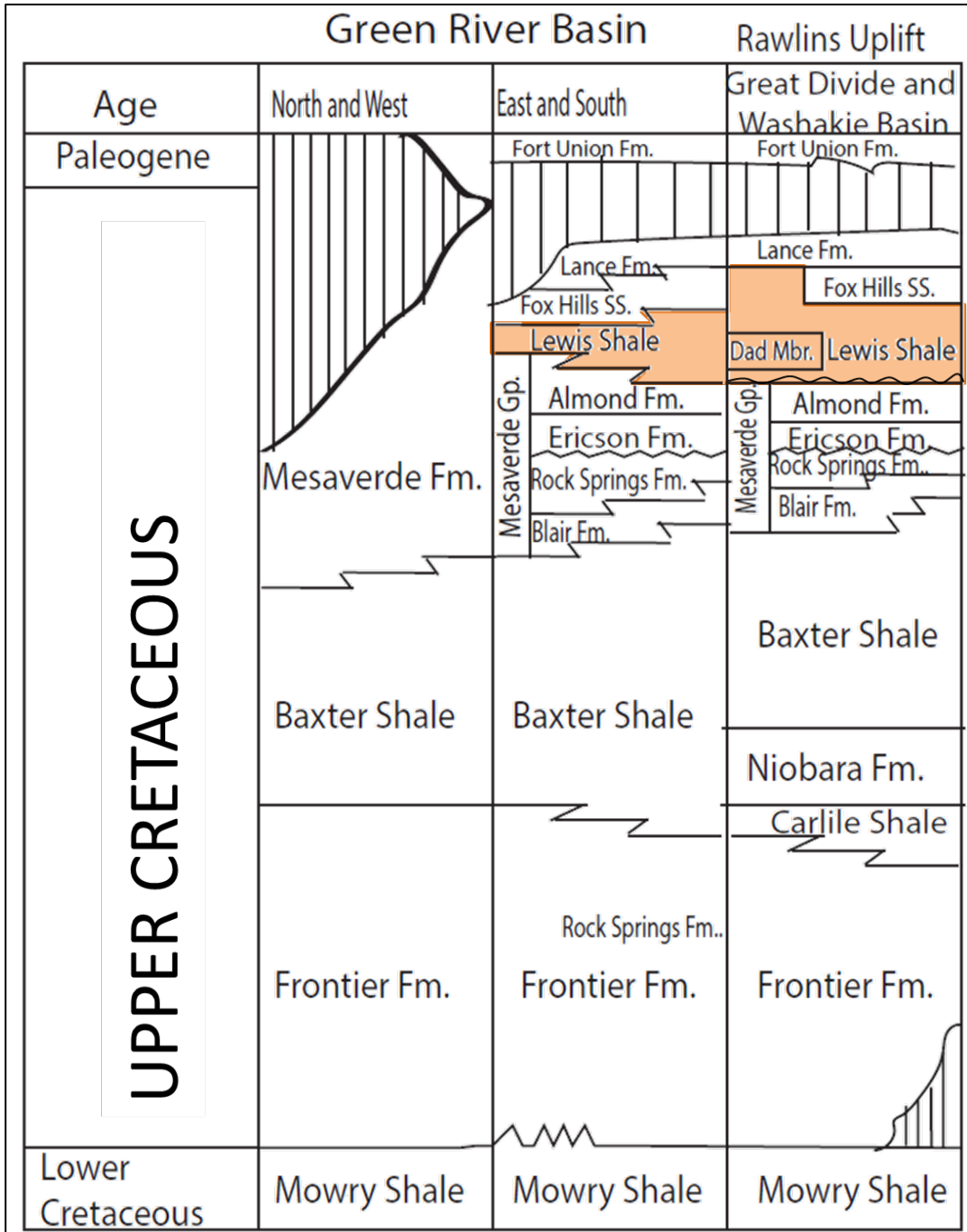
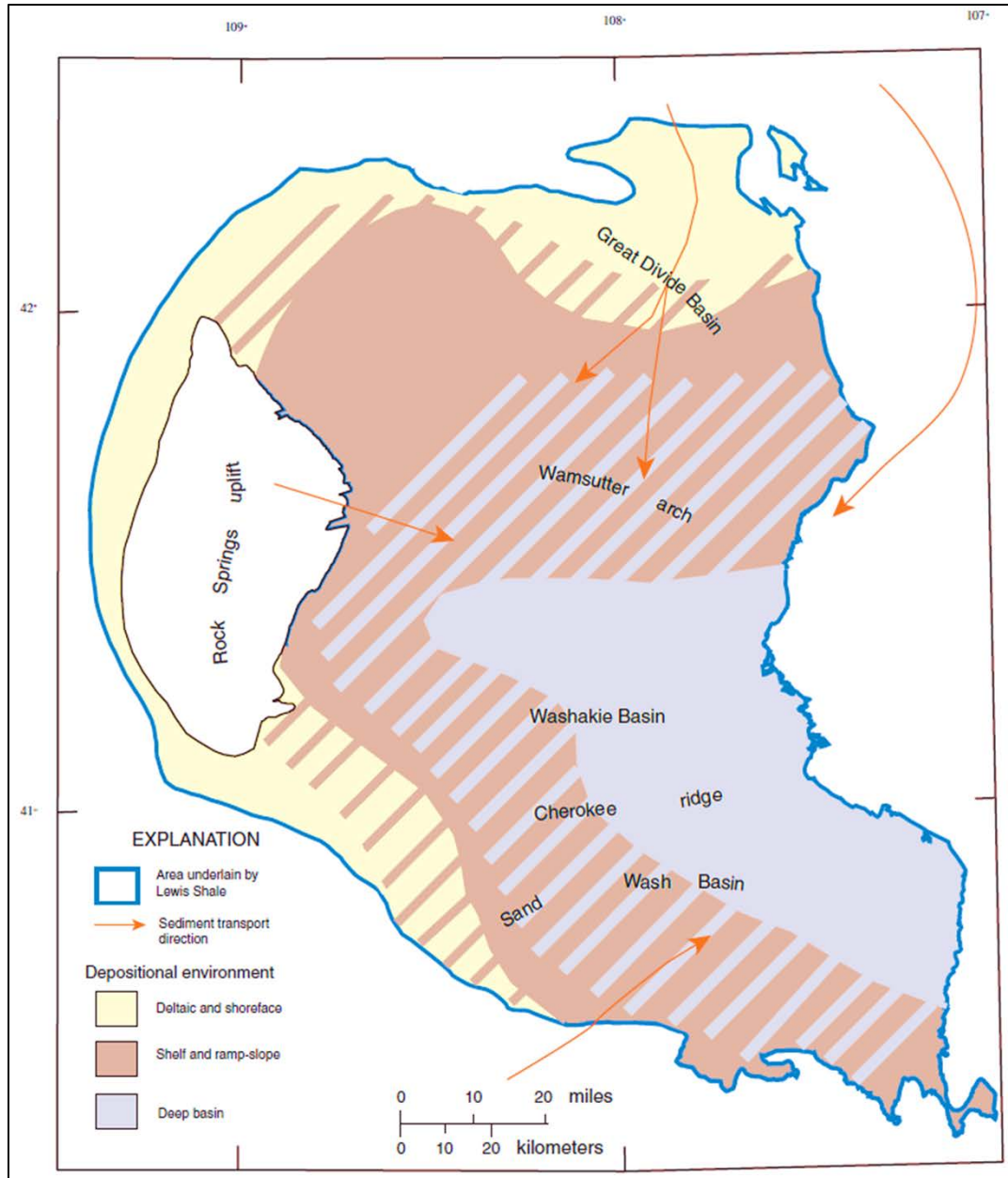


Figure 8. Stratigraphic chart of the Greater Green River Basin. Modified after Schell (1973) in Pyles (2000).

### *Depositional Environment*

Due to the shape of the basin (Figure 5) the depositional environment is sometimes difficult to define. Several authors have had different interpretations from transitional shelf, slope and basin floor environments (Asquith, 1970) to delta plain, delta front, and prodelta prograding over a ramp [(Winn et al., (1987) and Perman (1986, 1987, and 1990) in Pyles 2000)].

During the Laramide orogeny several uplifts occurred in the basin that provided the source material for the basin. Therefore, changes in direction from different submarine fans were identified by McGookey et al., (1972), McMillen and Winn (1991), and Hamilton (2006) converging from the north and changing with time from north-east, west and southwestern part of the basin (Figure 9). But the main source of sediments was constant throughout the deposition coming from north from the Lost Soldier anticline.



**Figure 9. Paleogeographic map showing the different directions of sediment transport and the various depositional environments during the deposition of the Lewis shale. Hachures show where the different environments overlap making the geology of the area more complex. From U.S. Geological Survey Digital Data Series DDS-69-D.**

### **Chapter 3: Maps and Correlations**

Several authors have used the Asquith Marker as a datum which can be correlated throughout the entire region, for example, Pyles (2000) and Pasternack (2005). It is represented as a high gamma ray kick in the logs. In order to develop correlations, the first step is to obtain well logs or stratigraphic columns. In this case well logs were available from the Wyoming oil and gas Conservation Commission.

In some cases the Wyoming Oil and Gas Conservation Commission website also has information about the geological markers for each well that were used as reference when identified on well logs. Since the Asquith Marker is easily differentiated in the gamma ray log, all well logs where the Asquith Marker was easily identified were used to make correlations for this thesis.

Stratigraphic correlations along the basin were made in order to locate structural and stratigraphic distributions of the Asquith Marker in the Greater Green River Basin. A total of 133 wells obtained from the Wyoming Oil and Gas Conservation Commission website were used for correlation and mapping purposes (Appendix 1). Top and base of the Asquith Marker were picked on each gamma ray log. In some cases the gamma ray log was not available and SP, Resistivity, Neutron, Density and Sonic logs were used instead to pick the Asquith Marker. Also, information about the tops of the Lewis Shale and Almond formation was useful to help identify the Asquith Marker. Figure 10 shows the wells that were correlated. Asquith Marker tops from fourteen wells were obtained from Minton (2002).



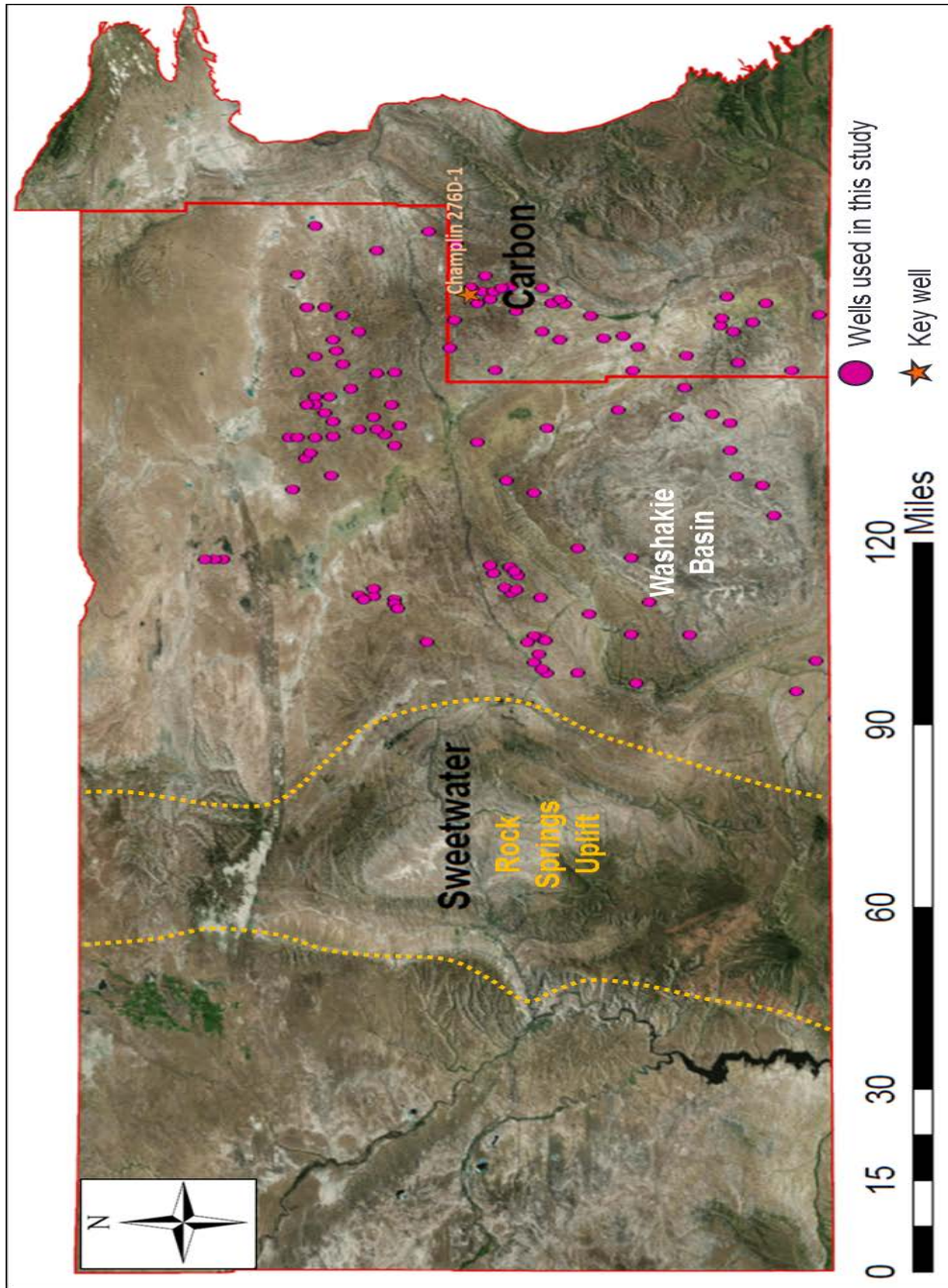


**Figure 10. Wells used in the basin for cross sections and mapping purposes. Amoco Champlin 276 D-1 well was used as a referenced well and is highlighted in orange on the map.**



Amoco Champlin 276 D-1 well was used as a reference well since it has been widely studied (Pyles (2000), Pyles and Slatt (2000), Almon et al., (2001), Almon et al., (2002) and Pasternack (2005). This is one of the few wells with core of the entire Asquith Marker and has the typical gamma ray signature. Geochemical analyses, thin sections and core description were performed by Pasternack (2005) in this well. Pyles (2000) completed a core description, sequence stratigraphy and geochemical analysis of the core.

Figure 11 corresponds to the structural cross-section with direction A-A' north-south where variability in depth and thickness within the Lewis Shale in the basin can be observed. The uplift of the Wamsutter Arch during the Eocene caused the entire structure to be higher as evidenced on the cross section. The Washakie basin to the southwestern section and Great Divide basin at the northeastern part represent the deepest part of the section.

The second cross section B-B' has an east-west trend, and shows clearly the changes in thickness of the Lewis Shale (Figure 12). This change in thickness is due to wedging towards the Rock Springs uplift that was structurally high during the time of deposition, thus restricting the available accommodation space. The Rock Springs Uplift caused the Lewis Shale and time-equivalent formations (Lance Formation and Fox Hills Sandstone) to intertongue, with the Lewis Shale at a distal position and the other two in a more proximal position within the basin (Figure 5). Gamma ray logs show lateral facies variations where sandier rocks are found within shales of the Lower member of the Lewis Shale. This lateral change in facies makes the placement of the top of the Lewis Shale more difficult. Towards the east, the lower member of the

Lewis shale thins due to the presence of the Sierra Madre Uplift and the position of the Interior seaway as shown previously in Figures 5 and 6.

The geometry of the formation followed the configuration of the basin during the time of deposition making it shallower towards the Rock Springs uplift and the Sierra Madre uplift and deeper towards the center (Washakie basin).

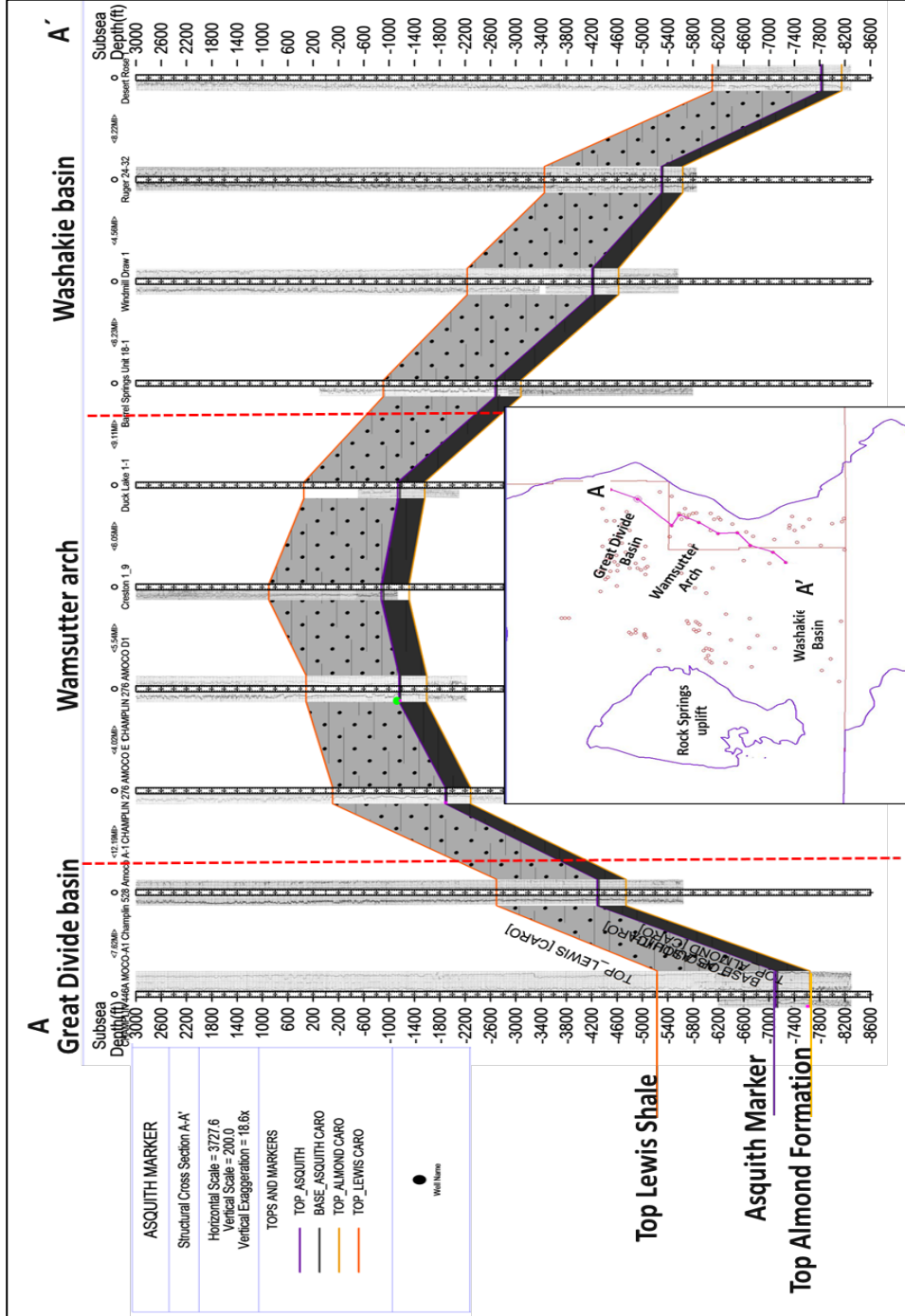
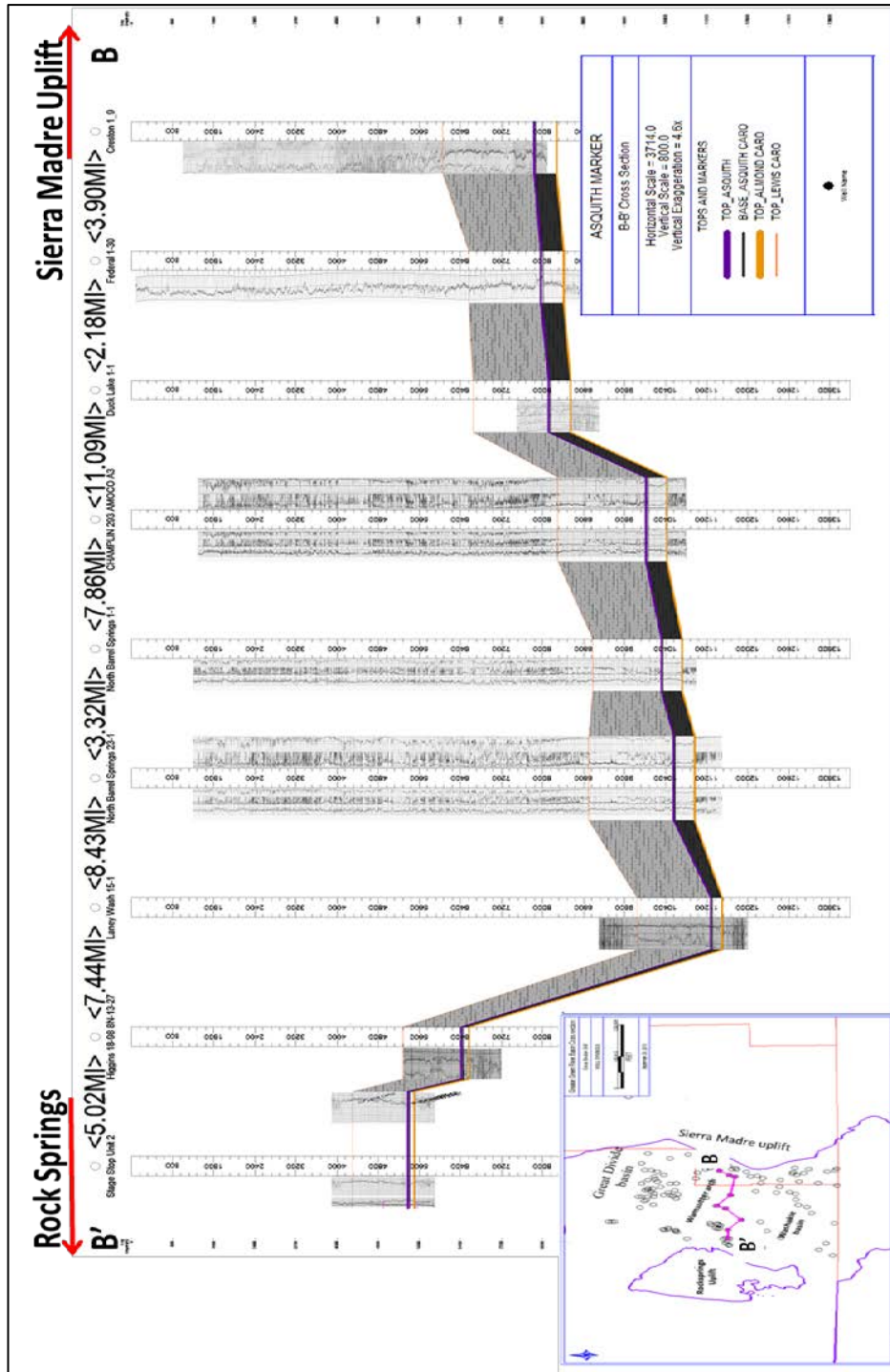


Figure 11. SW-NE Cross section (A-A') in the map from the Washakie Basin to the Great Divide Basin showing the geometry of the Basin. The Grey interval represents the sandier sections from the middle and upper Lewis Shale. The Asquith Marker is represented in purple.



**Figure 12. East-West cross section (B-B'). The shale facies thins towards the Rock Springs uplift where the depositional environment was shallower at the time of deposition. The grey interval represents the sandier sections from the middle and upper Lewis Shale. The Asquith Marker is represented in purple and the black shale is the lower section of the lower member of the Lewis Shale.**

### *Mapping*

From the tops interpreted from the correlations using Petra® software, structural and stratigraphic maps were generated to identify those areas where the Asquith Marker is thick enough and at appropriate depths to generate hydrocarbons.

The structural map is concordant with the geological history of the basin. The subsidence in the Washakie and Great Divide basins caused these two sub-basins to be in a structurally lower position in the basin. The Wamsutter Arch is the shallower zone in the basin (Figure 13).

Figure 14 corresponds to the isochore map from the Asquith Marker and shows the thickest Asquith Marker reaching as much as 42ft. This is interpreted as the depositional center of the basin during deposition of the Asquith Marker and follows the general trend source of sediment in the basin (north to south) as well as changes in the direction of sediment supply and tectonism present on the basin at the time of deposition might have caused the changes in topography and thus the difference in thickness showing a north-south trend of thicker deposition of the Asquith Marker.

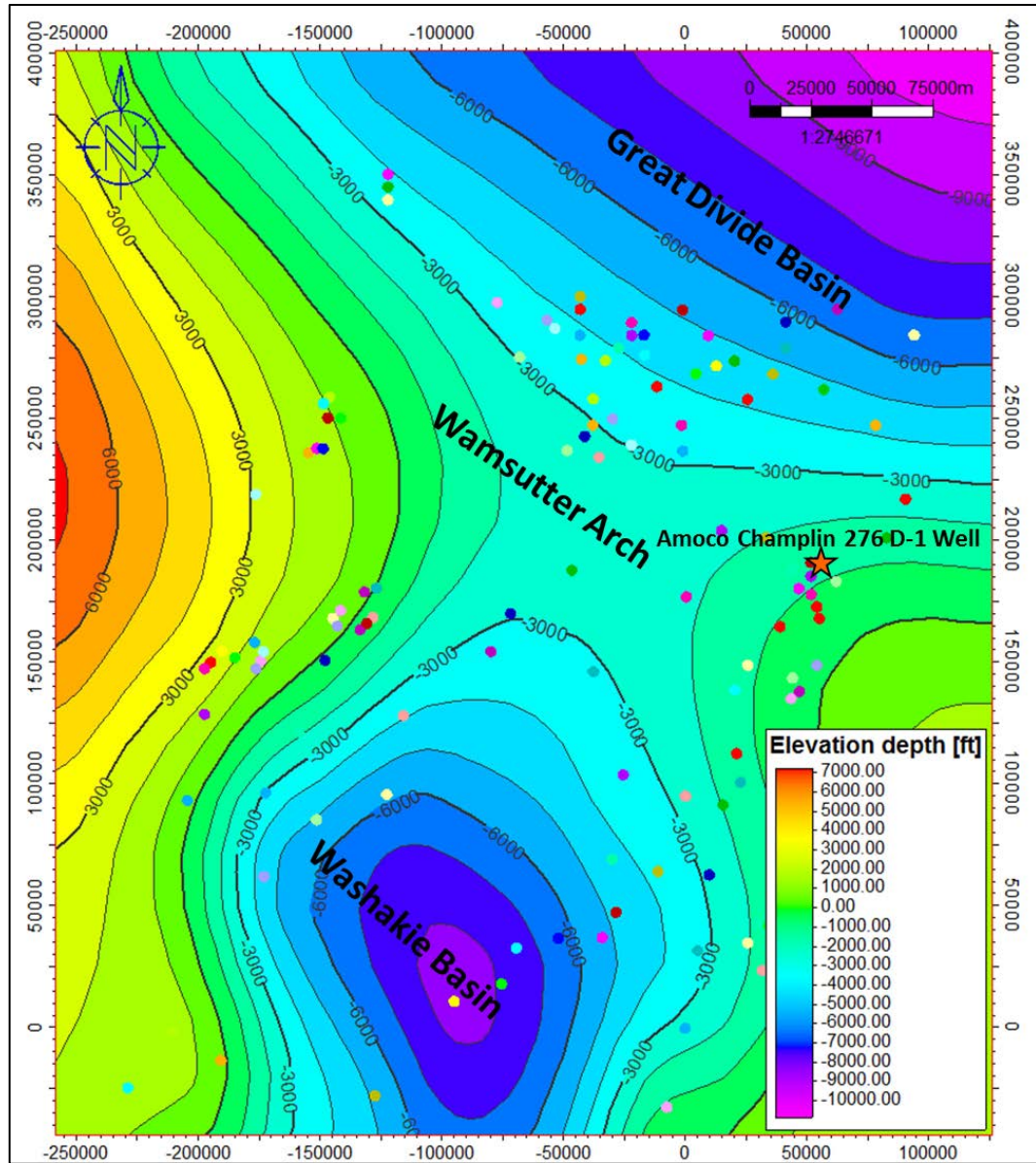


**Figure 13. Structural map at the top of the Asquith Marker. Wells are highlighted in red. Names are omitted for clustering effect. The orange star shows the location of the Rawlins outcrop and the Amoco Champlin 276 D-1 well.**



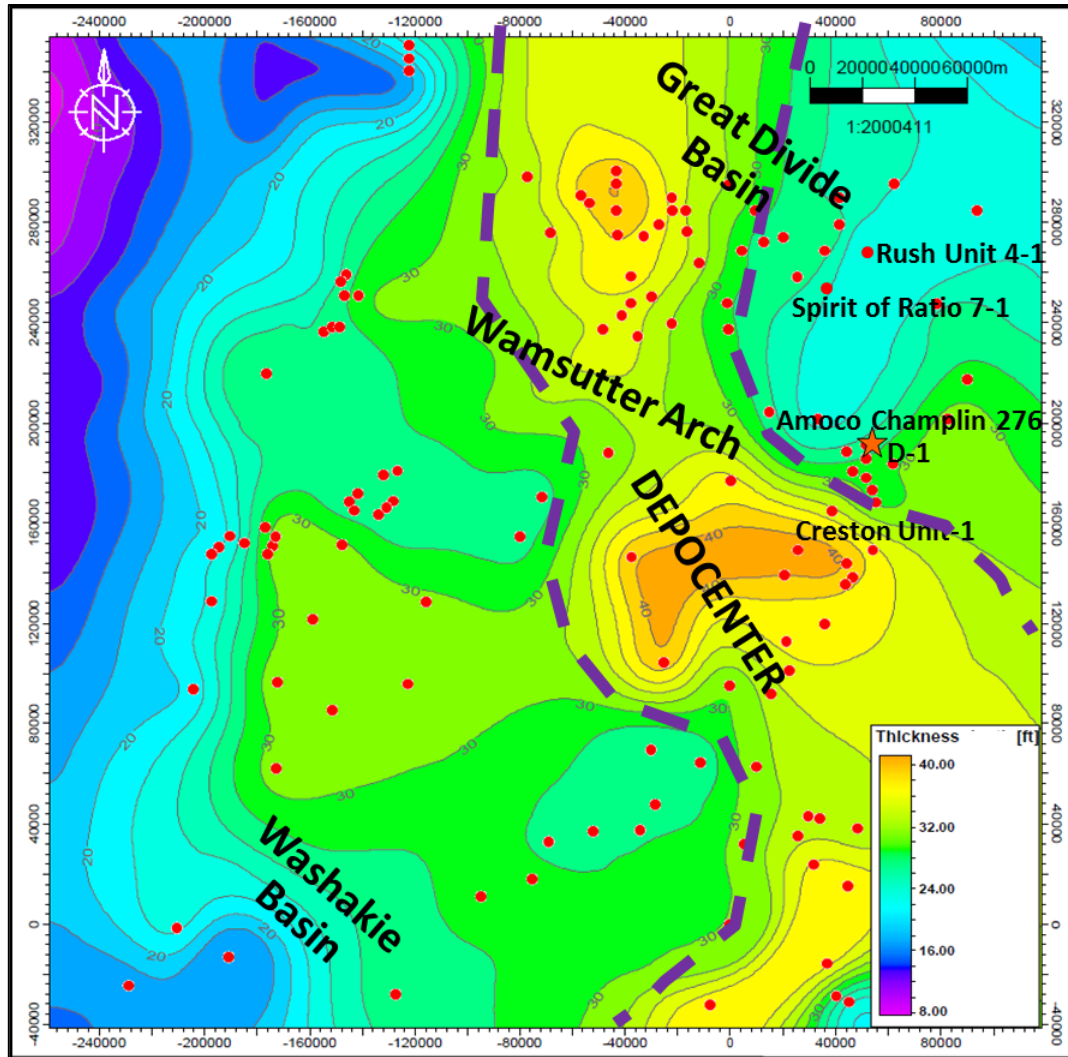


Figure 14. Isochore map of the Asquith Marker. Wells are highlighted in red. Dashed red line marks the limits of the depocenter. Names are omitted for clustering effect. The orange star shows the location of the Amoco Champlin D-1 well.

### *Outcrop Data*

The Asquith Marker outcrop located in Carbon County (Figure 15) is called the Rawlins outcrop by Pyles (2000). He described the outcrop strata as an amalgamated high-frequency deep-water sequence boundary and defined a major surface named the Asquith Marker.

The outcrop section was measured right above a limestone bed, where outcrop gamma ray measurements were recorded every two stratigraphic ft. and a gamma ray profile was built. Slatt (2011) established a direct relationship between TOC and gamma ray cps, where the higher the gamma ray the richer the TOC. Since the Asquith Marker is a condensed section capped by a mfs gamma ray counts are generally high for this section. The plot of gamma ray versus depth from the Asquith Marker is shown on Figure 16. The orange point refers to the limestone bed that Pyles (2000) refers to in his thesis as a “hardground”.

Figure 17 shows the entire Asquith Marker section measured with the points where the gamma ray and samples were taken. The section measures about 36ft. and is mainly composed of a clay-rich shale. The bedding plane is  $240^{\circ}/85^{\circ}$ . In general the outcrop seems very uniform, but once dug into, differences were evident at each of the measured points. The outcrop is highly faulted and weathered. Trenches of approximately 3.3ft. depth were dug on one of the sides of the outcrop, trying to avoid all the weathering that affects the geochemical analysis. At point one, broken parts of fossils were found (Figure 18). Point two has a 1foot thick limestone. Station four is one of the most weathered stations, and contained gypsum and some orange stains. At station



five a limestone bed occurs at the base of the shale and has the highest gamma ray response of the sequence (Figure 16). The samples at this point are very clay rich and disintegrate when in contact with water; very fine lamination is evident when the sample is wet. Some organic material can be observed on the hand sample and one fish vertebra was found (Figure 19).

Figure 20 shows a possible correlation from the outcrop to the Red Rim-1 well log. The gamma ray response from the well is taken every 0.5ft.; therefore the data was reduced to every two ft. to compare the trends. The well and the outcrop are 13.3 miles apart. Red Rim-1 well is in the deeper center of the basin. There is a change in thickness of the Asquith interval due to the Red Rim-1 well is located in a more distal part of the basin during the time of deposition. By contrast, the Rawlins outcrop is located in a shallower position of the basin. The thickness map shows a thinning trend towards the outcrop area. That is why the well section is thicker than the outcrop section (Figure 14).

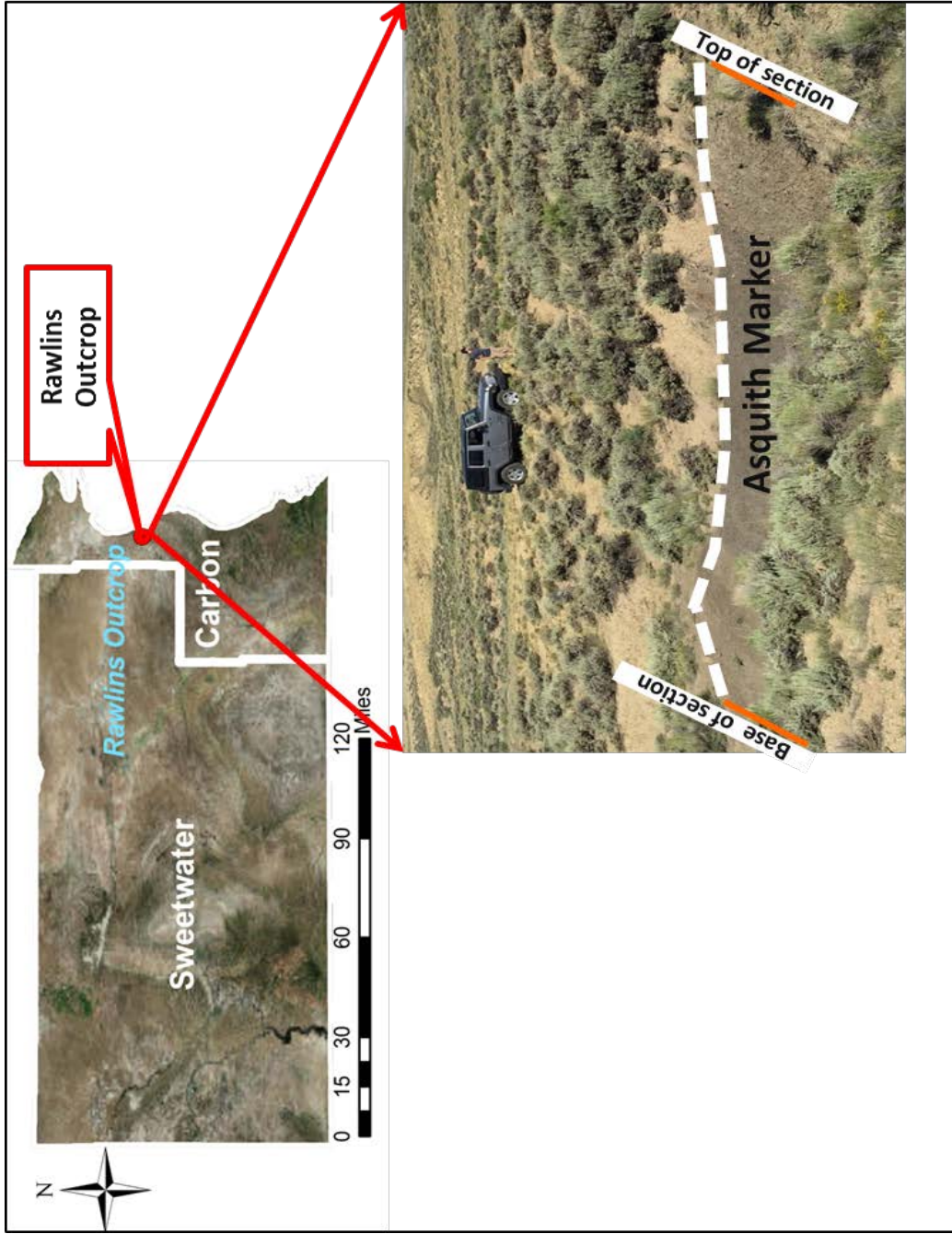
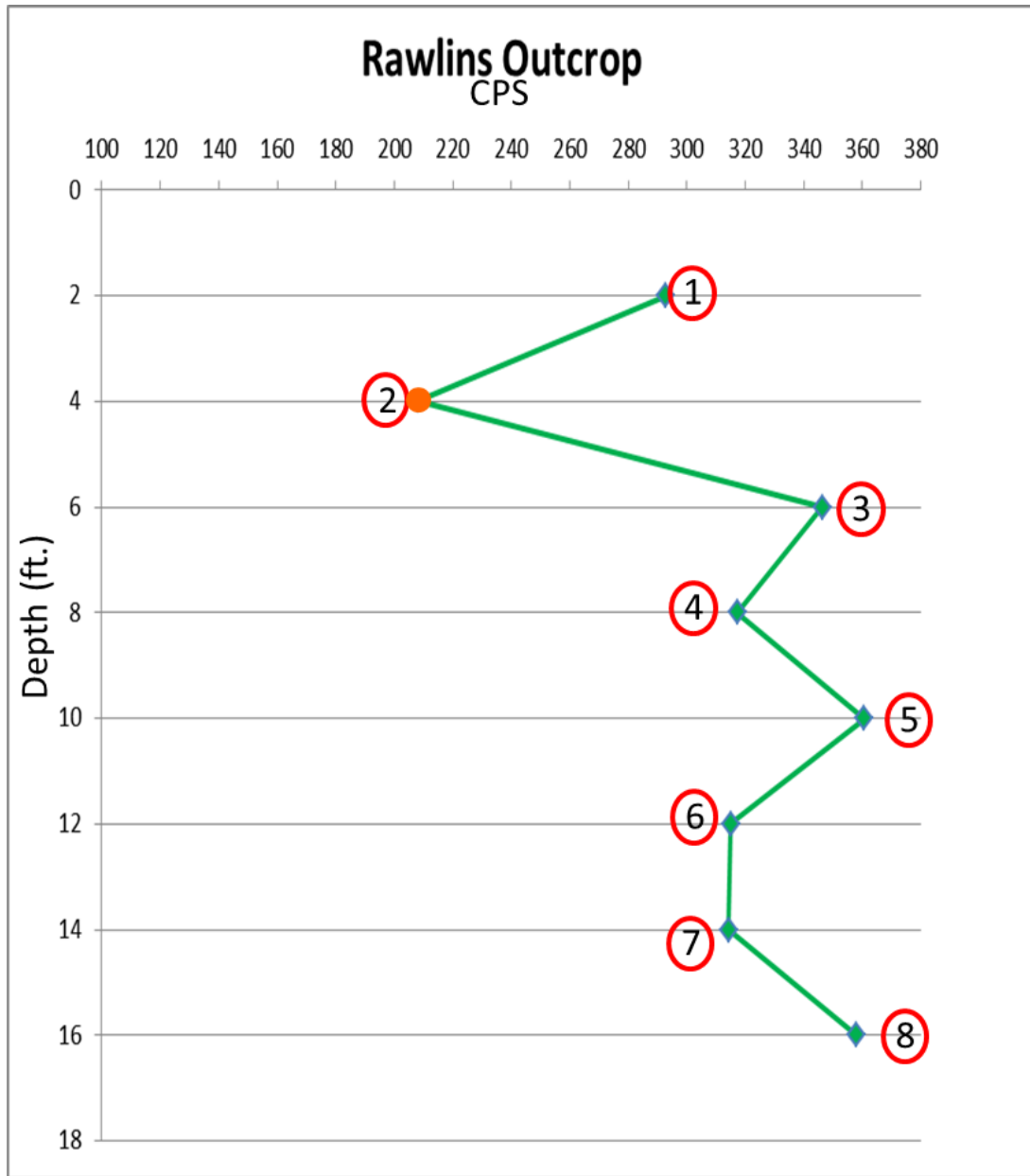
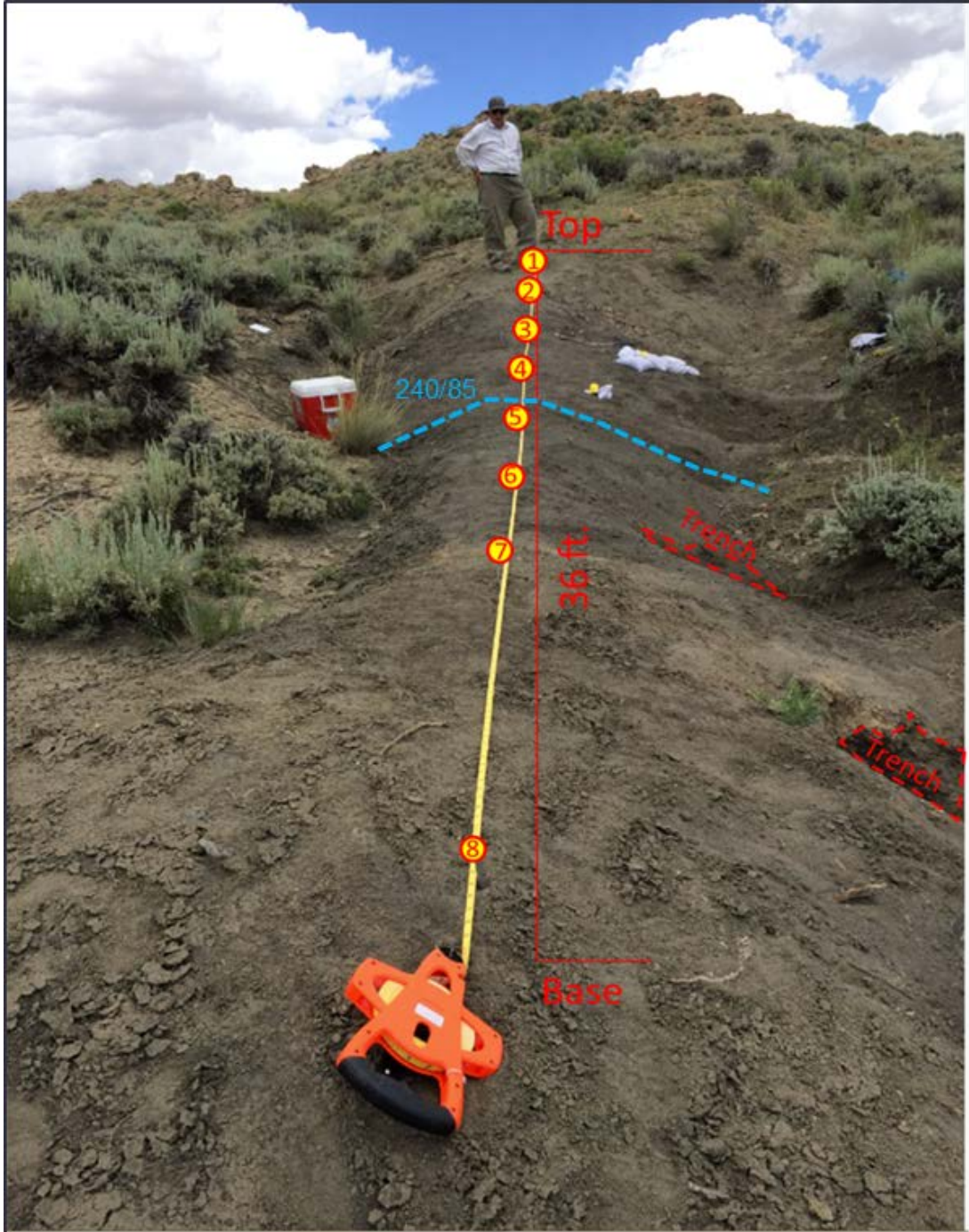


Figure 15. Location of the Asquith Marker's outcrop named the Rawlins Outcrop by Pyles (2000)



**Figure 16. Gamma ray plot from the Asquith Marker outcrop. The orange point corresponds to a limestone bed.**



**Figure 17. Picture of the extension of the outcrop. Trenches were dug on the right side of the mound every 2 stratigraphic ft. Numbers indicate these points.**





**Figure 18. Broken fossil from point 1.**

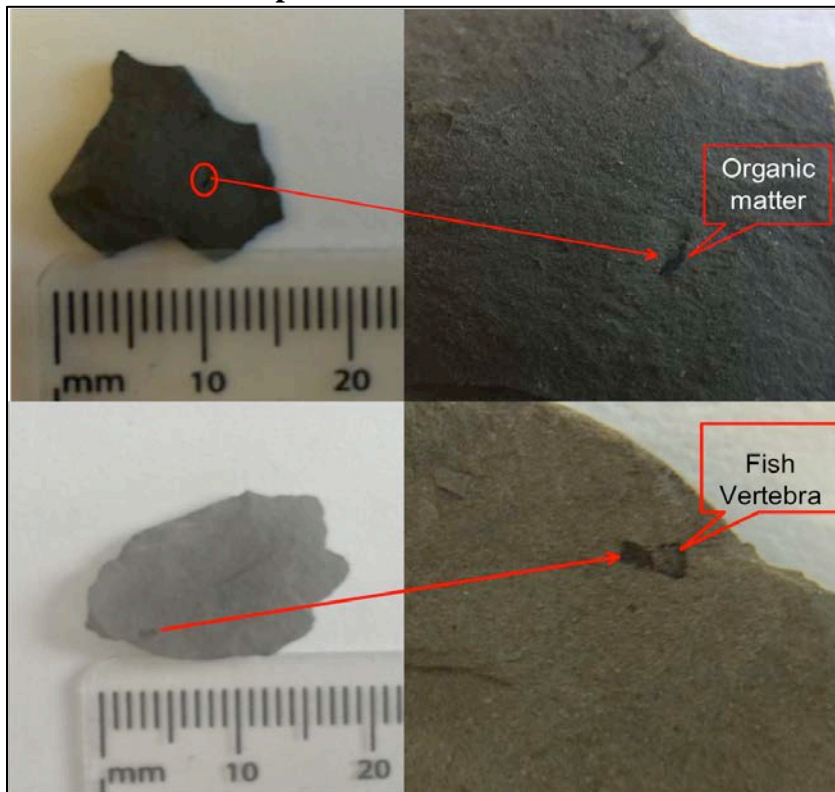


**Figure 19. Organic matter and fossil from point 5.**

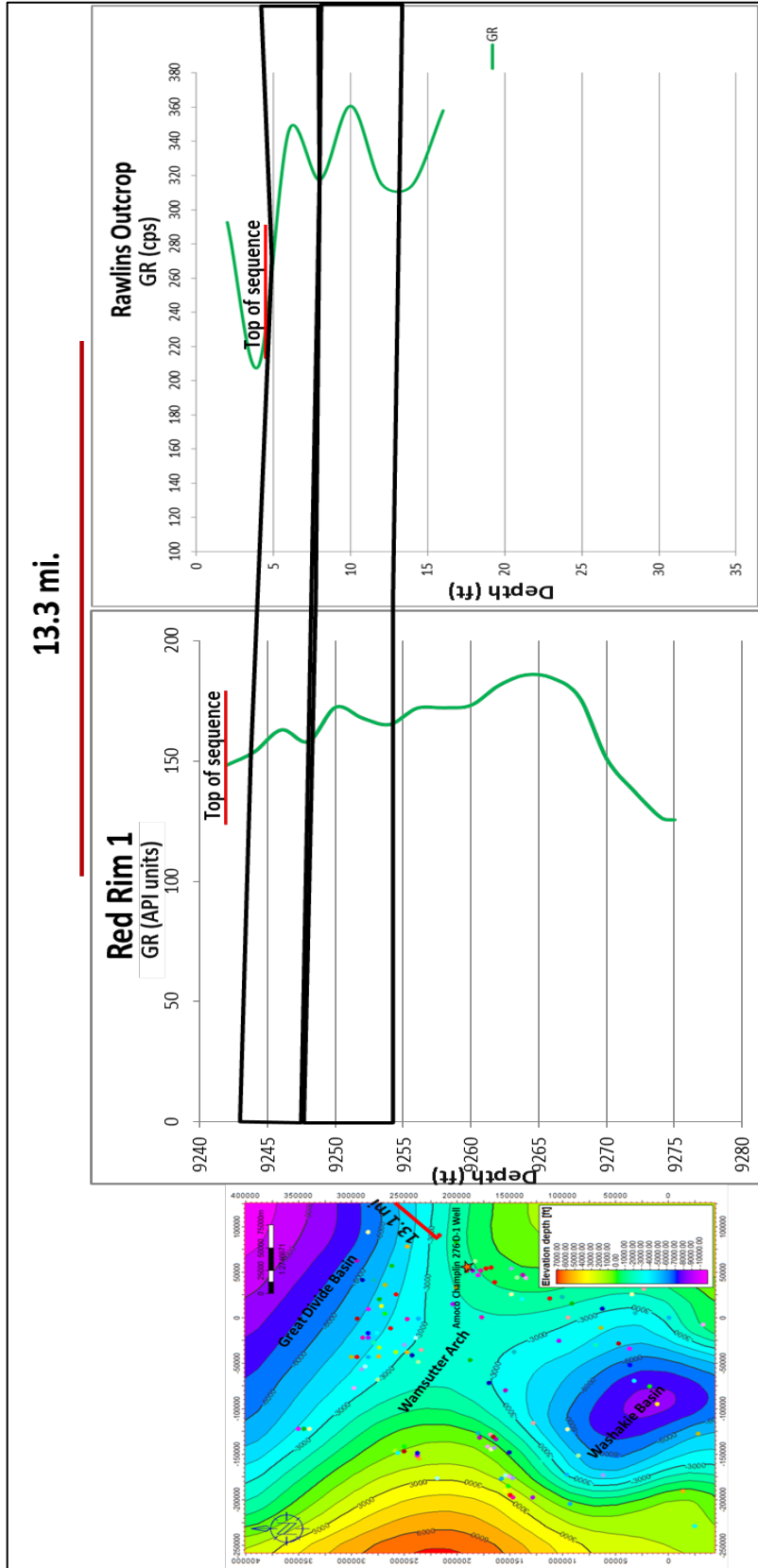


Figure 20. Possible correlation of the Rawlins Outcrop and Red Rim-1 well.

## Overpressure Analysis

The overpressure effect is caused by the thermal generation of gas in low permeability rocks. The Greater Green River Basin is a basin with low permeability rocks such as sandstones, coals and shales.

The overpressure effect starts when the oil cracks to gas and formation water turns to steam. The generation is much faster than the expulsion so the formation starts to become over-pressured (Surdam et al., 1995). By analyzing the change in transit time with the sonic log Law (1984) estimated the top of the overpressure regime in this area to be at 8000 to 10000ft. depth. Overpressure can be identified on the sonic log by a sudden increase in transit time (Figure 21) (Surdam et al., 1995). According to Law (1989), rocks subject to overpressure are generally producing gas, but in those areas where the Lewis Shale is above the overpressure zone towards the Wamsutter arch area it could be producing oil.

To identify prospective oil areas an overpressure analysis was performed on 9 wells across the basin from the deepest to the shallowest parts. Figure 22 shows the sonic log plotted versus depth for two wells. A blue line shows the general trend the log should follow. Towards the deeper part of the logs a sharp increase in transit time is evident as a “bump” on the sonic log and a different trend marked by the green line, which represents the top of the overpressure zone. The plots for the remaining 7 wells can be seen in Appendix 2.

Figure 23 is a cross section showing the top of the overpressure zone (green line) for seven wells in the eastern part of the basin close to the Wamsutter Arch. As

shown on the cross section, this surface is uneven and cuts across structural and stratigraphic boundaries below the middle and upper member of the Lewis Shale (upper light gray shales in the cross sections), but above the Asquith Marker (purple line). It is deeper in the deeper parts of the Washakie Basin.

For those wells located closer to the Wamsutter Arch the top of the overpressure is closer to the top of the Asquith Marker interval. This might mean that the interval is generating oil or condensate.



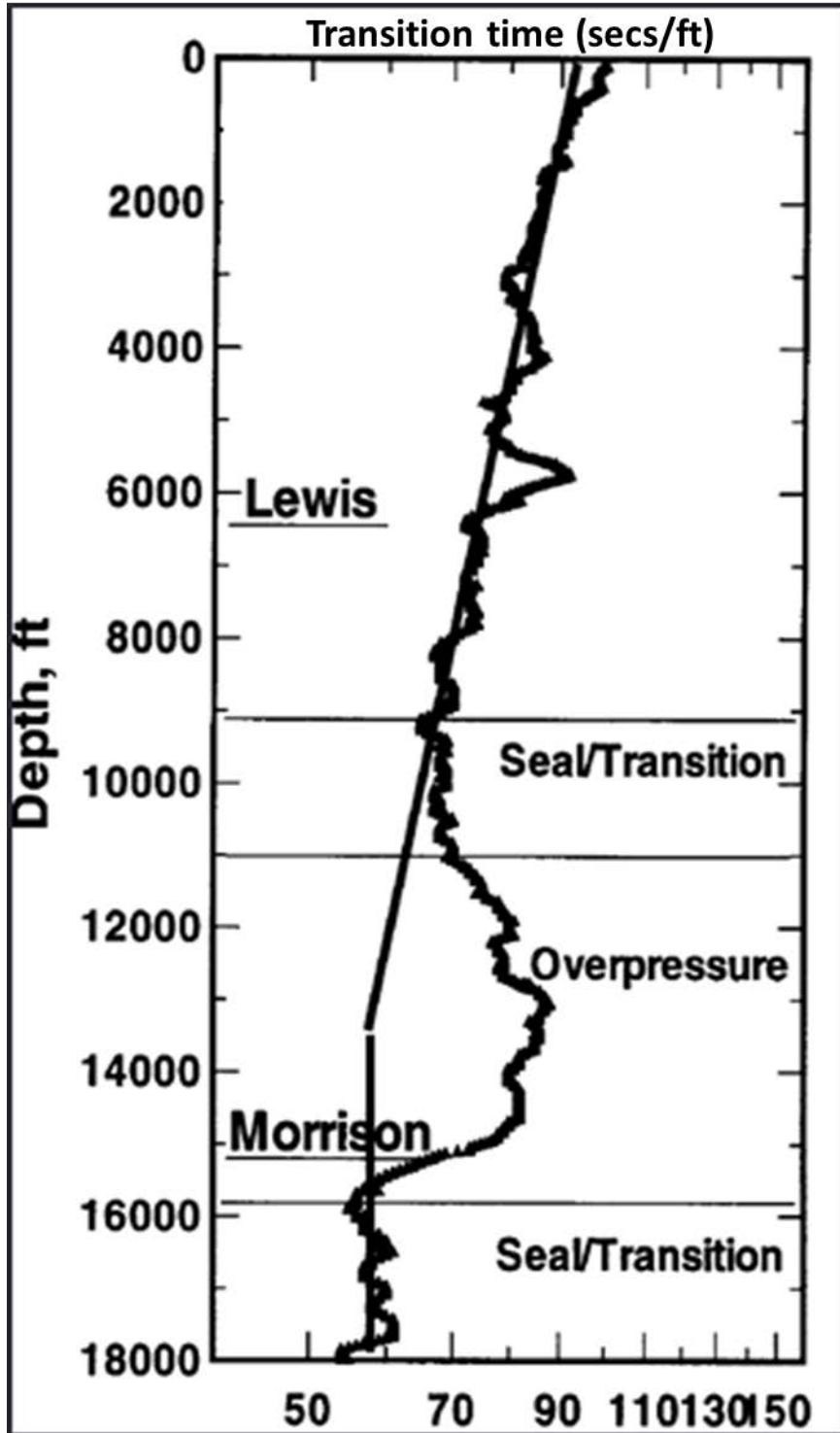
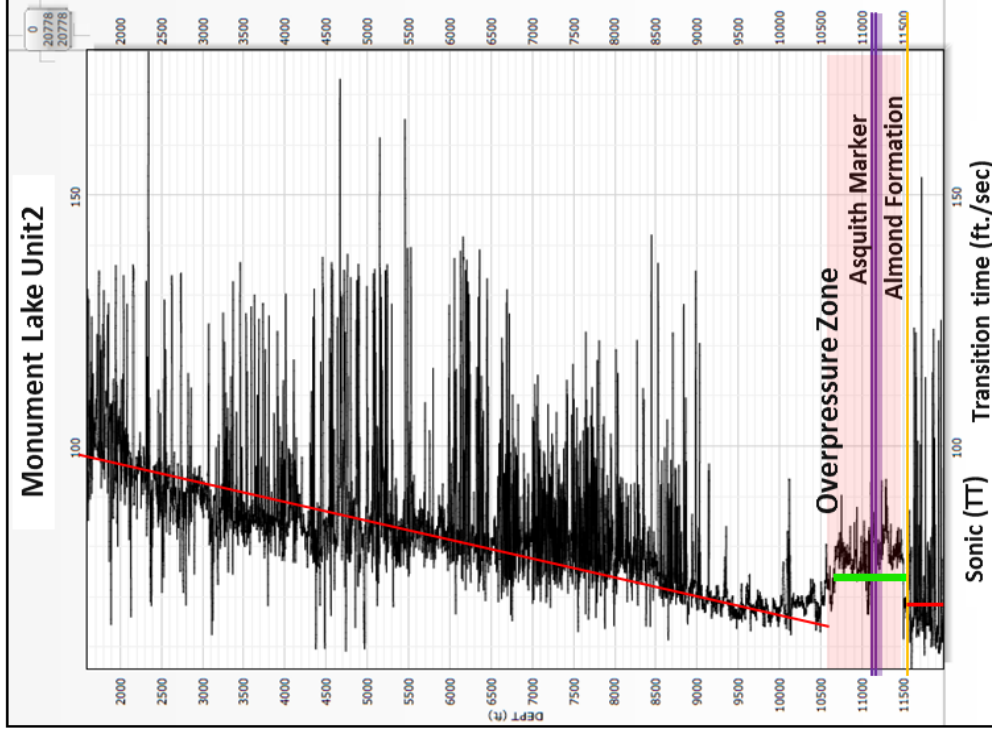
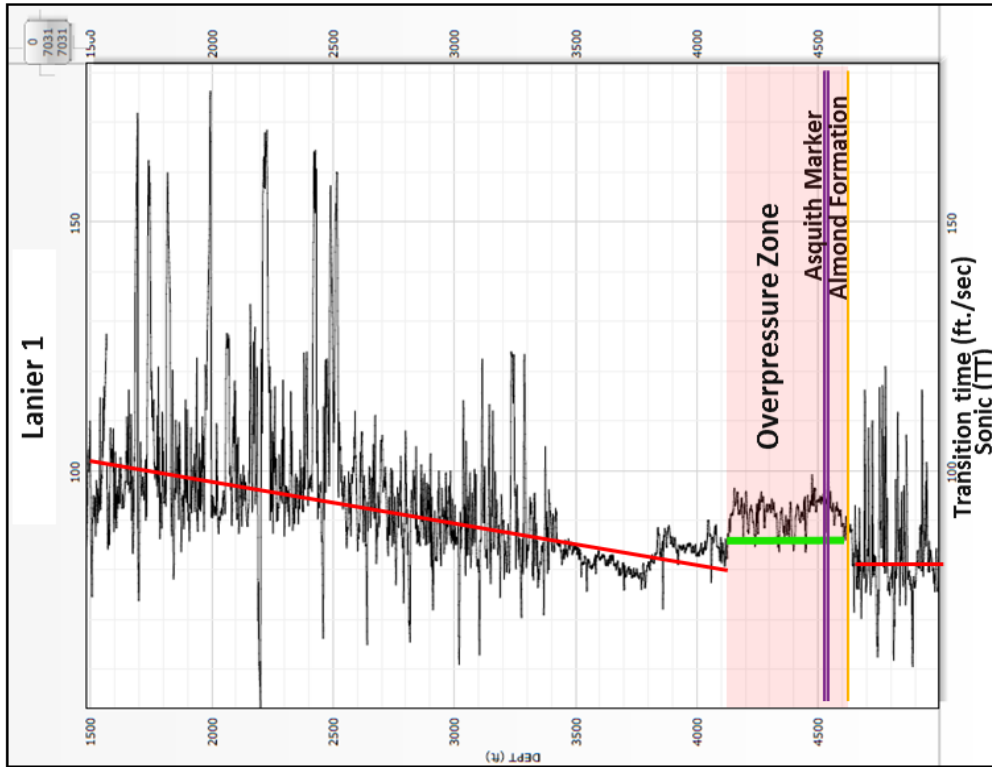


Figure 21. Plot of sonic log versus depth. The straight lines on the log represent the trend. The place where the line does not follow the trend is the top of the overpressure zone. This is the methodology proposed by Surdam (2005) to detect an overpressure zone.



**Figure 22. Overpressure analysis for two wells showing the change in the trend of the sonic log marked by the green line. The top of this green line represents the top of the overpressure zone**



## Mineralogy

### *XRD Analysis*

X- Ray diffraction analyses (XRD) were conducted on two samples from the Asquith Marker in the Amoco Champlin 276 D1 well in order to determine the mineralogical composition of the samples. Figure 24 shows the results obtained from these samples.

There is a high percentage of quartz, followed by the clay mineral illite. The second sample is located towards the bottom of the formation and shows a relatively high percentage of calcite. According to Wang and Gale (2009) calcite is classified as a ductile mineral, whereas quartz and dolomite are as brittle minerals. They use them to calculate the brittleness index shown on the following equation, but when the percentage of calcite is high, the rock is considered to be brittle (Slatt, personal communication).

$$Bi = \frac{(Dol + Qz + Ca)}{Qz + Dol + Ca + Cly + TOC}$$

For this formula the higher the Brittleness Index (BI) result the more brittle the rock is. In the present case, samples had values of 0.36 for the shallower sample and 0.52 for the deeper one. Values of 0.52 are considered to be within the brittle range whereas value 0.36 is considered to be more ductile.

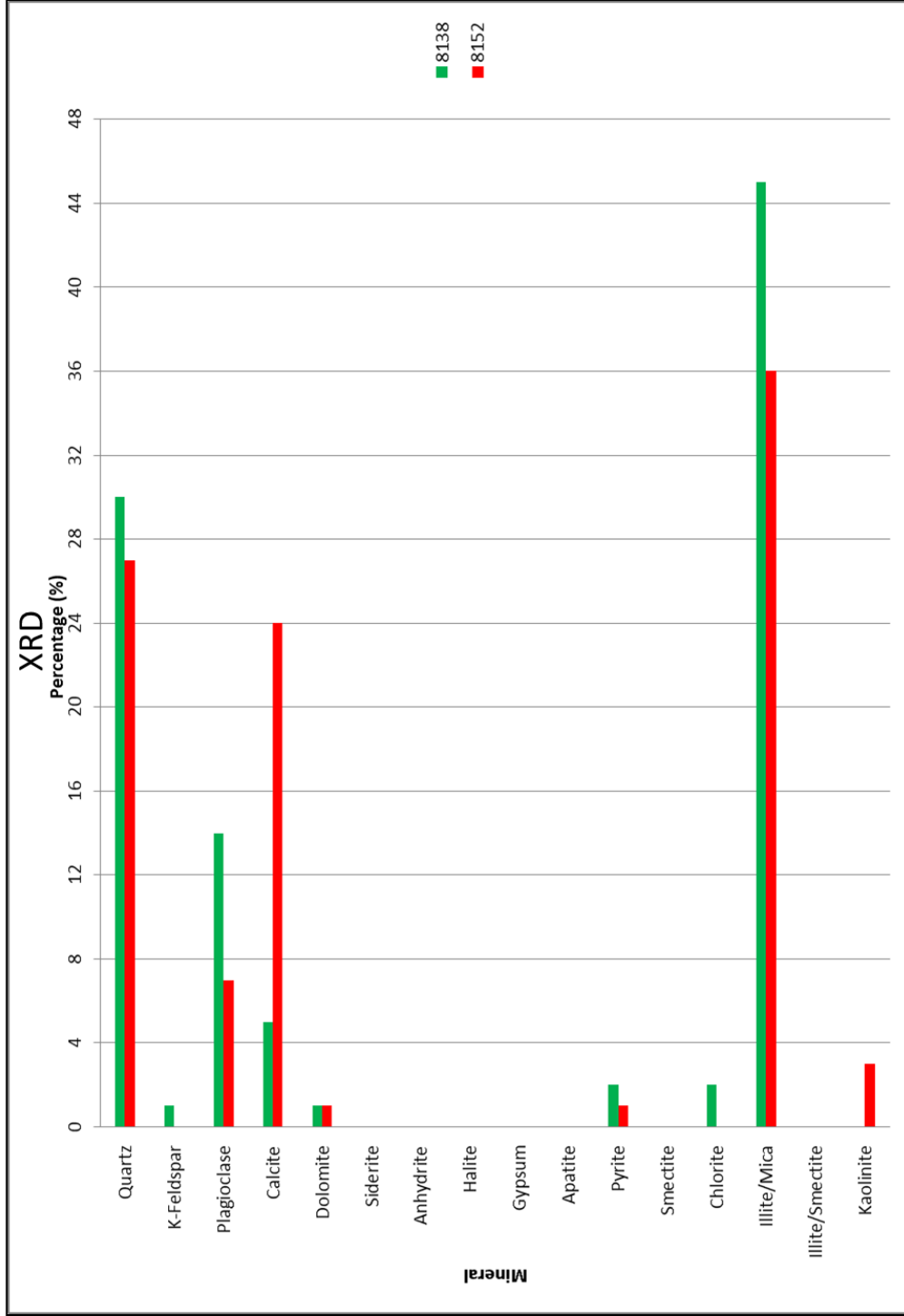


**Figure 24. X-ray diffraction analyses for two samples from the Amoco Champlin D-1 well at 8138ft. and 8152ft. depth.**

## Chapter 4: Geochemical Analyses

### Source Rock Quality

#### *TOC screening*

Organic matter has many different biological origins including plants, phytoplankton, zooplankton, and algae (Jarvie, 1991). Further information about the source of the organic matter will determine the type of kerogen present in the rock as well as the level of thermal maturity that the rock has at the present time (Jarvie, 1991). The organic carbon content in a rock sample is very small and it includes kerogen and bitumen (Peters and Cassa, 1994). Figure 25 shows a schematic of the proportion of organic carbon in sedimentary rocks.

Total organic carbon (TOC) measures the organic richness of a sedimentary rock making it a useful proxy to determine the potential of source rocks to generate hydrocarbons. LECO TOC analysis is the first screening process used in the assessment of a source rock (Jarvie, 1991). After this, additional analyses (Rock-Eval, vitrinite reflectance) will determine the source potential of the rock.

TOC value is compound of the following components: carbon in the extractable organic matter (EOM), which is composed of the carbon contained in the oil and gas already formed and is derived from the products of thermal cracking of kerogen that is later incorporated into biological markers. The second component of the TOC is the convertible carbon in the kerogen and the third component is the residual carbon fraction, which has no potential to generate hydrocarbons (Jarvie, 1991). The TOC value and TOC composition are very important in determining the potential of a source rock and the type of hydrocarbon the rock is more likely to produce.

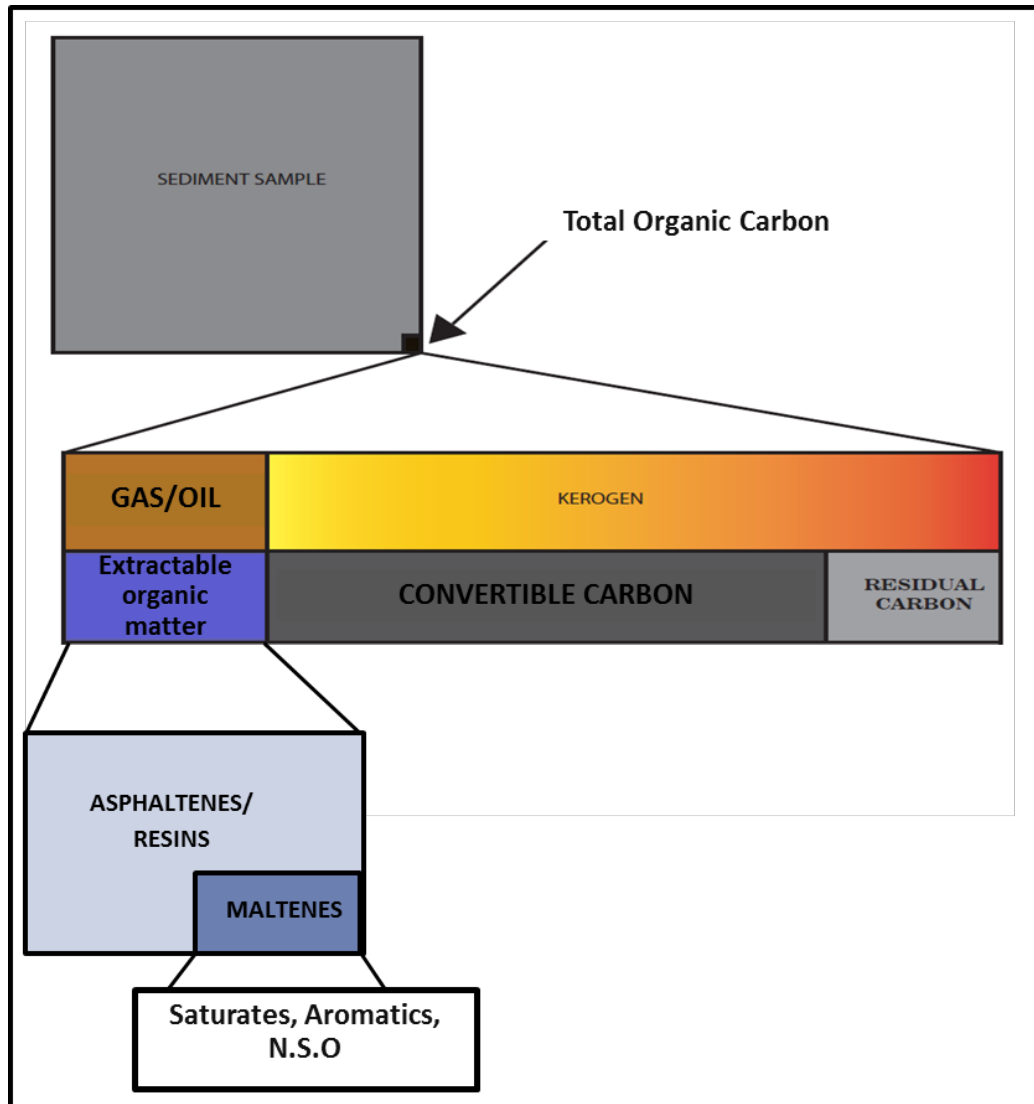


**Figure 25. Proportion of Organic Carbon in a rock sample and each one of its different constituents. Modified from Jarvie, (1991).**

Table 2 shows the interpretation of TOC content in sediments based on “early window maturity” (Jarvie, 1991).

Kerogen is a very complex structure formed when the organic matter is buried and goes through diagenesis. The type of kerogen varies with different types of organ-

ic matter present at the time of deposition; affecting the quality and quantity of the generated hydrocarbons (Jarvie, 1991).

In order to further determine the hydrocarbon potential of a rock, and integration of Rock-Eval, vitrinite reflectance, and biomarker analyses is imperative. For this study samples from other Lewis shales intervals were analyzed to contribute additional information to the database. A total of 29 samples from cuttings, cores and outcrop were from the Asquith Marker and the organic rich intervals from the Lewis Shale in the basin were collected for analysis. Only one well has core samples from the Asquith Marker, the remaining core samples are from other organic rich shales. All the cutting samples are from the Asquith Marker. Table 3 shows all the samples used to determine TOC in the study area as well as their potential to generate hydrocarbons based on Table 2.

**Table 2. TOC content in shales based on early oil window maturity (Jarvie, 1991).**

Generation Potential	TOC in Shales (wt.%)
Poor	0.0-0.5
Fair	0.5-1.0
Good	1.0-2.0
Very Good	2.0-5.0
Excellent	>5.0



**Table 3. List of the entire suite of samples including those that does not correspond to the Asquith Marker. It also shows their potential to generate hydrocarbons based on the parameters introduced by Jarvie, 1991.**

WELL	DEPTH	TOC	GENERATION POTENTIAL	FORMATION
Sample (2)	1	0.51	Fair	Asquith Marker
Sample (4)	2	0.53	Fair	Asquith Marker
Sample (6)	3	0.76	Fair	Asquith Marker
Sample (8)	4	1.04	Good	Asquith Marker
Sample (10)	5	0.68	Fair	Asquith Marker
Sample (12)	6	0.52	Fair	Asquith Marker
Sample (14)	7	0.72	Fair	Asquith Marker
Horseshoe Creek	4937	1.12	Good	Organic Rich Shale
Stage Stop unit 2	5390	1.13	Good	Asquith Marker
Stage Stop Unit 2	5410	1.64	Good	Asquith Marker
19 desert Springs	5946	0.70	Fair	Organic Rich Shale
Creston Unit 1	7482	1.39	Good	Organic rich Shale
Champlin 276 D-1	8138	3.89	Very Good	Asquith Marker
Champlin 276 D-1	8151	3.51	Very Good	Asquith Marker
Champlin 276 D-1	8152	3.69	Very Good	Asquith Marker
Champlin 276 D-1	8153	3.32	Very Good	Asquith Marker
Champlin 276 D-1	8154	2.02	Very Good	Asquith Marker
Champlin 276 E-1	8975	1.95	Good	Asquith Marker
Champlin 448	10570	1.30	Good	Asquith Marker
Chorney	11380	0.97	Fair	Asquith Marker
Chorney	11400	1.21	Good	Asquith Marker
2 monument Lake	11430	0.75	Fair	Organic rich Shale
2 monument lake	11447	1.00	Good	Organic rich Shale
2 monument lake	11467	0.91	Fair	Organic rich Shale
Amoco Bog	13330	0.84	Fair	Asquith Marker
Amoco Bog	13340	0.86	Fair	Asquith Marker
Champlin 446	14195	0.80	Fair	Organic Rich Shale
Champlin 446	14205	0.96	Fair	Organic rich Shale
Champlin 446	14224	0.86	Fair	Organic rich Shale

Jarvie (1991) established that even the leanest TOC rock can generate minor amounts of hydrocarbons as a result of thermal maturation. Figure 26 shows the samples from the Asquith Marker and their potential based on the classic interpretation of TOC content. This plot of TOC with depth (ft.) shows that the samples range from fair to very good potential to generate hydrocarbons. This variability in potential in the samples can be related to thermal maturity of the samples, TOC origin, TOC content, and weathering (Peters, 1986). Also, according to Jarvie et al., (2005) cutting samples can exhibit some caving from other formation causing a dilution effect. This dilution effect lowers the TOC values compared to the ones obtained from core samples and

affecting the other Rock-Eval parameters such as the S1, S2, S3, and S4 peaks. This also will affect other geochemical parameters as generation potential (based on Hydrogen Index) and thermal maturity. Jarvie et al., (2005) established that core samples had 2 to 2.5 times more TOC percentage than those measured from cuttings. Thus, it is possible that the values obtained for the cutting samples are actually higher than reported by the analysis. Samples listed as “sample 2, 4, 6, 8, 10, 12, and 14” are the samples obtained from the outcrop and all of them had fair TOC potential. Sample number 5 showed good potential and the highest outcrop gamma ray measurement. The outcrop was very weathered and the samples seemed wet and fractured, with some gypsum crystals. Low TOC in outcrop samples may be caused by oxidation of the organic matter in the rock.

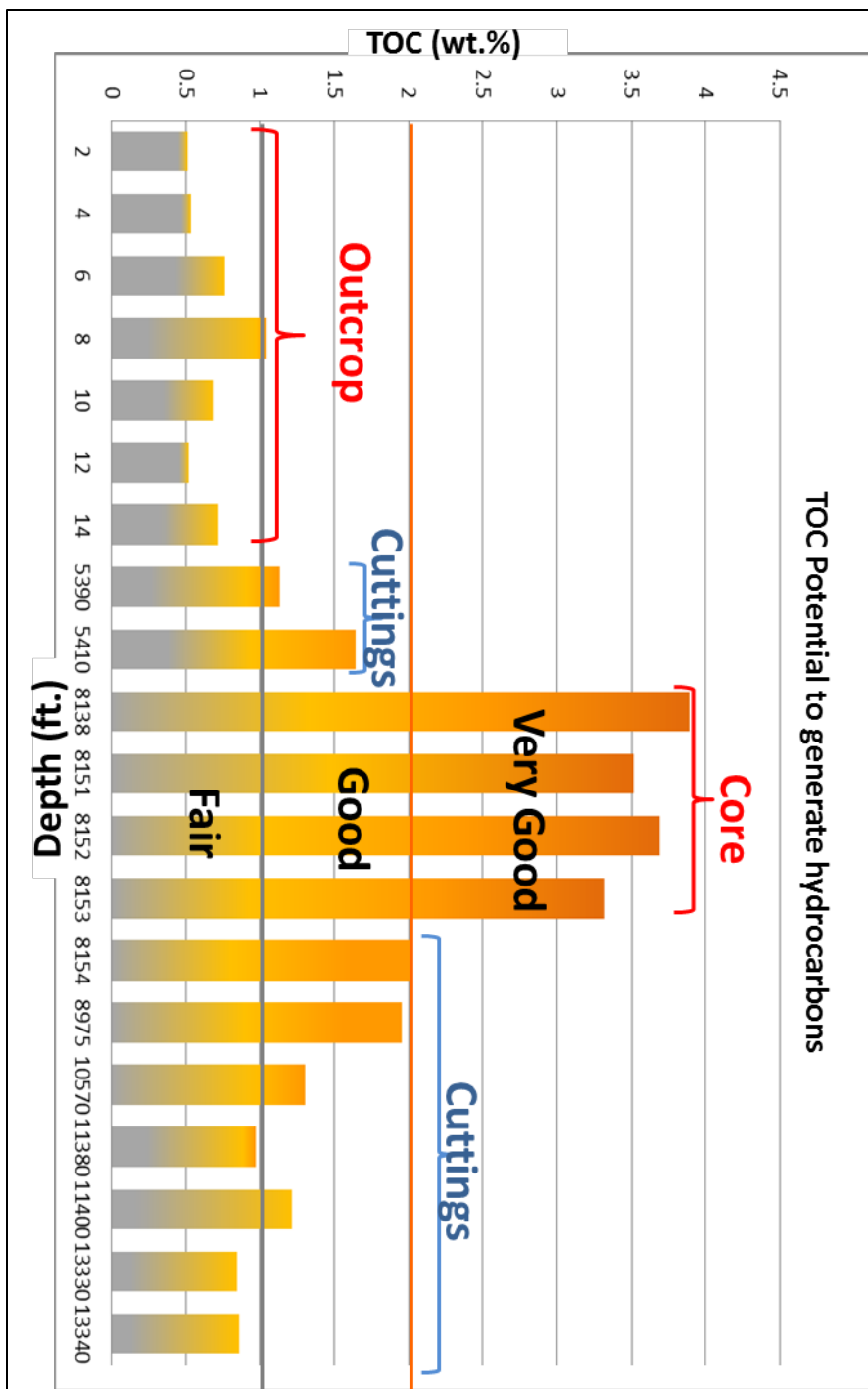


Figure 26. Plot of TOC vs. Depth based on the TOC potential shown in table 2. From LECO TOC analysis.

Figure 27 shows a cross section with present day TOC values obtained from the Asquith Marker samples. The cross section displays a slight decrease in TOC towards deeper areas. Several factors affect TOC (e.g. changes in depositional environment, weathering, and maturity) (Jarvie, 2005). Present-day TOC does not indicate that the rock generated hydrocarbons or the amount of generated hydrocarbons. However lower present-day TOC; relative to original TOC can indicate that organic matter has been converted into hydrocarbons under optimal pressure and temperature (Jarvie, 1991).

Jarvie (2003) proposed the following formula to calculate the original TOC of the source Rock from the present day TOC value:

$$\text{TOC}_{\text{original}} = \text{TOC}_{\text{present}} / 0.64$$

This formula is used to calculate the original TOC of the source rock and determine the potential to generate oil that the source rock had at the time of deposition. For the analyzed samples, changes in TOC with depth might be associated with maturity of the rock. However, TOC calculated using the formula proposed by Jarvie (2003) shows that the original TOC was also low (Table 4).

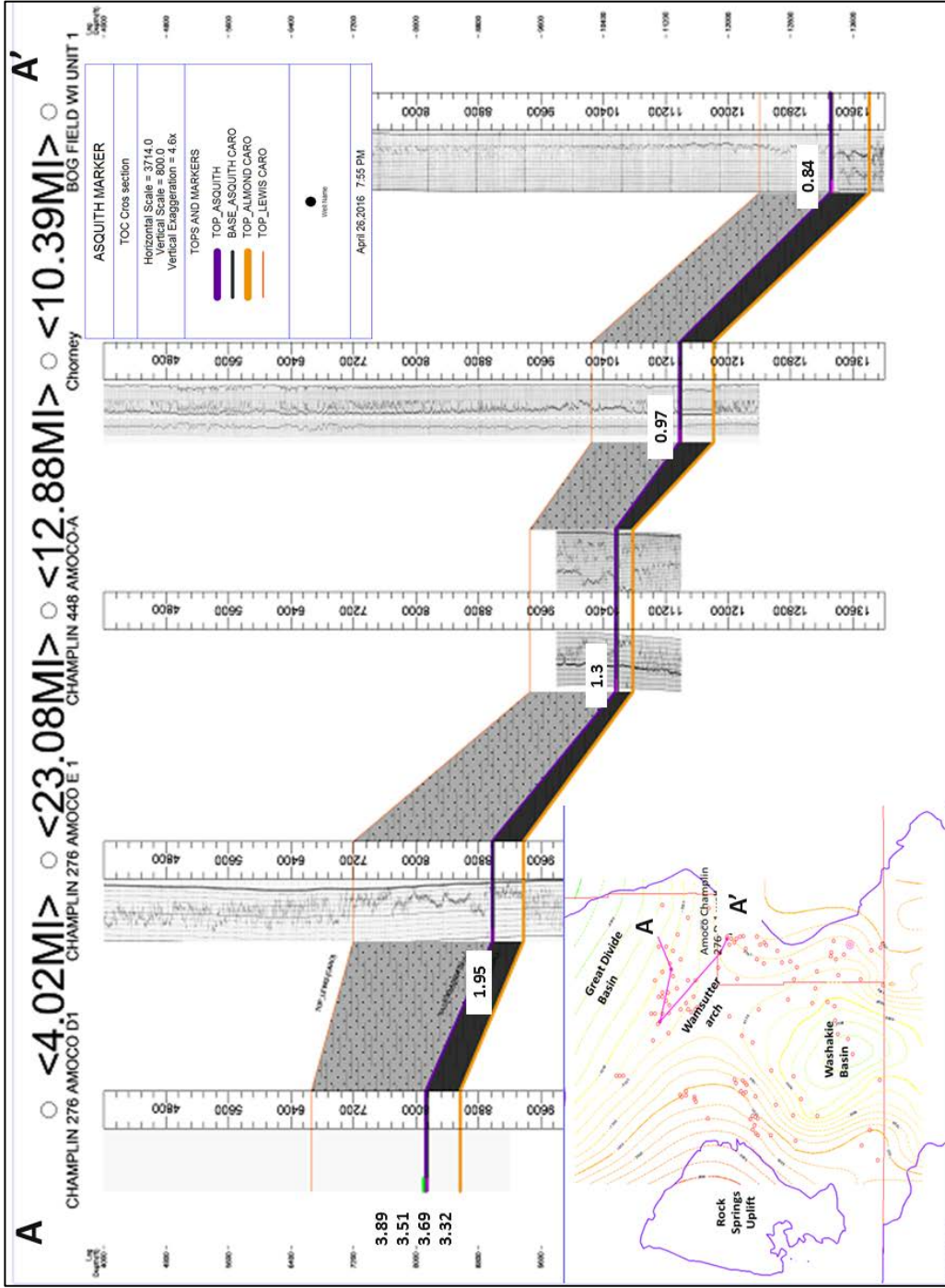


Figure 27. Cross section of the wells with TOC measurements showing a decrease in TOC content with depth.

**Table 4. TOC present and TOC original calculated with the formula introduced by Jarvie 2003.**

Sample	Depth	TOC <sub>present</sub>	TOC <sub>0</sub>
Outcrop Sample 1	2	0.51	0.80
Outcrop Sample 3	4	0.53	0.83
Outcrop Sample 4	6	0.76	1.19
Outcrop Sample 5	8	1.04	1.63
Outcrop Sample 6	10	0.68	1.06
Outcrop Sample 7	12	0.52	0.81
Outcrop Sample 8	14	0.72	1.13
Stage Stop Unit 2	5390	1.13	1.77
Stage Stop Unit 2	5410	1.64	2.56
Champlin 276 D-1	8138	3.89	6.08
Champlin 276 D-1	8151	3.51	5.48
Champlin 276 D-1	8152	3.69	5.77
Champlin 276 D-1	8153	3.32	5.19
Champlin 276 D-1	8154	2.02	3.16
Champlin 276 E-1	8975	1.95	3.05
Champlin 448	10570	1.3	2.03
Chorney	11380	0.97	1.52
Chorney	11400	1.21	1.89
Amoco Bog	13330	0.84	1.31
Amoco Bog	13340	0.86	1.34

The limited amount of data available of the Asquith Marker in some wells presented a challenge to determine its potential to generate hydrocarbons. However, the Asquith Marker potential to generate hydrocarbons was calculated by determining the TOC from other organic-rich shales available, extrapolate the TOC value to the Asquith Marker in those wells and determine the potential based on that value. For this purpose, the gamma ray curve and the TOC points obtained from Pasternack (2005) in the Amoco Champlin 276 D-1 well were plotted trying to find a correlation between them (Figure 28). With the plot obtained, a correlation factor was established and the

function obtained was applied to the Creston Unit 1 and Monument Lake Unit 2 wells (Figure 29). The points of TOC obtained by direct measurement on the sample were also plotted in order to calibrate the curve and compare the results (Figure 29). TOC values for the Asquith Marker obtained from the TOC calculated curve for Creston Unit 1 well had a range between 1.5 and 2.5 wt. % (this range was obtained calculating the standard deviation of the curve and setting it as limits for the TOC calculated curve). The values for Monument Lake Unit 2 ranged from 2.5 and 4.4 wt. %. Table 2 indicates “good to very good” potential to generate hydrocarbons for both Creston Unit 1 and Monument Lake Unit 2 wells. The calculated curve can have some vertical as well as horizontal error since we are plotting the average values of TOC, the correlation coefficient is not 100%, and depth shifting can occur.

An additional method to obtain the TOC in a well is using the resistivity log, sonic log, and the gamma ray log. Passey et al., (1990) establishes a base line in a fine grained non source-rock interval. Then, organic rich intervals will be recognized by the separation between the curves and not parallelism (Passey et al., 1990).

Figure 30 shows Passey’s methodology applied to the Creston Unit 1 well. Pink curve represents the sonic log whereas dashed blue line is resistivity log. The TOC value obtained for the Asquith Marker is 1.54 wt. %. This is not considered a high TOC but it is within the values obtained from the curve calculated in Figure 29 and according to Table 2 it shows good potential to generate hydrocarbons.

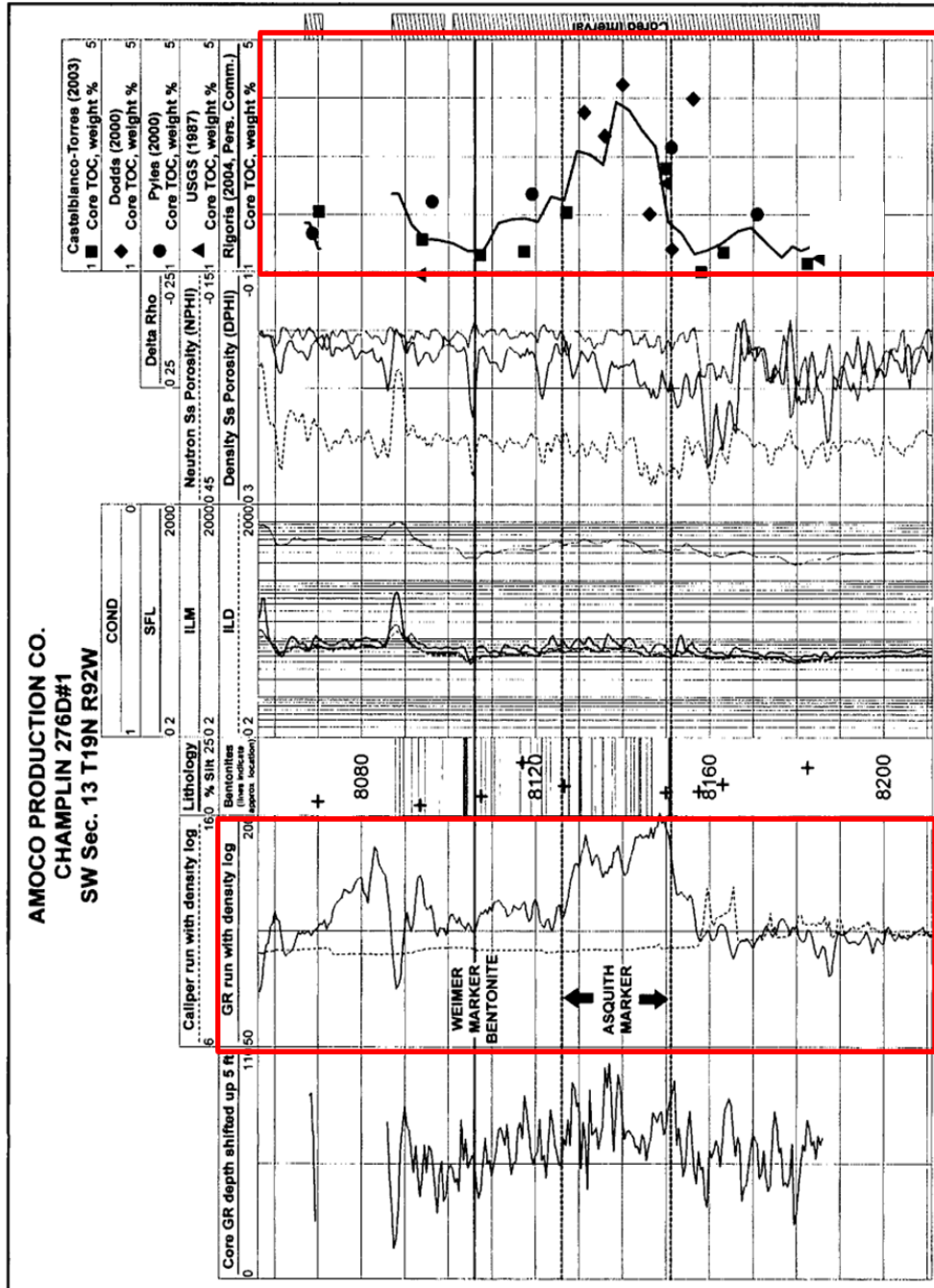


Figure 28. Figure showing the TOC curve and GR curve used to make a correlation and extrapolate to the other wells. The other points are measurements taken by others and analyzed by different labs. From Pasternack, 2005.



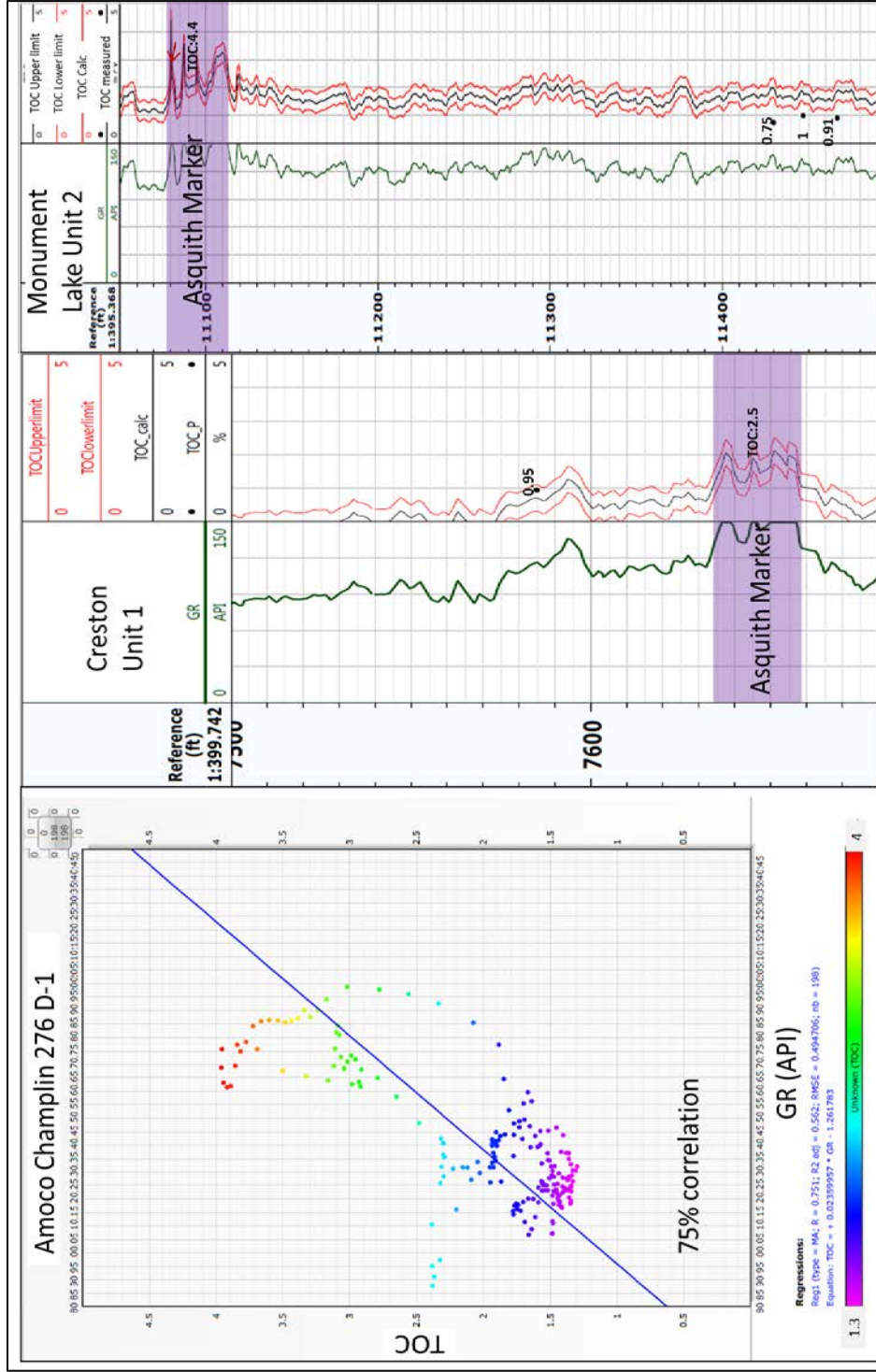


Figure 29. TOC Curves obtained from the correlation obtained by plotting the GR vs. TOC data from core from Pasternack (2005) on the left. Black dots represent the location of the samples taken for TOC analysis, used as a check point for the TOC curves obtained. The TOC points and the curve match in some points but not for all the wells.

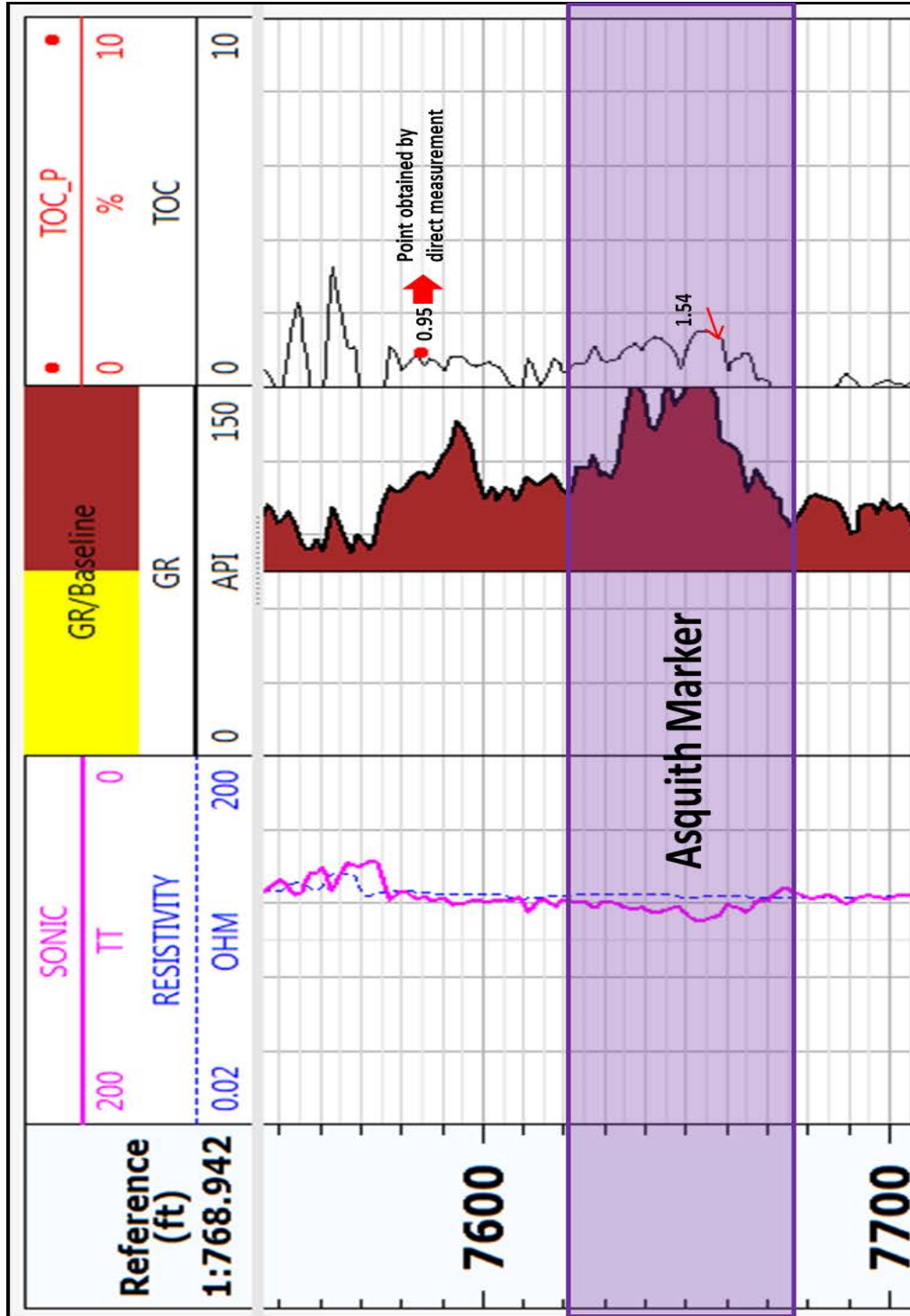


Figure 30. TOC curve (black line on the right) obtained using the methodology proposed by Passey et al., (1990). The red point represents the TOC measured from core sample.

### *Rock-Eval Analysis*

This is usually the second analysis performed in source rocks to determine their potential, after TOC screening. It gives information about the maturity, type of kerogen, depositional environment, and possible contamination that the rock could have been subjected to (Peters, 1986). Pyrolysis is the heating of organic matter in an inert environment. Pulverized samples are gradually heated under an inert atmosphere (Peters, 1986). This allows the extractable organic compounds, or bitumen, to be released, after which the insoluble organic matter or kerogen begins to crack (Peters, 1986). With this method is given the quantity of organic compounds that can be released from a rock upon increase in maturity (Peters, 1986).

The temperature programmed pyrolysis generates four peaks, named S1, S2, S3 and S4. The first peak represents the free hydrocarbons in the rock; the second peak (S2) represents the hydrocarbons generated by pyrolytic degradation of the kerogen in the rock. The third peak (S3) represents the carbon dioxide generated during temperature programming up to 390°C from the kerogen before the release of the earliest inorganic carbon dioxide (Figure 31) (Peters, 1986). S4 peak corresponds to the residual organic carbon; it does not generate any kerogen. These parameters can be reflected in a pyrogram. The pyrogram is going to show the evolution of the organic matter from the sample with increasing temperature and time (x axis from left to right).

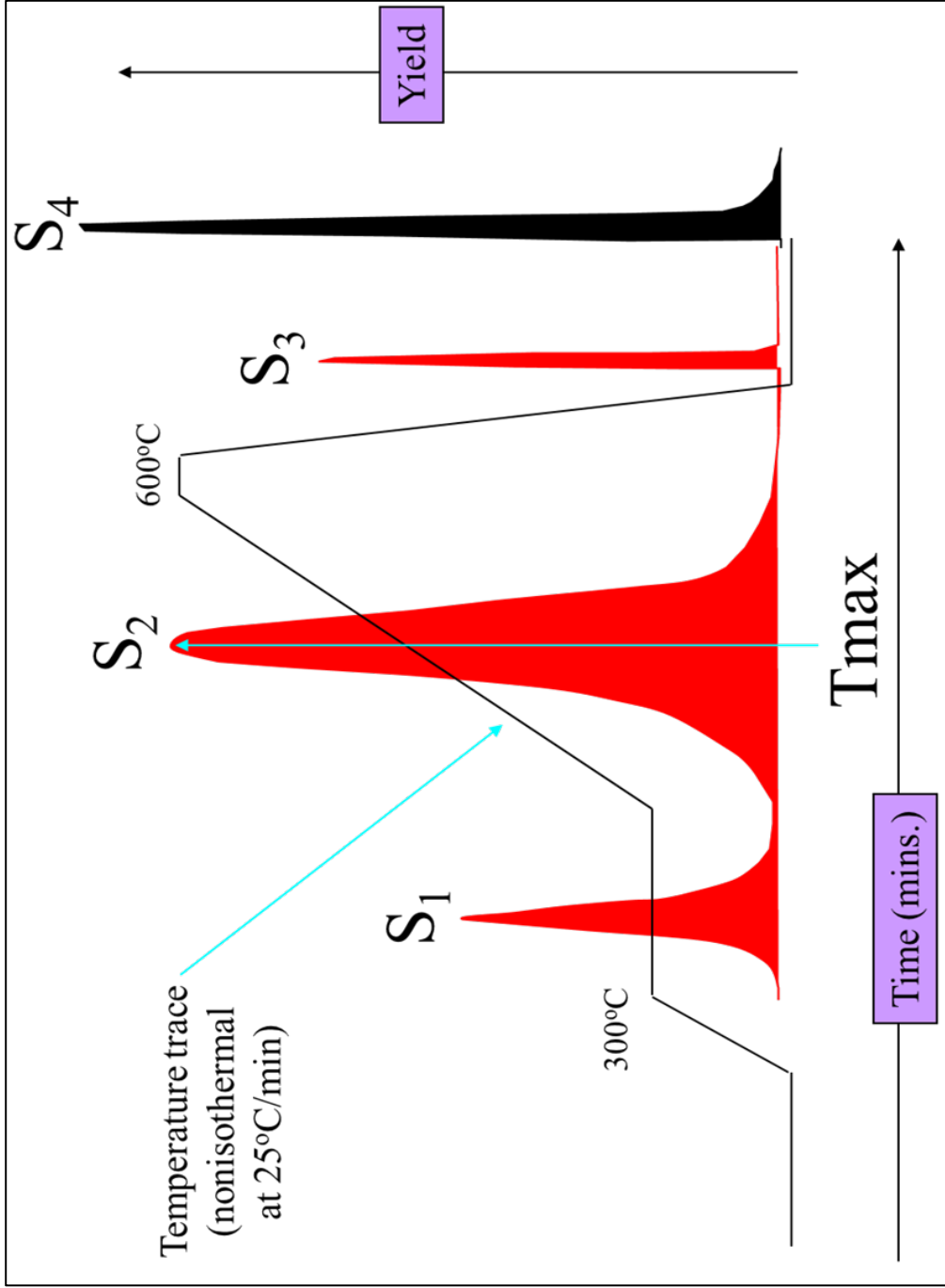


Figure 31. Typical pyrogram showing the three peaks (S1, S2 and S3) and the Tmax associated with the S2 peak. Modified from Hart and Steen, 2015.

Other parameters such as Tmax, Hydrogen Index (HI) and Oxygen Index (OI) are obtained from the pyrolysis data. Tmax corresponds to the temperature at which S2 maximizes. HI is the quantity of hydrocarbons that are pyrolyzable from S2 relative to the total organic carbon content (mg HC/g C<sub>org</sub>). OI corresponds to the quantity of organic oxygen in the kerogen relative to the TOC (mg CO<sub>2</sub>/g C<sub>org</sub>) (Peters, 1986). This data is also shown in the form of pyrograms (Peters, 1986). The pyrograms can inform us about possible unreliable data associated, for example, with a low Tmax value (Peters, 1986).

Table 5 shows the relationship between TOC data, S1, S2 peaks and the generation potential introduced by Peters (1986). Approximate 1g of sample was used for Rock-Eval analysis. Table 6 is the list of Asquith Marker's samples, depth, S1, S2, S3, TOC values from the Rock-Eval and their potential to generate hydrocarbons (Table 9).

**Table 5. Source rock potential associated with the S1 and S2 peaks. Modified from Peters (1986)**

<b>Quantity</b>	<b>TOC (wt.%)</b>	<b>S1 mg HC/g rock</b>	<b>S2 mg HC/g rock</b>
<b>Poor</b>	<b>0-0.5</b>	<b>0-0.5</b>	<b>0-2.5</b>
<b>Fair</b>	<b>0.5-1</b>	<b>0.5-1</b>	<b>2.5-5</b>
<b>Good</b>	<b>1-2</b>	<b>1-2</b>	<b>5-10</b>
<b>Very Good</b>	<b>2+</b>	<b>2+</b>	<b>10+</b>

**Table 6. List of samples from the Asquith Marker by depth with TOC values obtained from LECO TOC and S1, S2 and S3 values obtained from Rock-Eval. S1**

and S2 peaks are associated with their potential to generate hydrocarbons based on table 5.

Sample	Depth	TOC	S1 (mg HC/g Rock)	Potential S1	S2 (mg HC/g Rock)	Potential S2	S3 (mg HC/g Rock)
Outcrop Sample 1	2	0.51	0.02	Poor	0.12	Poor	0.44
Outcrop Sample 2	4	0.53	0.07	Poor	0.07	Poor	0.52
Outcrop Sample 3	6	0.76	0.07	Poor	0.16	Poor	0.66
Outcrop Sample 4	8	1.04	0.02	Poor	0.28	Poor	0.65
Outcrop Sample 5	10	0.68	0.04	Poor	0.14	Poor	0.5
Outcrop Sample 6	12	0.52	0.29	Poor	0.11	Poor	0.63
Outcrop Sample 8	14	0.72	0.04	Poor	0.26	Poor	0.59
Stage Stop Unit 2	5390	1.13	0.2	Poor	1.36	Poor	0.67
Stage Stop Unit 2	5410	1.64	1.57	Good	4.81	Fair	0.54
Champlin 276 D-1	8138	3.89	1.7	Good	18.02	Very good	0.43
Champlin 276 D-1	8151	3.51	1.52	Good	16.56	Very good	0.5
Champlin 276 D-1	8152	3.69	1.78	Good	19.2	Very good	0.56
Champlin 276 D-1	8153	3.32	1.1	Good	14.05	Very good	0.45
Champlin 276 D-1	8154	2.02	0.54	Fair	5.18	Good	0.33
Champlin 276 E-1	8975	1.95	0.2	Poor	2.56	Fair	0.37
Champlin 448	10570	1.3	0.27	Poor	1.46	Poor	0.34
Chorney	11380	0.97	0.28	Poor	0.85	Poor	0.26
Chorney	11400	1.21	0.45	Poor	1.4	Poor	0.29
Amoco Bog	13330	0.84	0.29	Poor	0.66	Poor	0.29
Amoco Bog	13340	0.86	0.3	Poor	0.73	Poor	0.26

Rock-Eval has some pitfalls especially when analyzing small amounts of samples. These include contamination at the time of sampling, weathering, and low TOC (Peters, 1986). For example, outcrop samples usually show low S1, S2 and high S3 peaks and values due to weathering. S1 peak can be minimized due to the evaporation of the lighter hydrocarbons, and water washing is also going to affect it by taking them away from the sample. S1, S2, S3 and S4 peaks can be enhanced by the oxidation of the organic matter produced by weathering or a prolonged storage in the case of cuttings (Peters, 1986). The S2 peak can be affected by several factors including maturity and it is also correlated with the type of organic matter and the tendency of having higher or lower HI and OI explained early on (Peters, 1986). As stated before, according to Jarvie (2005), cutting samples can have lower TOC values from cuttings than those obtained from core samples. Samples in this study that correspond to the Asquith Marker are mainly from cuttings and showed low values of TOC compared to the ones obtained from the only core samples available from the Asquith Marker. These low values in TOC will affect other parameters such as HI, OI, and S1, S2, S3 and S4 values. This can explain why samples in Table 6 showed poor to good potential to generate hydrocarbons and only samples from the cored well showed very good potential.

Figure 32 shows a pyrogram from the Amoco Bog Field well where the low TOC of the sample affected the S2 peak (Peters, 1986). According to Katz (1983) and Hartmand-Strout, (1987), the mineral matrix can affect the pyrolysis; some clay minerals (kaolinite, calcite, illite...) adsorb the pyrolyzate and show lower HI and S2 peaks (Hartman-Stroup, 1987). For cutting samples the heating or drying during stor-

age can reduce the S1 peak, since the hydrocarbon that is already generated in the rock can be lost by evaporation during the process. Also, oil-based or water-based mud and other additives can change the S1, S2 and S3 peaks (Peters, 1986).

In this present case, the wells were drilled with water-based mud, therefore is not affecting the S1, S2, S3 and S4 peaks. As shown on Figure 33, there is a small S1 and S2 peak, for Stage Stop Unit 2 the hydrocarbon potential based on the Hydrogen Index was to generate oil and gas. The small S1 and S2 peaks from the pyrogram could be due to the handling of the cutting samples and the length of time in which they were stored. Part of the hydrocarbons may have evaporated from the sample and the S1 peak might have been affected. Figure 34 is the pyrogram resulting from one of the core samples obtained from the Amoco Champlin 276 D1 well. It shows a high S2 peak and the Tmax was easy to determine in this case thanks to the high S2. The other pyrograms for the remaining samples are shown in Appendix 3.



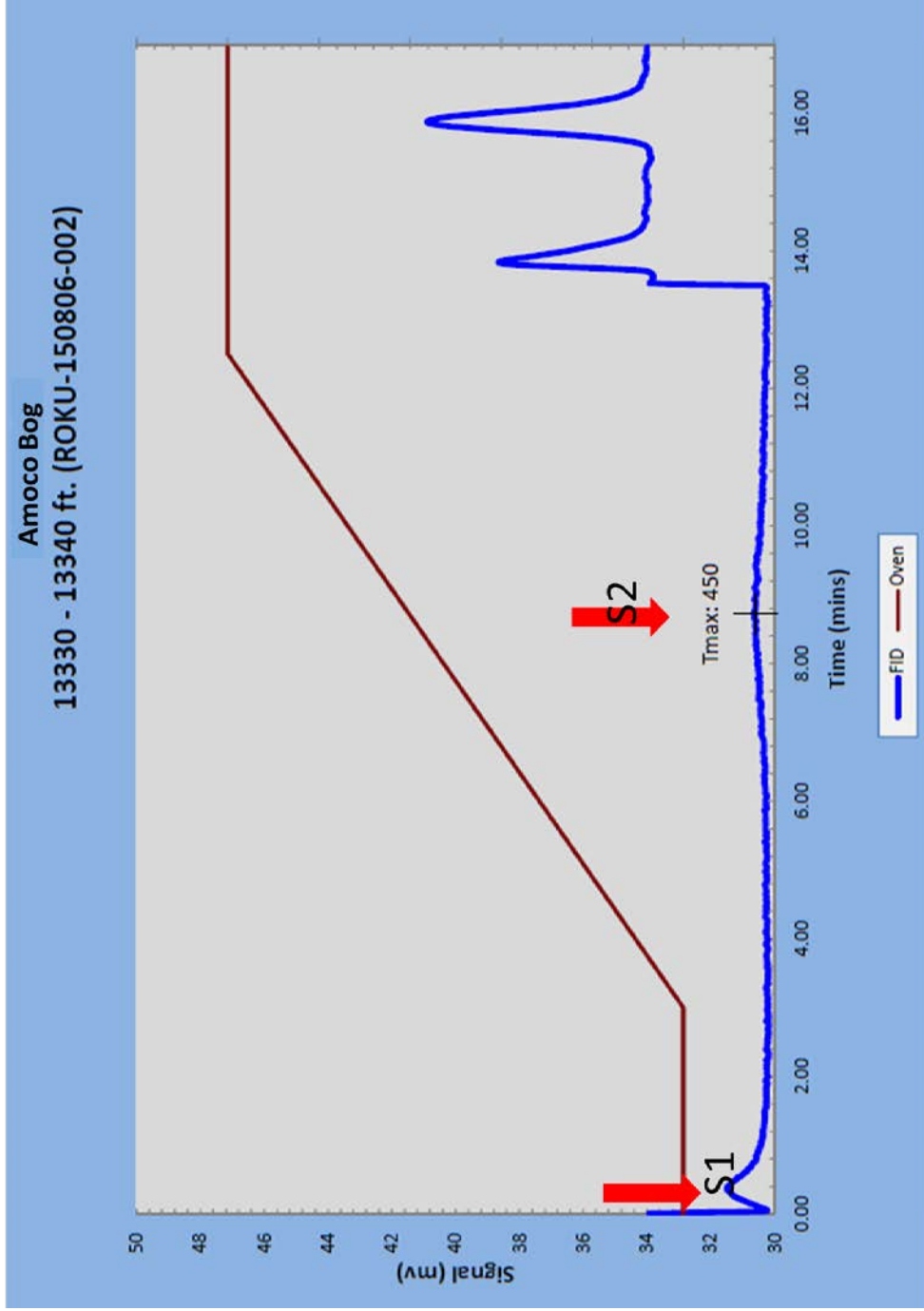
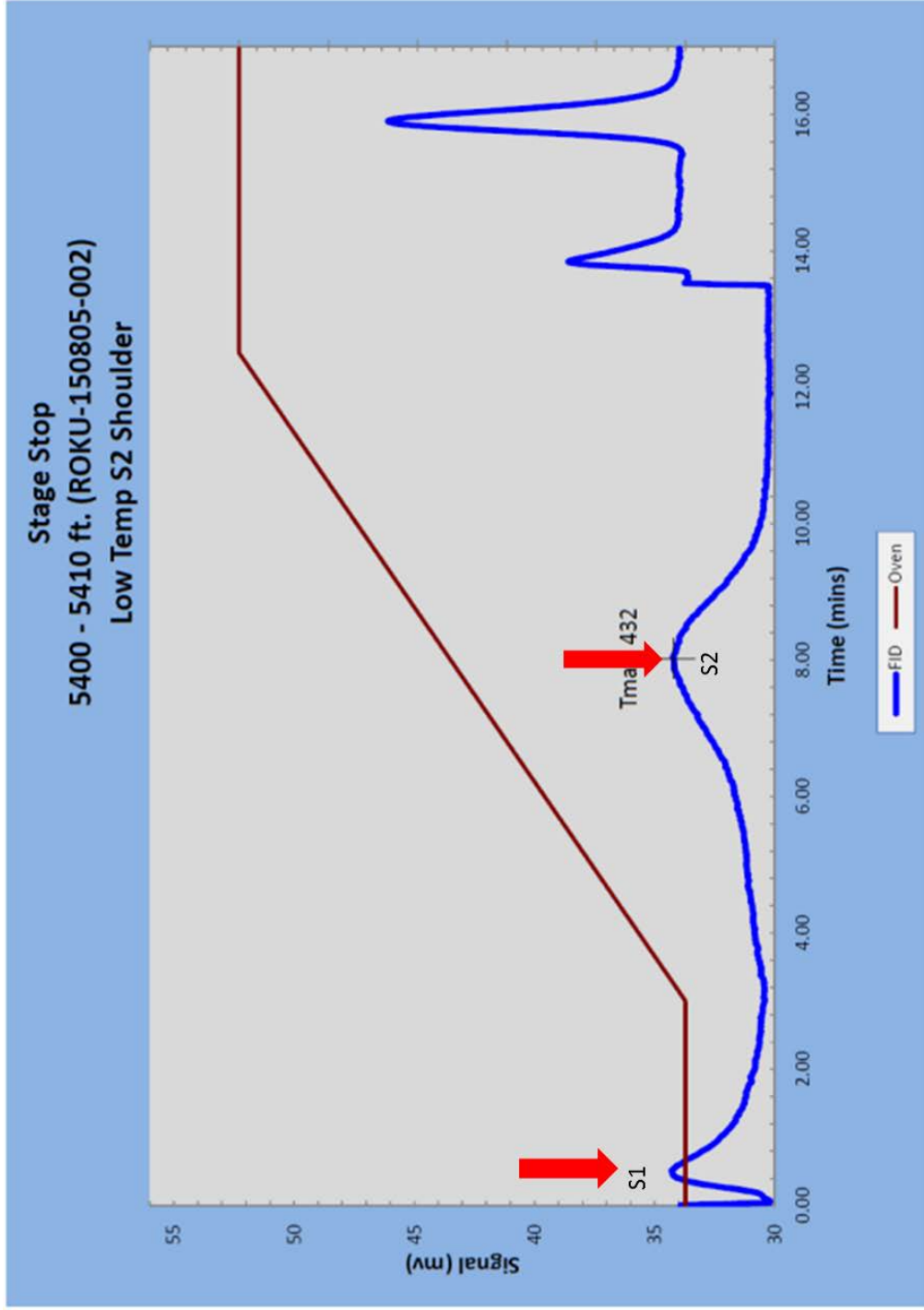
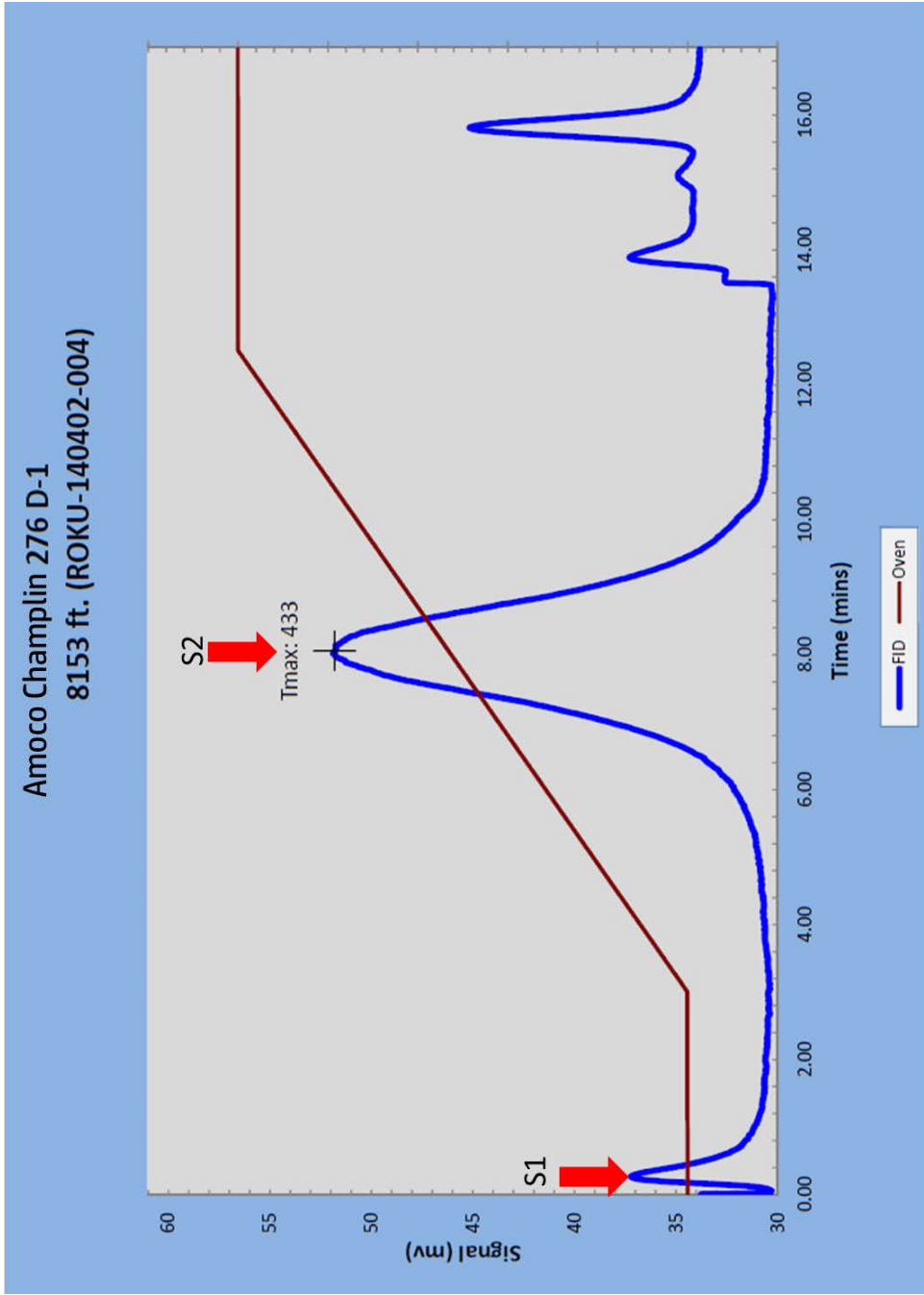


Figure 32. Pyrogram from Amoco Bog Field well. This is one of the wells with a low S2 peak, which makes the Tmax difficult to determine.



**Figure 33. Pyrogram from Stage Stop Unit 2 well. There is a small S1 and S2 peak.**



**Figure 34. Pyrogram from Amoco Champlin 276 D-1 Well. It shows a high S2 peak earning a high potential to generate hydrocarbons. This is one of the samples obtained from core that was not affected by caving or handling as was the case of the cutting samples.**

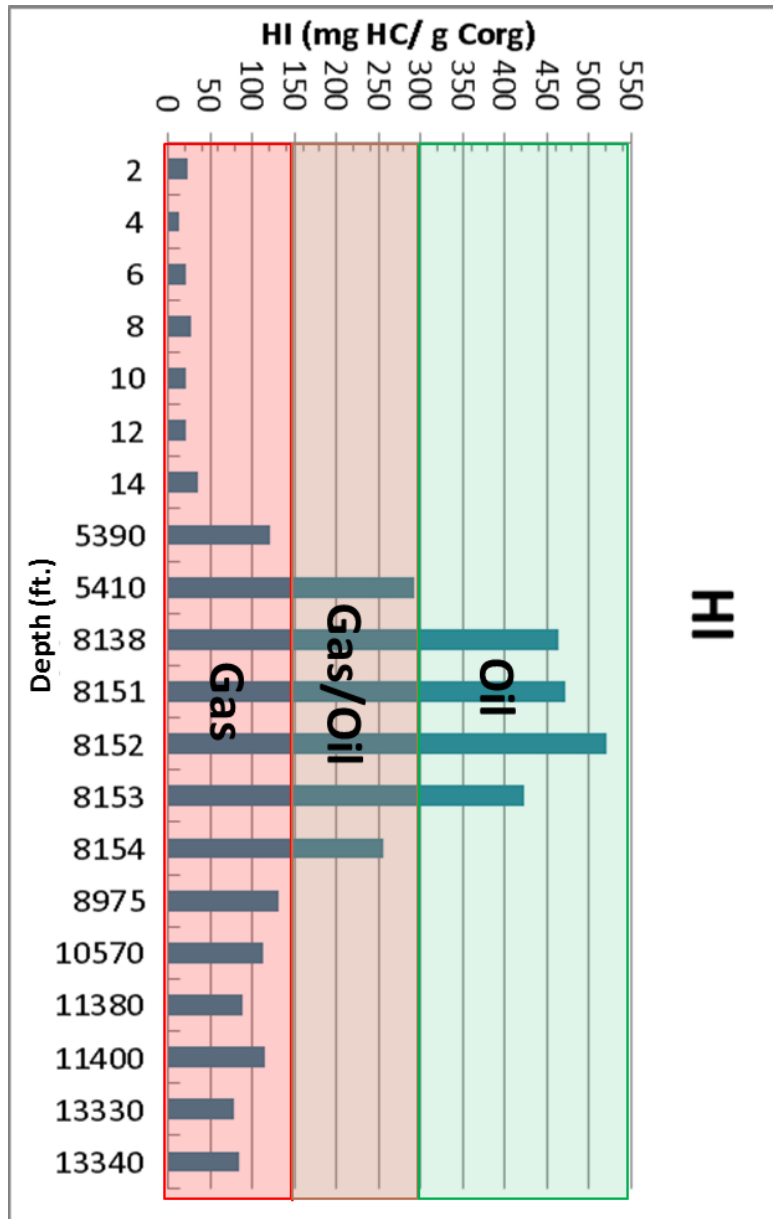
Some of the samples had questionable Tmax. S2 values less than 0.2 mg HC/ g rock are not reliable and should not be used (Peters, 1986). These samples correspond to all the outcrop samples except for outcrop sample number 4.

Figure 35 shows the potential to generate oil, gas or mixed based on HI (Peters, 1986). Samples taken from the Asquith Marker and their potential to generate hydrocarbons were evaluated according to Peters' parameters (1986) (Table 7). The first 7 samples are from the outcrop. These all have poor potential to generate hydrocarbons since they were subject to weathering as explained earlier from the effects of weathering in Rock-Eval analysis. One of the Stage Stop samples showed good potential to generate hydrocarbons (oil and gas).

The other samples corresponding to cutting samples showed fair potential to generate hydrocarbons. As explained before, cutting samples can be affected by oxidation during the handling and storage and have caving from other shales during drilling (Jarvie, 2005).

**Table 7. Type of hydrocarbon generated based on HI and S2/S3 values from the pyrolysis. Modified from Peters (1986)**

Type	HI (mg HC/g Corg)
Gas	0-150
Gas and Oil	150-300
Oil	300+



**Figure 35. Plot of Hydrogen Index (HI) vs. Depth and the type of hydrocarbon it can generate.**

In Table 8 there are some samples from other shales within the Lewis Shale. All of them had low TOC values. Based on the HI values indicate poor to fair potential to generate gas. According to Table 8 higher hydrogen Index values indicate more potential to generate oil (Peters, 1986).

**Table 8. Samples from the Organic rich facies of the Lewis Shale.**

Well	Depth (ft.)	TOC	S1 (mg HC/g Rock)	S2 (mg HC/g Rock)	S3 (mg CO <sub>2</sub> /g Rock)	HI	Type of HC
Horseshoe Creek	4937	1.12	0.25	1.28	0.14	114.3	Gas
19 desert Springs	5946	0.7	0.21	1.06	0.2	152.3	Oil and Gas
Creston Unit 1	7482	1.39	0.57	3.6	0.28	259	Oil and Gas
2 monument Lake	11430	0.75	0.26	0.53	0.33	70.5	Gas
2 monument lake	11447	1	0.28	0.72	0.24	72	Gas
2 monument lake	11467	0.91	0.28	0.68	0.19	75	Gas
Champlin 446	14195	0.8	0.21	0.35	0.15	43.9	Gas
Champlin 446	14205	0.96	0.25	0.44	0.09	45.9	Gas
Champlin 446	14224	0.86	0.21	0.34	0.11	39.7	Gas

### *Kerogen Type*

Kerogen is a very complex mixture; it forms when the organic matter is buried and goes through diagenesis. The type of organic matter present at the time of deposition will define the type of kerogen formed in the rock (Jarvie, 1991). There are four types of kerogen determined by the hydrogen and oxygen content relative to the carbon content present in the sample that are the major constituents of a kerogen (Espitaliè et al., 1977). Type I has high hydrogen/carbon and low oxygen/carbon ratios, the organic material source for this type of kerogen is phytoplankton and zooplankton which is oil prone. Type II kerogen has a medium ratio of both hydrogen/carbon and oxygen/carbon ratios, and the organic material for this type is algae. This Type II kerogen is largely oil prone. Type III is the opposite of Type I with low hydrogen/carbon and high oxygen/carbon ratios; it originates from woody material and is mainly gas prone.

Figure 38 shows the diagram for the Amoco Champlin 276 D-1 well. Kerogen in this well is Type II (marine) which is oil prone. The axes of the diagram are S2 and TOC. The S2 peak obtained from the Rock-Eval represents the remaining hydrocarbon potential the sample has; it is measured in mg of HC/g of sample. With this diagram the petroleum potential for different sets of samples can be conducted establishing petroleum potential and sedimentary environments (Langford and Blanc-Valleron, 1990). This diagram eliminates the problems with the S3 from which the OI is obtained because it can be rendered in rocks with high carbonate content and also affects the Hydrogen Index. Hydrogen and Oxygen Index are related to maturity in a rock (Langford and Blanc-Valleron, 1990). The hydrogen content is proportional to the

hydrocarbons liberated (S2) and the oxygen present in the kerogen is proportional to the carbon dioxide liberated pyrolysis (S3) (Peters, 1986). Usually more mature samples plot towards the left corner of the diagram due to the low hydrogen and oxygen indexes. In the plot from Figure 36 samples are immature and the position is given by the type of kerogen present in the rock. The maturity of the samples was later confirmed by the pyrograms from the Rock-Eval and the biomarkers.



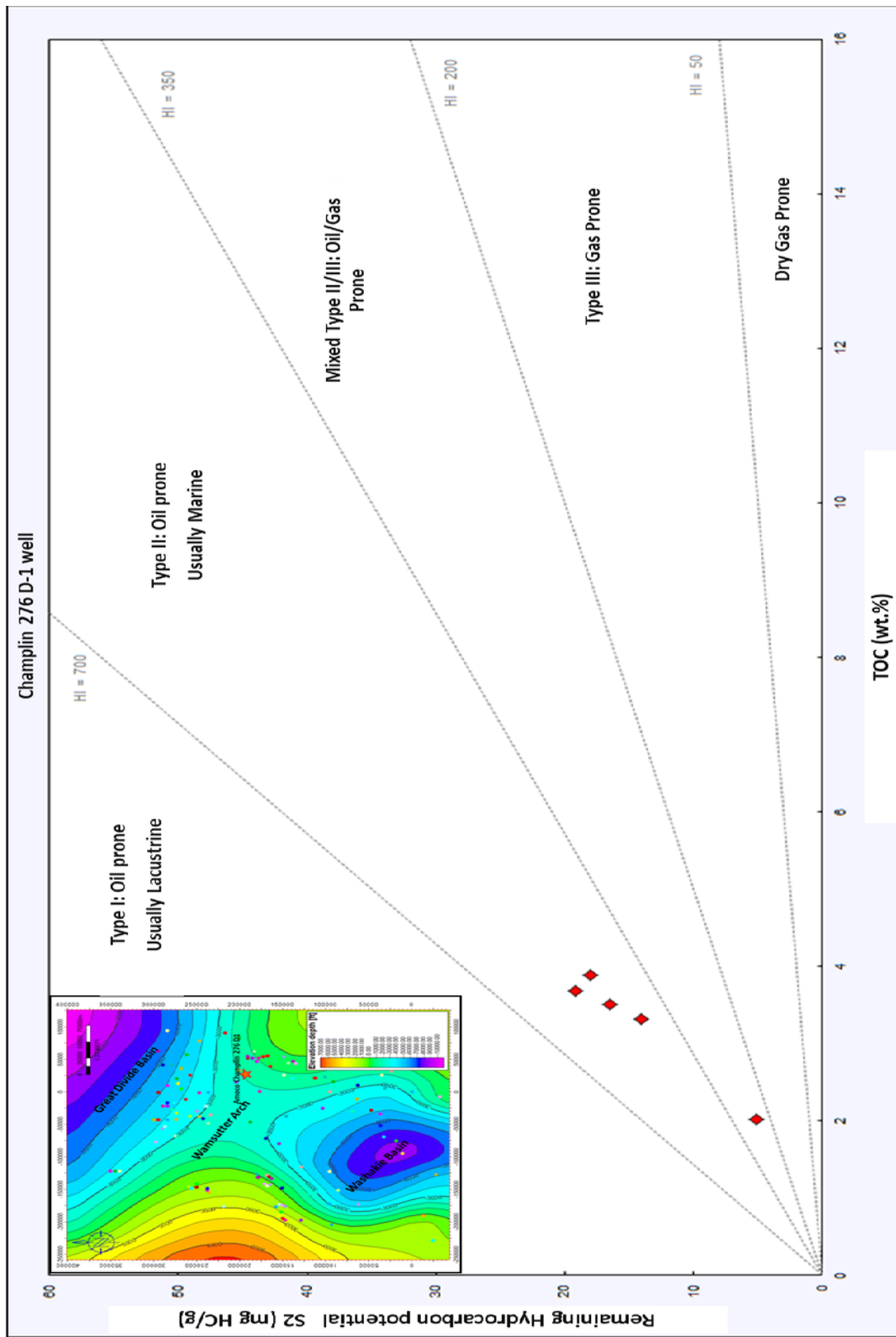


Figure 36. S2 vs. TOC diagram from the Amoco Champlin 276 D-1 well.

### *Thermal Maturity-Vitrinite reflectance.*

Vitrinite reflectance was historically used to determine coal rank but it can also be used to determine the thermal maturity of a rock. It is a measurement of the percentage of light reflected off the vitrinite maceral at 500x magnification in oil immersion (Cardott, 2012). Vitrinite reflectance ( $R_o$ ) is another way to measure the maturity of a rock. The percentage of reflected light will correspond to a certain thermal maturity or “how cooked” the rock is and what type of product is expected to be found there. (Figure 37) shows the reflectance percentage and the thermal maturity expected for each percentage of reflected light (McCarthy et al., 2011).

Vitrinite is a maceral that comes from woody material (Tissot and Welte, 1984); woody particles have to be small enough to be transported by water or by wind away from its continental source in order to find it in a marine environment, as is the case of the Asquith Marker. Also, similar appearance of vitrinite to bitumen makes it especially difficult to detect and measure using the microscope (Cardott, 2012).

One available sample from the Creston Unit 1 well was used to measure vitrinite reflectance. Vitrinite particles were considerably small in this sample making this measurement more a quantitative than a qualitative one (Cardott, personal communication). Vitrinite reflectance in Creston Unit 1 well at 7575ft. gave values between 0.72 and 1.02%, within the oil window (Figure 37). Three measurements at 7282ft. were between 0.70 and 0.92% (courtesy of Brian Cardott from the Oklahoma Geological Survey).

But other parameters such as the presence of the marine spore Tasmanites and its fluorescent color allowed us to have an approximation of the thermal maturity of

the sample (Figure 38) (Taylor et al., 1998). These algal spores are often used as a petrographic qualitative thermal maturity indicator based on the fluorescence. The color index goes from green to orange corresponding with low maturity to post mature. When the sample from Creston Unit 1 well was examined under fluorescent light at 500X magnification, Tasmanites fluorescence appeared weak orange. Taylor and others (1998) stated that Tasmanites loses its fluorescence when the sample has a vitrinite reflectance between 0.9-1.0% Ro. This indicates once again a thermal maturity within the oil window for this Creston Unit 1 sample and values of vitrinite reflectance close to ones measured within the vitrinite particles.

One sample from the outcrop was analyzed but all the vitrinite found was pitted. When a vitrinite particle is pitted, makes the calculated reflected light to be lower than it truly is, therefore the measurement is not reliable (Cardott personal communications).

Due to the low amount of data, values of vitrinite reflectance from the Mesaverde Group were obtained from Pawlewicz and Finn (2002). Figure 39 gathers this data together with the ones obtained by direct measurement from the Creston Unit 1 well overlaid by the structural map (grey lines). As shown on Figure 37 vitrinite reflectance increases with maturity. From Figure 39 it was also established for the Asquith Marker that vitrinite also increases with depth (grey lines). The value of vitrinite also increases with depth, since the more mature rocks are located towards the deeper parts of the basin (Washakie and Great Divide basin). In general the rocks are within the oil window or in the late oil window. This supports the idea that the more deeply buried the rocks are the more mature they are. The map has some uncertainty due to

the small amount of data. Also, oil generation boundaries shown on Figure 37 are not definitive and values can vary depending upon type of kerogen and organic matter (Tissot and Welte, 1984) but they give an approximation that combined with thickness, TOC and biomarkers can help define potential areas for oil development within the Asquith Marker.

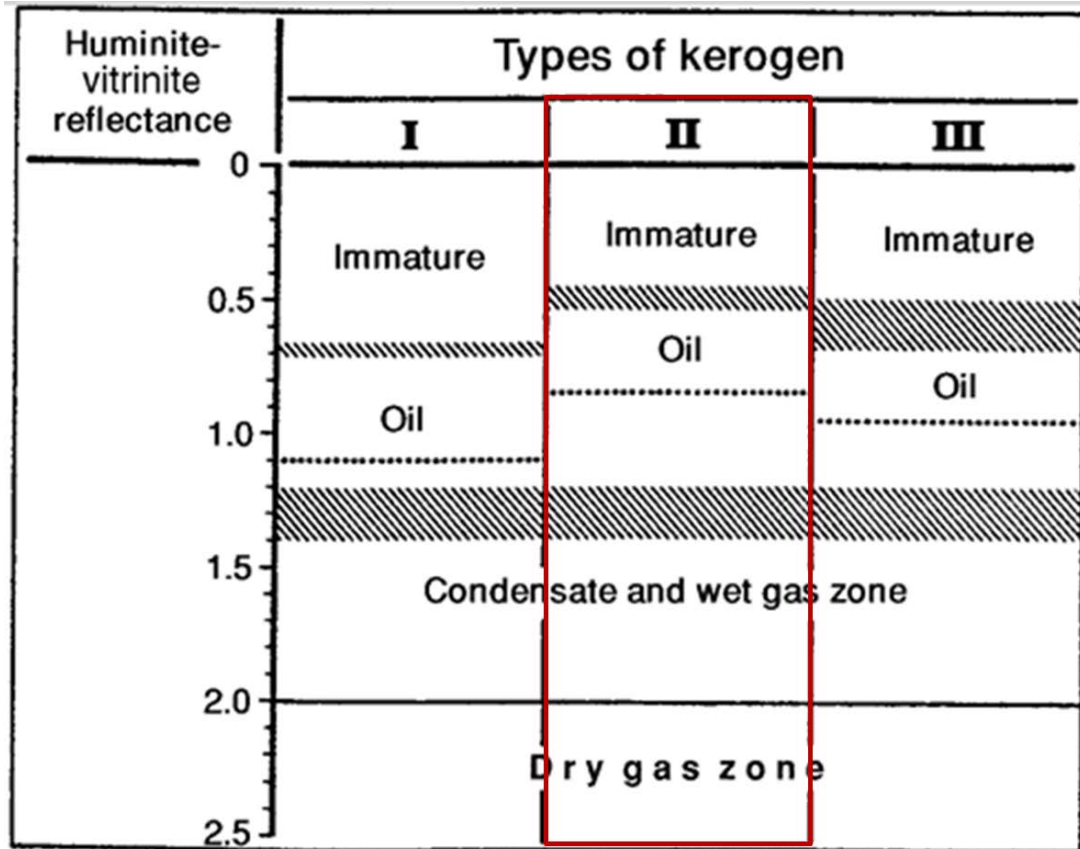
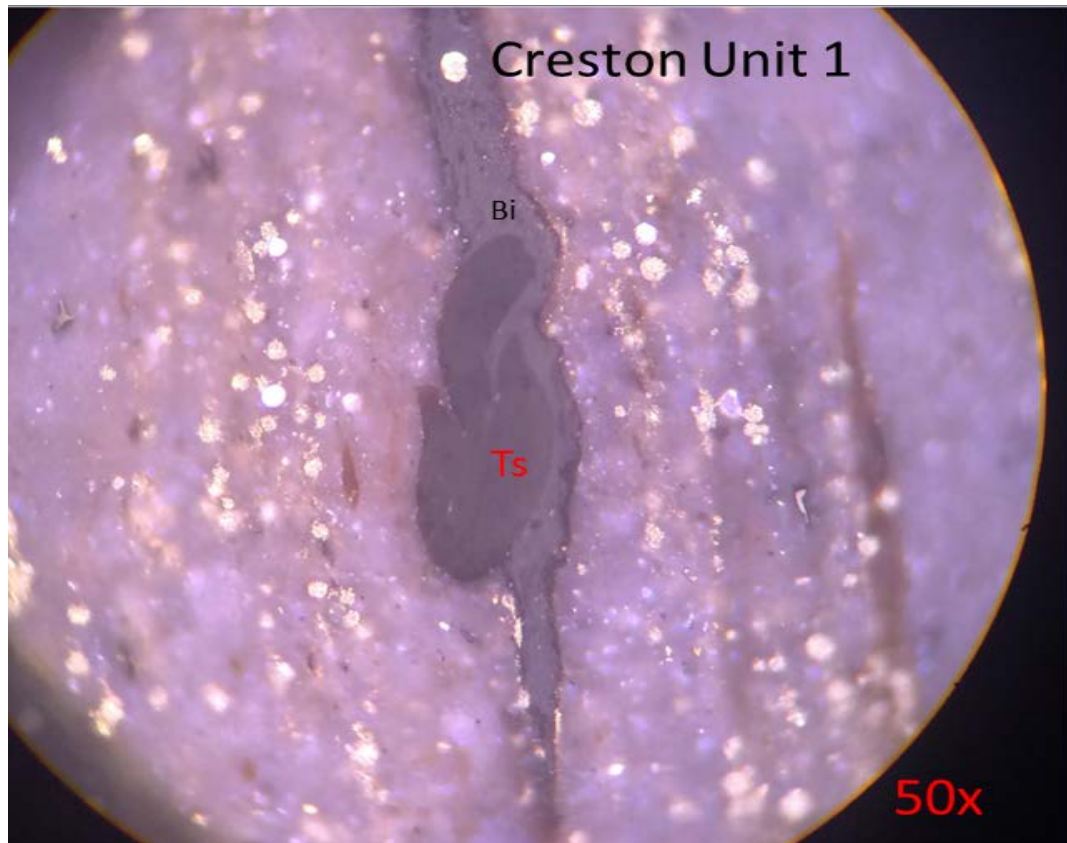


Figure 37. Thermal maturity from Vitrinite reflectance. From Tissot and Welte, 1984.



**Figure 38. Tasmanites (Ts) picture from Creston Unit 1 well.**

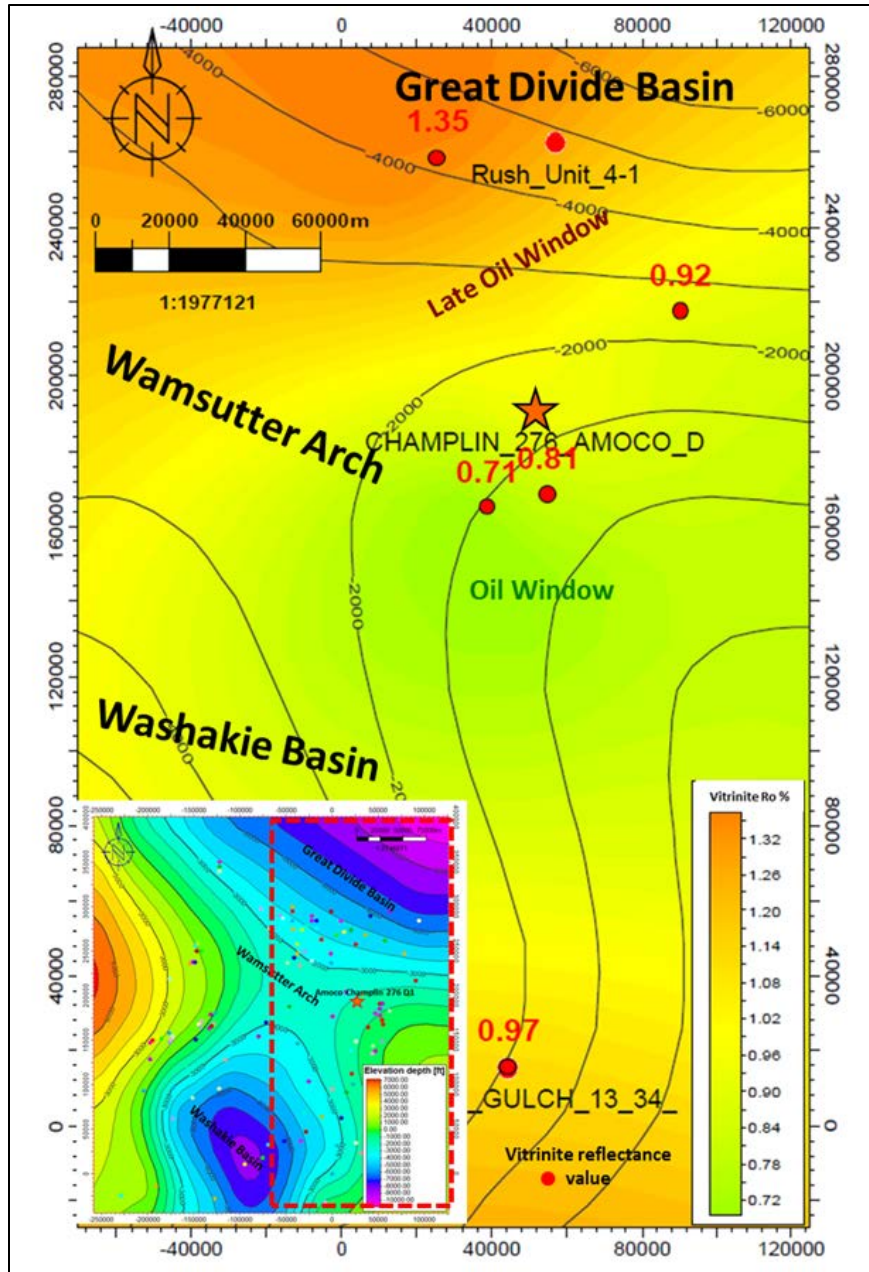


Figure 39. Vitrinite Reflectance values map overlaid by the structural map (grey lines) from the Mesaverde Group and some values from the Lewis Shale in the basin. According to Figure 37, the boundary between immature and oil-condensate is not very definitive and varies depending upon the type of organic matter present in the rock (Tissot and Welte 1981). The general trend of the map shows an increase in thermal maturity (increase in vitrinite reflectance) towards the North and South which also corresponds to the deeper trends in the basin. Vitrinite values decrease towards the center of the map that corresponds to the shallower area in the basin.

### *Biomarker Analysis*

Biomarkers are usually known as molecular fossils that retain chemical similarities with their precursor, such as plant, animal, bacteria, spore, fungi or any other possible organic source (Philp and Lewis, 1987). Biomarkers are extremely useful for determining the depositional environment, and maturity in source rocks (Hunt et al., 2002). The depositional environment determines the amount and type of organic matter found in a rock. The ideal environment for the accumulation and preservation of organic matter is an anoxic environment (Calvert and Pedersen, 1992).

Three samples: one sample from the Amoco Champlin 276 D-1 well depth, one cutting sample from the Amoco Champlin E-1 well, and one cutting sample from the Stage Stop Unit 2 were analyzed by the Organic Geochemistry Group in the University of Oklahoma. Gas chromatography and gas chromatography-mass spectrometry (GC-MS) were performed for specific biomarker groups such as, alkanes and steranes (m/z 217) and terpanes (m/z 191).

The Amoco Champlin 276 D-1 sample was extracted from the Asquith Marker interval at 8138ft. depth. The GC chromatogram for this sample at 8138ft. depth shows an unimodal distribution of n-alkanes maximizing at  $n\text{-C}_{16}$  to  $n\text{-C}_{17}$  (Figure 40). There was not an odd/even predominance in the n-alkane distribution. These characteristics were interpreted as a sample from mainly marine environment with marine plankton, bacterial and photosynthetic algae are the main source of the organic matter, and an early window maturity stage for the sample (Philp personal communication).

Pristane and phytane are the most common isoprenoids that are derived from chlorophyll (Gossens et al., 1984). It is believed that these compounds originate from

degradation of the phytol side chain of chlorophyll (Hughes et al., 1995). Pr/Ph ratio is used as a redox indicator of the depositional environment in which a ratio less than 1 corresponds to an anoxic environment, whereas samples with ratio much greater than 1 correspond to an oxic environment (Hughes et al., 1995). For the Amoco Champlin 276 D-1 sample the ratio of 1.5 suggesting an suboxic environment.

Pr and Ph can be combined with the  $n$ -C<sub>17</sub> and  $n$ -C<sub>18</sub> normal alkanes to evaluate maturity of the sample. It is expressed as a ratio C<sub>17</sub>/Pr and C<sub>18</sub>/Ph ( $n$ -alkanes /isoprenoids). This ratio increases with maturity as  $n$ -alkanes are generated faster than isoprenoids (El Nady et al., 2003). Results from the GC gives a ratio of 1.2 and 1.221 from the C<sub>17</sub>/Pr and C<sub>18</sub>/Ph ratios and is indicative of a thermally immature sample (Table 9).

**Table 9. List of well used for the analysis, ratios used to measure maturity and other parameters and the result of the maturity analysis.**

Well Name	Ratio	Meaning
Champlin 276 D1 core sample (8138 ft.)	$n$ -C <sub>17</sub> /Pr:1.2	Low maturity
	$n$ -C <sub>18</sub> /Ph:1.221	Low maturity
	Pr/Ph: 1.5	Suboxic environment
	Ts/(Ts+Tm):0.482	Main Oil window
Champlin 276 E1 cutting sample (8770-9000 ft.)	Ts/(Ts+Tm):0.284	Early Oil Window
	C <sub>31</sub> 22s/22s+22r:0.545	Immature
	C <sub>29</sub> (S/S+R):0.26	Early Oil Window
	C <sub>29</sub> ββ/ββ+αα:0.56	Main Oil window
Stage Stop 2 cutting sample (5400-5410 ft.)	Ts/(Ts+Tm):0.55	Main Oil window
	C <sub>31</sub> 22s/22s+22r:0.542	Immature
	C <sub>29</sub> ββ/ββ+αα:0.563	Main Oil window
	C <sub>29</sub> (S/S+R):0.49	Main Oil window

Terpanes are a wide class of branched and cyclic alkanes that include tricyclic, tetracyclic and pentacyclic terpanes (Peters et al., 1993). Terpanes are important to identify bacterial reworking during early diagenesis (Moldowan et al., 1985). They are usually monitored using the m/z 191 mass fragmentogram. Figure 41 shows the m/z



191 chromatogram and the terpane distribution for the Amoco Champlin 276 D-1 at 8138ft. depth sample. Tricyclic terpanes are derived from bacterial membranes by cyclization of regular polyprenols (Tissot and Welte, 1984). The presence of these tricyclic terpanes is linked to the presence of Tasmanites algae and increase with increasing maturity (Peters et al., 2005). For the Amoco Champlin 276 D-1 well tricyclic terpanes presented low abundance which means low maturity and could also mean a distal marine depositional environment due to the presence of Tasmanites.

Pentacyclic terpanes are very diverse in their use as biomarkers. C<sub>30</sub> (17 $\alpha$  (H), 21 $\beta$ (H)-hopane) or H30, and 17 $\alpha$  (H), 21 $\beta$ (H)-30-norhopane H29 and hopanes are used as depositional environment indicators. High abundance of H29 over H30 is indicative of organic rich carbonates (Connan et al., 1986 in Roushdy et al., 2010). For this sample the predominance of H30 shows that this is not a carbonate environment and it is usually derived from marine depositional environment (Philp and Lewis, 1987) (Figure 41).

Homohopanes (C<sub>31</sub>-C<sub>35</sub>) are derived from bacteriopolyhopanol from a prokaryotic cell membrane. It can be used as an indicator of oxic or anoxic environments. High C<sub>35</sub>-homohopane indices are typical of marine, low Eh environments of deposition. The presence of this C<sub>35</sub> compound for this sample (8138ft. depth from Amoco Champlin 276 D-1) is indicative of a reducing environment (Figure 41).

Norhopanes are widely used to determine maturity of the source rock but it depends strongly on the depositional environment. Ts refers to 18 $\alpha$ (H)-22,29,30-trisnorhopane and Tm 17 $\alpha$ (H)-22,29,30-trisnorhopane. The (Ts/Ts+Tm) ratio between these two compounds increases with the presence of shale in calcareous facies (Figure

41). Tm is less stable than Ts, with maturity the abundance of Tm decreases while the Ts abundance increases (Peters et al., 2005). In Amoco Champlin 276 D-1 well this ratio (0.48) suggests the sample is in the main oil window (Table 9).

Oleanane is a pentacyclic triterpenoid that is indicative of higher plant material (angiosperms) input. It serves to identify terrigenous input since its precursor is presumed to be oleanane triterpenoids (ten Haven and Rullkotter, 1988 in Jung-Nan, 1989). It also narrows the age of deposition to Late Cretaceous-Early Tertiary (Philp and Gilbert, 1986). Oleanane was also present in the terpanes distribution for the Amoco Champlin 276 D-1 sample at 8138ft. depth.

Steranes are mainly derived from sterols that come from algae and higher plants (Peters et al., 2005). Sterane distribution for the Asquith marker was determined using the analysis of saturates from the m/z 217 ion (Figure 42).

Diasteranes are formed by backbone rearrangement of regular steranes. High abundance of the diasteranes indicates a clay rich rock as a result of the reactions of steranes catalyzed by clays (Philp, 1987). For the sample of Amoco Champlin 276 D-1 well the presence of diasteranes compounds is interpreted as a shale sample from a marine environment (Figure 42).

C<sub>30</sub> Steranes are derived from sterols synthesized by marine algae, consequently, the presence of this C<sub>30</sub> compound will indicate a marine depositional environment (Moldowan et al., 1990). M/z 217 chromatogram and sterane distribution for Amoco Champlin 276 D-1 at 8138ft. depth is shown on Figure 42 and the presence of the C<sub>30</sub> compound showing again that this sample correspond to a marine setting.

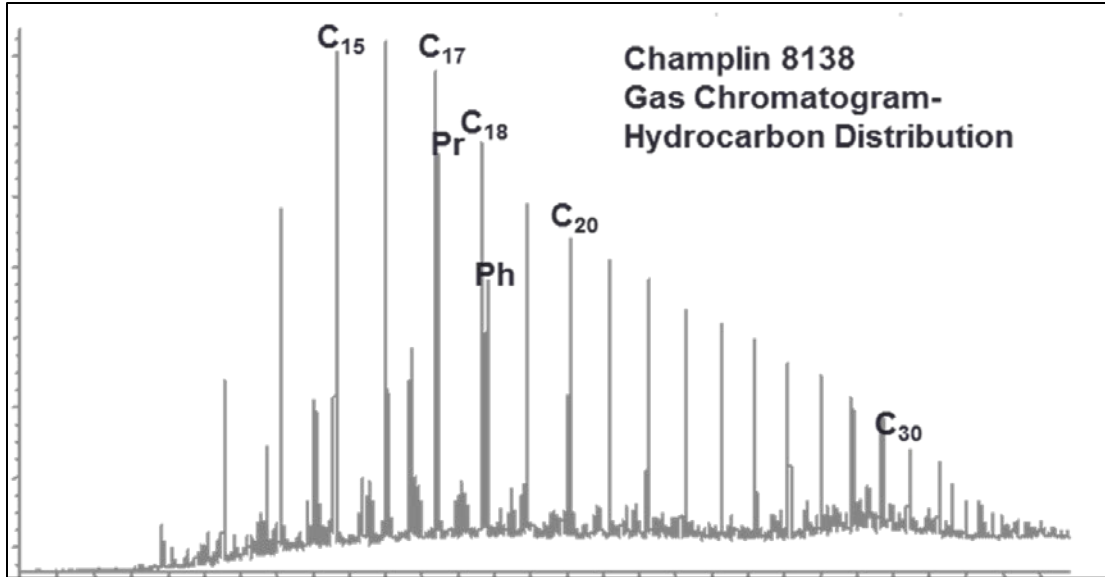


Figure 40. Amoco Champlin 276 D-1 GC chromatogram for the Amoco Champlin 276 D-1 well at 8138ft. depth. It shows the location for C17, C18, Pr and Ph n-alkanes.

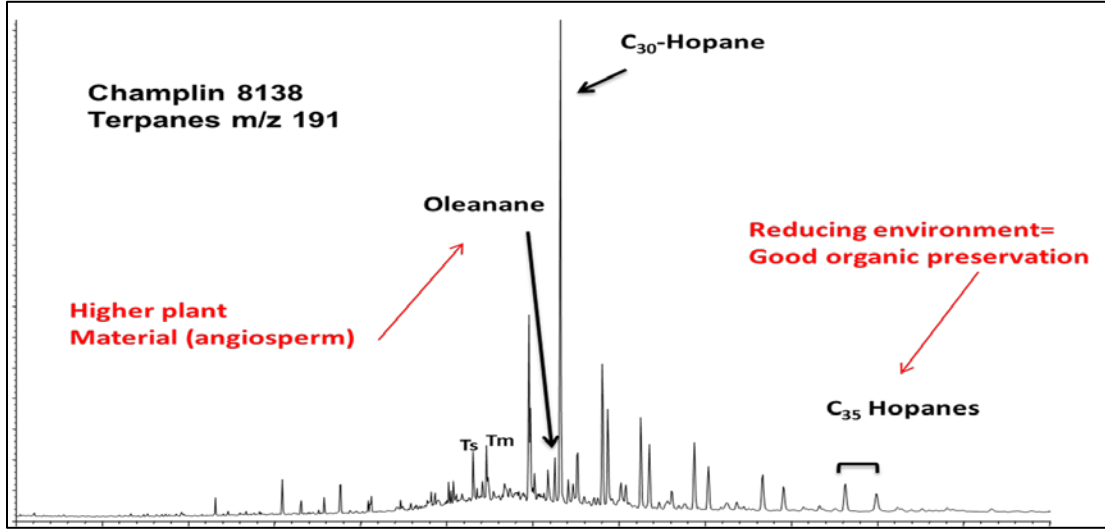
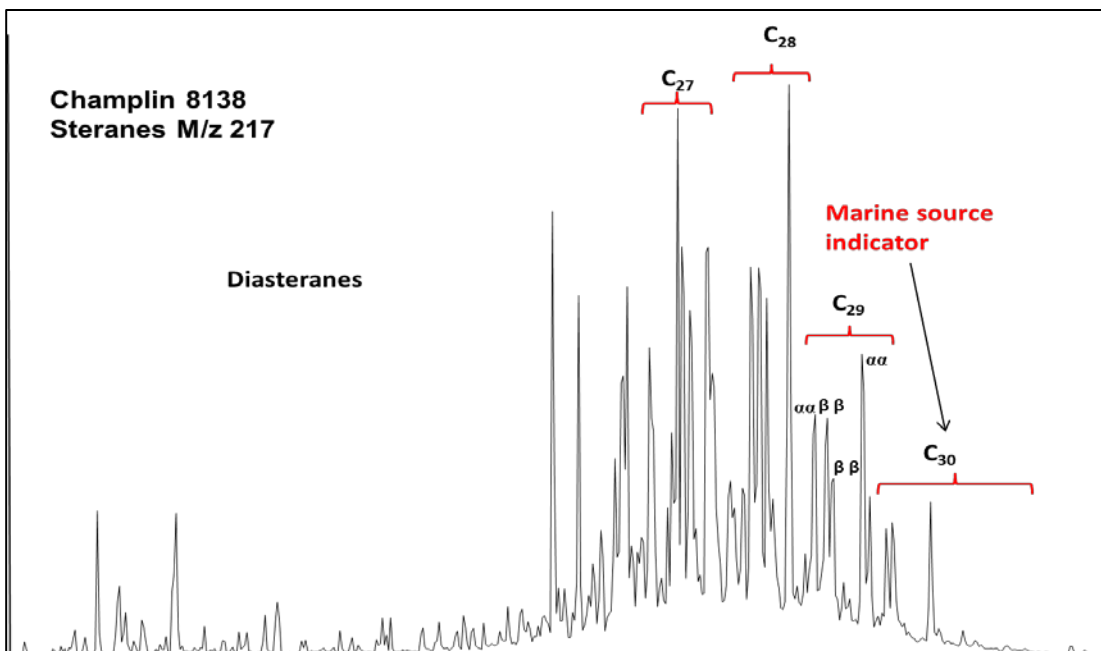


Figure 41. Amoco Champlin 276 D-1 GCMS from the m/z 191 ion showing the oleanane, C35 hopanes, and the C30 hopanes.



**Figure 42. Amoco Champlin 276 D-1 well GCMS from the m/z 217 ion, it shows the high abundance of diasteranes and the presence of C30.**

The Amoco Champlin 276 E-1 sample was extracted from Asquith Marker cuttings at 8770-9000ft. depth. Tricyclic terpanes low abundance is indicative of low maturity and linked to Tasmanites presence, which means this sample is from a marine environment and low maturity (Figure 43).

Terpane distribution for this sample at 8770-9000ft. depth shows a C<sub>30</sub> over C<sub>29</sub> abundance, which indicates a marine, non-calcareous environment (Figure 43); (Ourisson et al., 1982). The doublets found in the C<sub>31</sub>-C<sub>35</sub> compounds from the m/z 191 hopanes are called homohopanes. The precursor carries a 22R configuration that changes to a mixture of 22R and 22S with maturity (Peters et al., 2005). Thus in mature rocks the S optical isomer is going to be more abundant than the R. The S/R ratio for C<sub>31</sub> hopane suggests the sample from the Amoco Champlin 276 E-1 well is immature (Table 9) (Peters et al., 1993). High C<sub>35</sub>-homohopane indices are typical of marine environment, low Eh environments of deposition and indicative of a reducing environment (Figure 45). The terpanes (Ts/Ts+Tm) ratio suggests the sample is in the early oil window (0.284) (Table 9). Another hopane analog is the C<sub>29</sub> moretane which is highly unstable and tends to disappear with increasing maturity (Peters et al., 1993). Its presence was identified on the chromatogram indicating that this sample is highly immature (Figure 43).

Gammacerane is a terpane that has been identified in samples from hypersaline marine and non-marine environments (Damsté et al., 1995). Its precursor is the tetrahymanol (gammacer-3 $\beta$ -ol) from protozoa (Damsté et al., 1995). The presence of this compound was identified in the m/z 191, thus indicating a hypersaline marine envi-

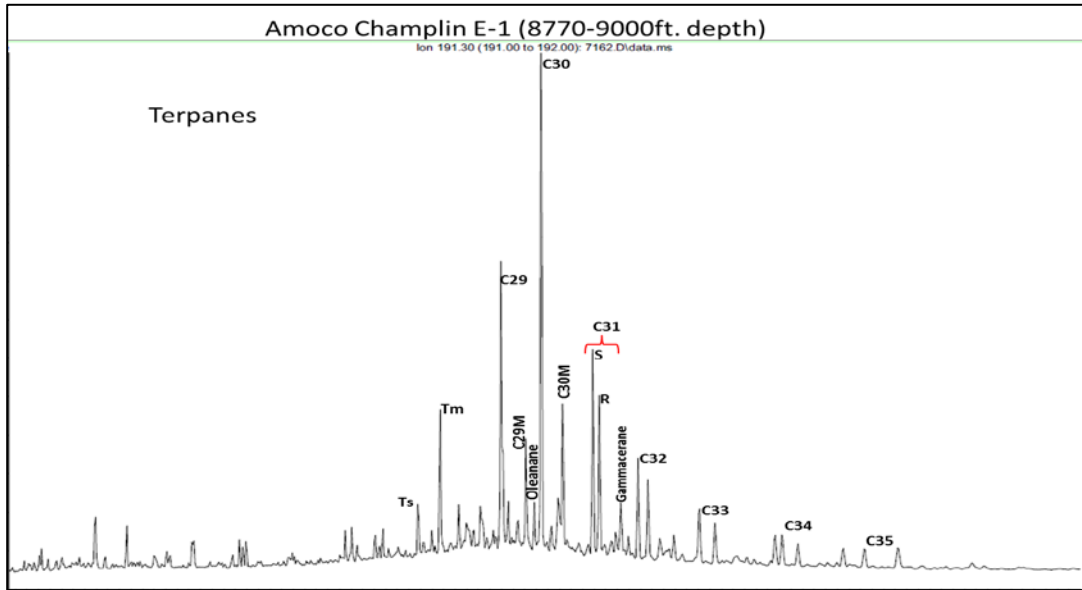
ronment of deposition. As in the previous sample, oleanane is present in the sample which indicates higher plant input (Figure 43).

Figure 44 shows the m/z 217 chromatogram and sterane distribution for the Amoco Champlin E-1 well at 8770-9000ft. depth. High concentrations of diasteranes indicate a shale rich rock, and from the C<sub>30</sub> compound, the presence of a high abundance is from a marine environment. C<sub>29</sub> steranes are useful to determine thermal maturity derived from sterols synthesized by marine algae (Moldowan et al., 1990) (Figure 44). The  $\alpha\alpha$  gradually changes into a mixture of  $\alpha\alpha$  and  $\beta\beta$ . The change of the two hydrogens from alpha positions to beta positions occurs with maturity (Seifert and Moldowan, 1986). From the  $\beta\beta/\alpha\alpha$  ratio (0.56) the steranes indicates that the sample is in the main oil window (Figure 44) (Table 9). From the C<sub>29</sub> S and R isomers ratio, this sample is in the main oil window (Table 9).

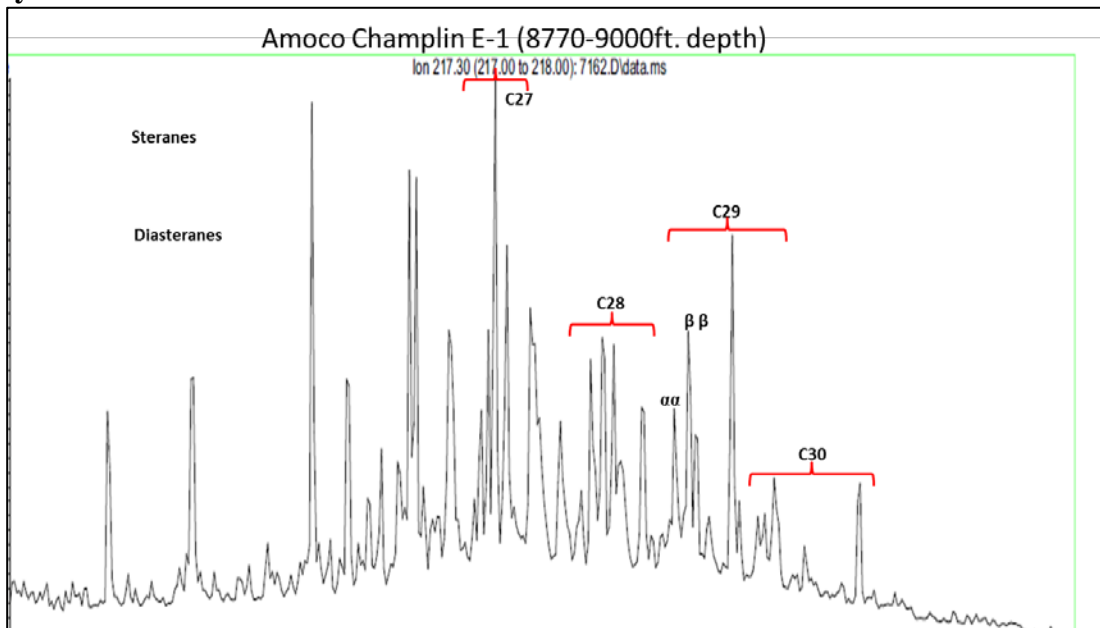
The Stage Stop Unit 2 well sample was extracted from Asquith Marker cuttings at 5400-5410ft. depth. Figure 45 shows the chromatogram for the Stage Stop well and m/z 191 and the terpane distribution. The  $T_s/(T_s+T_m)$  ratio is 0.55 which means main oil window (Table 9). The S/R ratio for C<sub>31</sub> hopane suggests the sample is immature (0.542) (Table 9). The presence of C<sub>30</sub> steranes indicates a marine environment as previously established (Figure 45). Oleanane is less abundant than in the other samples, which indicates a lower amount of the higher plant material input, which mean a more distal position within the basin. Moretanes are present which indicates low maturity.

Figure 46 shows the chromatogram for the m/z 217 steranes ion for the Stage Stop Unit 2 sample. The presence of C<sub>30</sub> sterane indicates the sample is from a marine

environment. The  $\beta\beta/\alpha\alpha$  steranes ratio (0.56) indicates that the sample is in the main oil window (Table 9).  $C_{29}$  steranes isomers ratio indicates this sample is in the main oil window.



**Figure 43. Amoco Champlin 276 E-1 well GCMS from the m/z 191 ion. The ratio of Ts/Tm suggests the sample is very immature. The S/R ratio suggests is early mature. The presence of C29 moretane indicates that this rock is highly immature since they are highly unstable and tend to disappear with increasing maturity.**



**Figure 44. Amoco Champlin 276 E-1 well GCMS m/z 217, showing the high**

abundance of diasteranes that as stated before indicate a shale rich rock and marine environment.

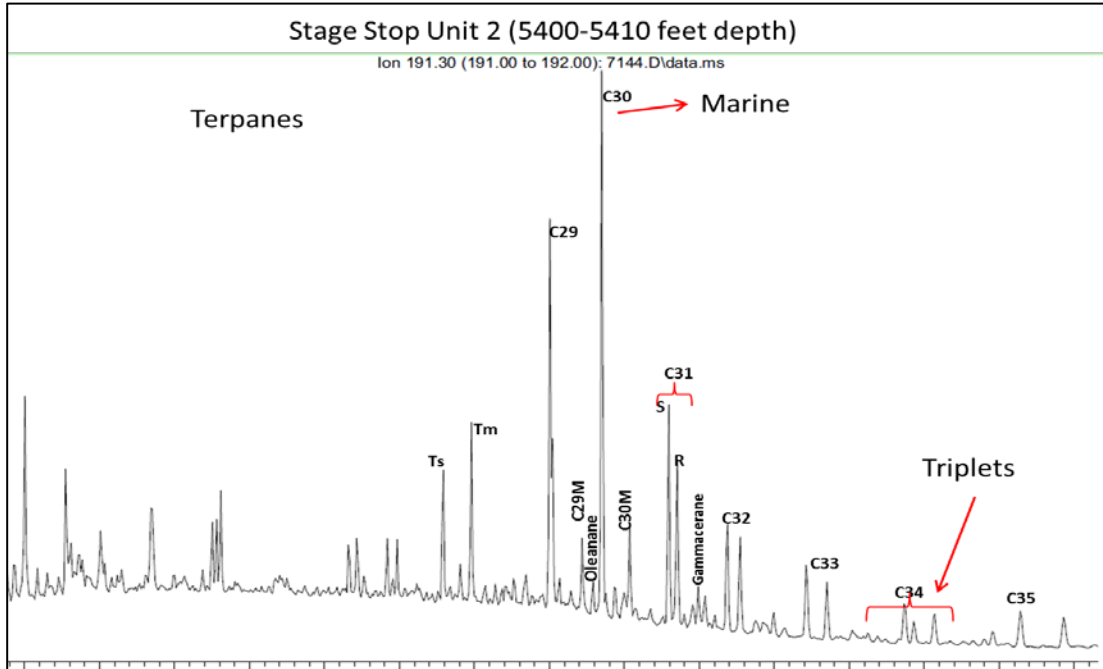


Figure 45. Stage Stop Unit 2 well GCMS from m/z 191 ion showing the C30 hopane, moretane, gammacerane, oleanane and the C32, C33, C34 and C35 triplets, which indicate that the sample is highly immature, from stratified waters, with higher plant material input.

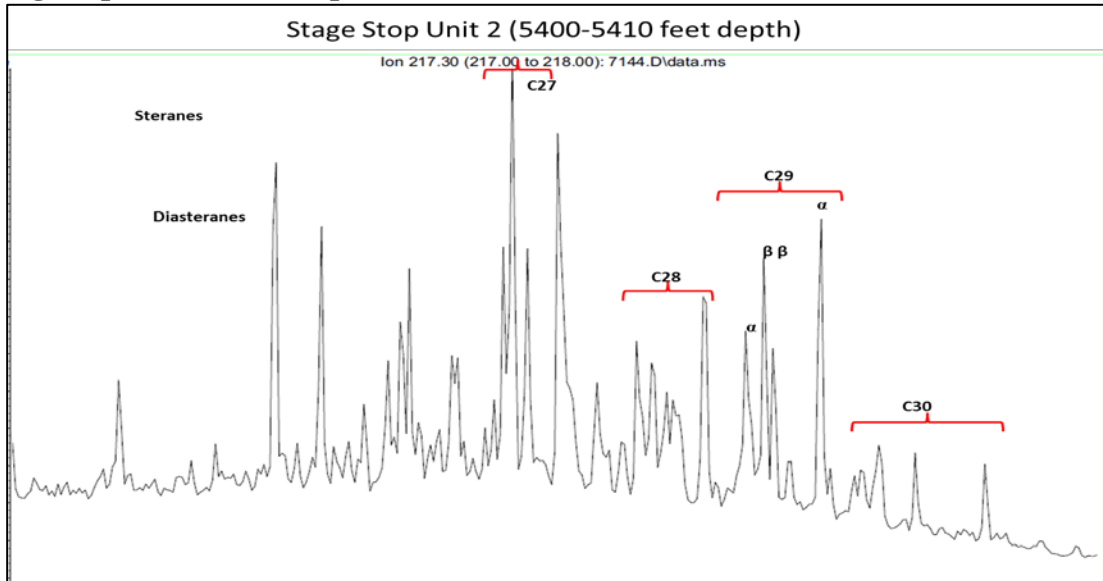


Figure 46. Stage Stop Unit 2 well GCMS from m/z 217 ion showing the C27, C28, C29 and C30 steranes, which indicate a shale.



## Chapter 5: Identification of Potential Areas of Oil Accumulation

Several constraints were used to determine potential oil-prone areas. TOC, thickness, and vitrinite reflectance were plotted on maps. According to Jarvie, 2005, low TOC samples should, at least, have a thickness of 100ft. to be prospective. Therefore, for this present study a thickness between 30 and 50ft. was used. TOC seemed to slightly decrease with depth, this change in TOC could refer to hydrocarbon production and maturity of the sample but it has high potential for the samples within 1400 and -6600ft. depth. Thus, depths within ~1400 and ~-6600 ft. depth (TVDSS) were chosen as depths constraints (Table 10).

**Table 10. List of constraints used to define potential areas.**

Constraint	Value
Thickness	30-50ft.
Depth (based on TOC potential to generate hydrocarbons)	1400-(-6700)
Vitrinite reflectance	In the area is within the oil or late oil window
Oil field, Oil well (Stage Stop 2, Rush Unit 4-1)	Stage Stop has produced oil from the Lewis Shale.

Vitrinite reflectance showed that the samples are within the oil window, late oil window and in some cases (value of 1.32) could be placed in the condensate and wet gas window. Definitive limits for these windows are not placed because the generation of hydrocarbons depends highly on the type of organic matter present. It was observed that vitrinite values correlate with depth for this present case, where the deeper the sample the more thermally mature it is. Information about oil wells from the Asquith Marker was also used as a constraint in defining potential areas. Figure 49 is the resulting potential area with all the constraints applied. It has an approximate area of  $2.53 \times 10^7$  acres.

There is one field that is being producing oil from the Lewis Shale which was also used as a constraint. I gathered new information regarding two wells located towards the area of the Great Divide basin. They are producing oil from the Asquith Marker in horizontal wells. The Rush Unit 4-1 (Figure 47, between vitrinite values of 1.35 and 0.92 Ro.%) and Spirit of Ratio well also close to that area (Figure 47).

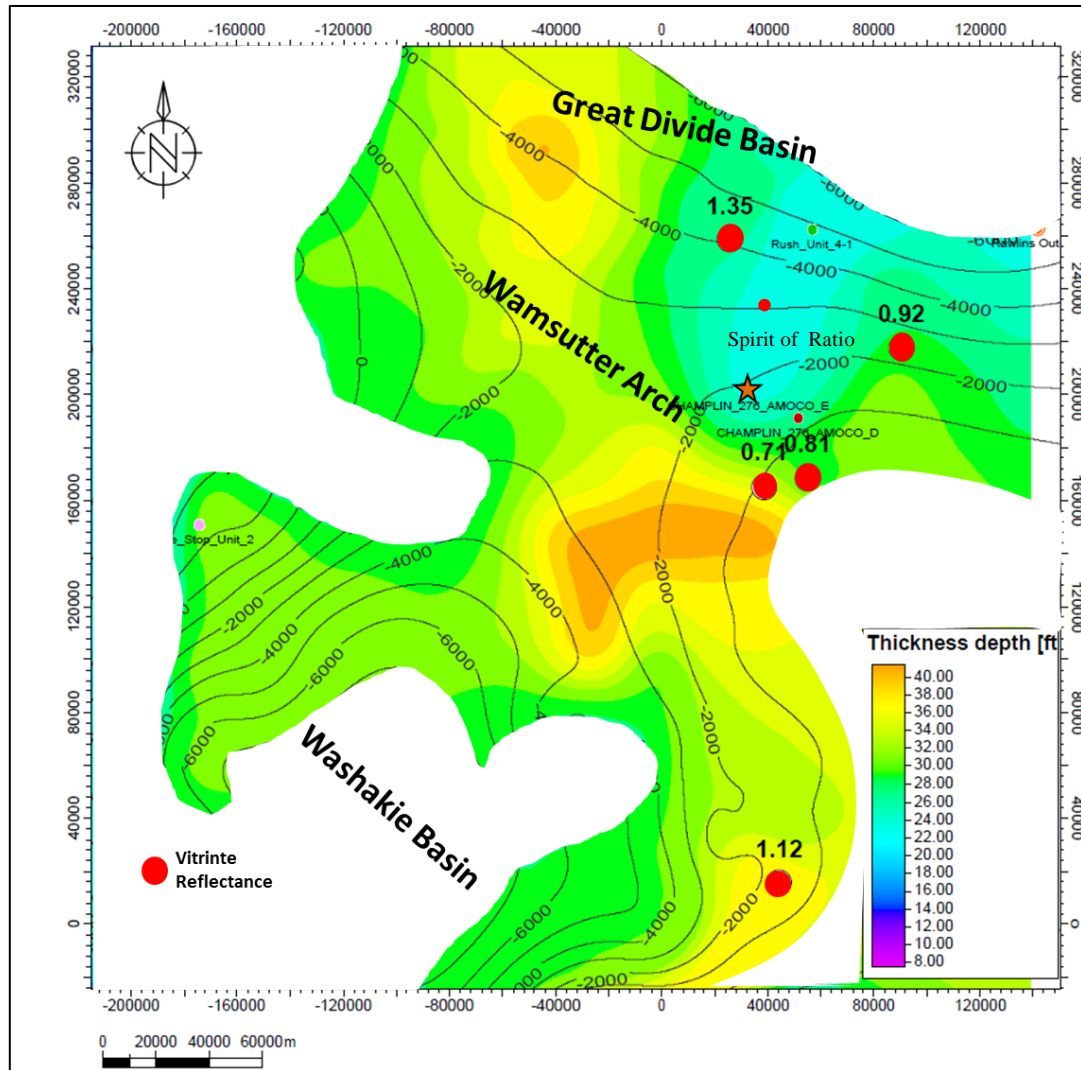


**Figure 47. Map showing the resulted potential area. Thickness, Ro, depth and were used as constraints to define the potential areas.**

## Chapter 6: Conclusions

From the data obtained and the screening process used, it was possible to define potential areas for development of the Asquith Marker as an unconventional oil play. The data also showed some of the pitfalls of Rock-Eval analysis related to weathering, low TOC, and scarce data.

The potentially productive areas are located towards the western side of the basin close to the Stage Stop Field and towards the Wamsutter arch area close to the Amoco Champlin 276 D-1 well (Figure 47). Wells where the Asquith Marker is between 1400-(-6600) are prospective (Figure 47). From the thickness maps it was possible to determine the maximum thickness of the Asquith Marker (50ft.). Thickness increases from west to east in the basin and reaches its maximum thickness towards the eastern margin of the Washakie basin near the Wamsutter arch.

The type of kerogen is typically Type II, which is oil prone. However, in some cases, the low TOC caused the Tmax. and HI values to be unreliable. This made it impossible to determine the type of kerogen for those samples. Further XRD analyses showed a predominance of quartz in the samples, followed by illite. In the deeper samples, an increased percentage of calcite and clay minerals was observed, suggesting that the deeper sample is more ductile.

The overpressure effect is important in this basin because it is a typical gas bearing rock. But, since the top of the overpressure is an uneven surface throughout the basin, there are areas where the Asquith Marker might be generating oil or condensates. To resolve the discontinuous distribution of potentially productive areas, biomarkers were analyzed. Biomarkers gave a large amount of information about ma-

turity, source material, age and depositional environment. In general all the samples were very similar with higher plant material input and a marine origin, in stratified, saline waters. In general, the rock just entered the oil window or in the main oil window. From The vitrinite reflectance values obtained the eastern section of the basin is within the oil window to late oil window.

Some of the assumptions made regarding the potential productivity of this basin were based on a very few samples, and therefore there is uncertainty in the results and interpretations. It is important to take into account the low TOC and thickness of the Asquith Marker when considering it as a new unconventional oil play.

The new information about two wells (Rush Unit 4-1 and Spirit of Ratio 7-1H) towards the Great Divide basin served as a proof of concept since both of these wells were drilled as horizontal wells through the Asquith Marker. They were produced 26775 Bbls and 14350 Bbls respectively. Spirit of Ratio 7-1H is still producing but the Rush Unit 4-1H was abandoned due to the high declination rate. This also proves the importance of taking into account the thickness and TOC of the interval.

### *Recommendations*

Further analysis needs to be conducted in order to better define the potential areas and to understand the play. It is preferable to have core samples for these analyses, since the sample is fresher and will reduce the pitfalls from Rock-Eval analyses.

An oil sample from one of the fields that produced oil from the Lewis Shale should be analyzed for biomarkers in order to correlate with the biomarkers from the samples and determine if the oil comes from the Asquith Marker.

XRD analyses were made in two samples from the Asquith Marker from the Amoco Champlin D-1 well. It is important to expand the analysis to more areas to see the facies changes in the formation and thus be able to identify more accurately the potential drillable areas.

New information about two oil producing wells (Rush Unit 4-1 and Spirit of Ratio 7-1H) from the Asquith Marker provided as proof of concept, but the decline rate suggested production-limits were being approached.

## References

- Almon, R.W., C.W. Dawson., S.J. Sutton, F.G. Ethridge., and B. Castelblanco, 2002, Sequence Stratigraphy, Facies Variation and Petrophysical Properties in Deepwater Shales, Upper Cretaceous Lewis Shale, South-Central Wyoming. Gulf Coast association of geological Societies Transaction, v. 52, p.1041-1053.
- Anna, L.O., 2013, Geologic assessment of undiscovered oil and gas in the Williston Basin Province, Montana, North Dakota, and South Dakota, chap. 3 of U.S. Geological Survey Williston Basin Province Assessment Team, Assessment of undiscovered oil and gas resources of the Williston Basin Province of North Dakota, Montana, and South Dakota, 2010 (ver. 1.1, November 2013): U.S. Geological Survey Digital Data Series 69–W, p.71.
- Asquith, D.O., 1970, Depositional topography and major marine environments, Late Cretaceous, Wyoming. AAPG Bulletin, v. 54(7), p.1184-1224.
- Calvert, S. E., and T. F. Pedersen, 1992, Organic carbon accumulation and preservation in marine sediments: how important is anoxia. Organic matter: productivity, accumulation, and preservation in recent and ancient sediments, v.533, p. 231-263.
- Cardott, B. J. 2012. Introduction to vitrinite reflectance as a thermal maturity indicator: AAPG search and discovery article No. 40928.
- Damsté, J. S. S., F. Kenig, M. P. Koopmans, J. Köster, S. Schouten, J. M. Hayes, and J. W. de Leeuw, 1995, Evidence for gammacerane as an indicator of water column stratification. *Geochimica et Cosmochimica Acta*, 59(9), p.1895-1900.
- Espitalie, J., M. Madec, B. Tissot, J. J. Mennig, and P. Leplat, 1977, Source rock characterization method for petroleum exploration. In Offshore Technology Conference. Offshore Technology Conference.

- Gill, J. R., E. A. Merewether, and W. A. Cobban, 1970. Stratigraphy and nomenclature of some Upper Cretaceous and lower Tertiary rocks in south-central Wyoming (No. 667). US Govt. Print. Off.,.
- Goossens H., de Leeuw J. W., Schenck P. A. and Brassell S. C. (1984) Tocopherols as likely precursors of pristane in ancient sediments and crude oils. *Nature* 312, p. 440-442.
- Hamilton, S.E., 2006, Cause of lost circulation in Lewis Shale wells South Central Wyoming. Master of Science Thesis, The University of Oklahoma, Norman, Oklahoma. p.9
- Hart, B. S., and A. S. Steen, 2015, Programmed pyrolysis (Rock-Eval) data and shale paleoenvironmental analyses: A review. *Interpretation*, v. 3(1), SH41-SH58.
- Hartman-Stroup, C. 1987, The effect of organic matter type and organic carbon content on Rock-Eval hydrogen index in oil shales and source rocks. *Organic geochemistry*, v. 11(5), p.351-369.
- Hettinger, R. D., and L. N. Roberts, 2005, Lewis total petroleum system of the Southwestern Wyoming province, Wyoming, Colorado, and Utah. *Petroleum Systems and Geologic Assessment of Oil and Gas in the Southwestern Wyoming Province, Wyoming, Colorado, and Utah*, US Geological Survey Digital Data Series DDS-69-D, 43.
- Hughes, W.B., Holba, A.G., Dzou, L.I.P., 1995. The ratios of dibenzothiophene to phenanthrene and pristane to phytane as indicators of depositional environment and lithology of petroleum source rocks. *Geochimica et Cosmochimica Acta* 59, p.3581-3598.
- Hunt, J. M., R. P. Philp, and K. A. Kvenvolden, 2002, Early developments in petroleum geochemistry. *Organic Geochemistry*, v. 33(9), p. 1025-1052.
- Jarvie, D. M., 1991, Total Organic Carbon (TOC) Analysis: Chapter 11: Geochemical Methods and Exploration: AAPG Special Volumes, p. 113-118.

- Jarvie D. M., R. J. Hill and R. M. Pollastro, 2005, Assessment of the gas potential and yields from shales: The Barnett Shale model. Oklahoma Geological Survey Circular 110, 37-50.
- Katz, B. J., 1983, Limitations of 'Rock-Eval' pyrolysis for typing organic matter. *Organic Geochemistry*, v. 4(3), p.195-199
- Khorasani, G.K., and J.K. Michelsen, 1994, The effects of overpressure, lithology, chemistry and heating rate on Vitrinite reflectance evolution, and its relationship with oil generation. *APEA journal*, p. 418-434.
- Law, B. E., 1984, Relationships of source rocks, thermal maturity, and overpressuring to gas generation and occurrence in low permeability Upper Cretaceous and lower Tertiary rocks, Greater Green River basin, Wyoming, Colorado, and Utah, in J. Woodward, F. F. Meissner, and J. L. Clayton, eds., *Hydrocarbon source rocks of the greater Rocky Mountain region: Rocky Mountain Association of Geologists Guidebook*, p. 469– 490
- McGookey, D. P., J. D. Haun, , L. A. Hale, H. G. Goodell, , D. G. McCubbin, R. Weimer, and G. R. Wulf, 1972, Cretaceous system. *Geologic Atlas of the Rocky Mountain Region: Rocky Mountain Association of Geologists*, p. 190-228.
- McMillen, K. M., and R. D. Winn Jr., 1991, Seismic facies of shelf, slope, and submarine fan environments of the Lewis Shale, Upper Cretaceous, Wyoming, in P. Weimer and M. H. Link, eds., *Seismic facies and sedimentary processes of submarine fans and turbidite systems: New York, Springer-Verlag*, p. 273–287.
- Minton, G., 2002, *Subsurface Study of the Lewis Shale in the Southern Washakie and Sand Wash Basin using Borehole Images, Core, Well log and Seismic Data*. Master of Science Thesis, Colorado School of Mines, Golden, Colorado.



- Moldowan, J. M., W. K. Seifert, and E. J. Gallegos, 1985, Relationship between petroleum composition and depositional environment of petroleum source rocks: AAPG Bulletin, v. 69, p. 1255–1268.
- Moldowan, J. M., F. J. Fago, C. Y. Lee, S. R. Jacobson, D. S. Watt, N. E. Slougui, A. Jeganathan, and D. C. Young, 1990, Sedimentary 24-n-propylcholestanes, molecular fossils diagnostic of marine algae: Science, v. 247, p. 309–312.
- Oung, J., 1989, The development and application of novel mass spectrometric techniques for the analysis of biomarkers in crude oils and rock extracts. Thesis dissertation, Oklahoma Univ., Norman, OK (USA). p 17.
- Passey, Q. R., S. Creaney, J. B. Kulla, F. J. Moretti, and J. D. Stroud, 1990, A practical model for organic richness from porosity and resistivity logs: AAPG Bulletin, v. 74, p. 1777–1794.
- Pasternack, I., 2005, The Weimer Marker Bentonite—A regionally persistent correlation horizon within the Upper Cretaceous Lewis Shale, eastern Greater Green River basin, Wyoming and Colorado: The Mountain Geologist, v. 42, no. 2, p. 67–84.
- Pawlewicz, M.J and M. Finn, 2002, Vitrinite reflectance data for the Greater Green River Basin, southwestern Wyoming, northwestern Colorado, and northeastern Utah. US Department of the Interior, US Geological Survey.
- Peters, K. E., 1986, Guidelines for evaluating petroleum source rock using programmed pyrolysis. AAPG bulletin, v. 70(3), p.318-329.
- Peters K. E., C. C. Walters and J. M. Moldowan, 2005, The biomarker guide, Volume 2: biomarkers and isotopes in petroleum exploration and earth history. Second Edition, Cambridge University Press. USA. v.2, p.612-613.

- Philp, R. P. 1985, Biological markers in fossil fuel production. *Mass Spectrometry Reviews*, v.4(1), p.1-54.
- Philp, R. P., and T. D. Gilbert, 1987, A review of biomarkers in kerogens as determined by pyrolysis-gas chromatography and pyrolysis-gas chromatography-mass spectrometry. *Journal of analytical and applied pyrolysis*, v. 11, p. 93-108.
- Philp, R. P., and C. A. Lewis, 1987, Organic geochemistry of biomarkers. *Annual Review of Earth and Planetary Sciences*, v. 15, p.363-395.
- Pyles, D., and R. Slatt, 2000, A high-frequency sequence stratigraphic framework for shallow through deep-water deposits of the Lewis Shale and Fox Hills Sandstone, Great Divide and Washakie basins, Wyoming, in P. Weimer, R. M. Slatt, J. Coleman, N. C. Rosen, H. C. Bouma, M. J. Styzen, and D. T. Lawrence, eds., *Deep-water reservoirs of the world (CD-ROM): Gulf Coast Section Society for 1376 Geologic Note Sedimentary Geology (GCSSEPM) 20th Annual Research Conference*, Houston, p. 836–861.
- Pyles, D.R. and R.M. Slatt, 2007, Stratigraphy of the Lewis Shale, Wyoming, USA: Application to Understanding Shelf Edge to Base-of-slope Changes in Stratigraphic Architecture of Prograding Basin Margins, in Nilsen, T.H., Shew, R.D., Steffens, G.S., and Studlick, J.R.J., eds., *Atlas of Deep-Water Outcrops: American Association of Petroleum Geologists Studies in Geology*, v. 56, p. 1-19.
- Ritzma, H. R., 1955, Late Cretaceous and Early Cenozoic structural pattern, southern Rock Springs Uplift, Wyoming: *Wyoming Geol. Assoc. 10th Ann. Field Conf. Guidebook*, p. 135-137.
- Roehler, H. W., 1992, Introduction to Greater Green River Basin geology, physiography, and history of investigations: *U.S. Geological Survey Professional Paper 1506-A*, 14 p, 1 plate.

- Roushdy, M. I., M. M. El Nady, Y. M. Mostafa, N. S. El Gendy, and H. R. Ali, 2010, Biomarkers characteristics of crude oils from some oilfields in the Gulf of Suez, Egypt. *Journal of American Science*, 6(11), p. 911-925.
- Rowe, H. D., R. G. Loucks, S. C. Ruppel, and S. M. Rimmer, 2008, Mississippian Barnett Formation, Fort Worth Basin, Texas: Bulk geochemical inferences and Mo–TOC constraints on the severity of hydrographic restriction. *Chemical Geology*, v. 257(1), p.16-25.
- Seifert, W.K. and J.M. Moldowan, 1978, Application of steranes, terpanes and monoaromatics to the maturation, migration and source of crude oil, *Geochimica et Cosmochimica Acta*, v.42.p. 77-95.
- Simoneit, B. R. 2002, Molecular indicators (biomarkers) of past life. *The Anatomical Record*, v. 268(3), p.186-195.
- Slatt, R. 2011, Important geological properties of unconventional resource shales. *Open Geosciences*, v. 3(4), p.435-44.
- Slatt R. M., P. Philp, N. O'Brien, Y. Abousleiman, P. Singh, E. V. Eslinger, , R. Perez, , R. M. Portas, , E. T. Baruch, K. J. Marfurt, , and S. Madrid-Arroyo, 2012, Pore- to Regional- Scale, Integrated Characterization Workflow for Unconventional Gas Shales, in J.A. Breyer, ed., *Shale reservoirs---Giant resources for the 21st century*, AAPG Memoir 97, p. 127-150.
- Surdam, R.C., Z.S. Jiao, and J. Liu, 1995, Pressure regime in the Upper Cretaceous shales and sandstones in the Washakie basin, Wyoming. *Resources of Southwestern Wyoming; Field conference guidebook*. p. 205-223.
- Taylor, G.H., M. Teichmuller, A. Davis, C.F.K. Diessel, R. Littke, and P. Robert,1998, *Organic petrology*: Berlin and Stuttgart, Gebruder Borntraeger, v.704, p. 137.

- Tissot B. P. and D.H. Welte, 1984, Petroleum Formation and Occurrence, 2nd ed. Springer-Verlag.
- The southwestern Wyoming Province. Introduction to a geologic Assessment of undiscovered Oil and Gas Resources, chap 2 of U.S. Geological Survey Southwestern Wyoming Province assessment Team. Denver, Colorado, 2005.
- Wang, F. P., and J. F. W. Gale, 2009, Screening criteria for shale -gas systems: GCAGS Transactions, v. 59, p.779–793.

### Appendix 1: Wells used in correlations

WELLNAME	SURFLAT	SURFLON
Red Creek 18_1	41.09398	-107.902744
South_Baggs_unit_15	41.0085	-107.73768
South_Baggs_unit_4	41.01577	-107.75681
GAMBLERS RES FED 43_	41.05131	-107.768958
ROBBERS GULCH 13_34_	41.13651	-107.741383
Champlin 14_25	41.50302	-107.705228
Creston 1_9	41.54661	-107.760598
Windy_hill_1	41.5974	-107.676107
MARATHON 1A_13	41.19025	-107.809232
Cige 1A_30	41.15923	-107.78784
Baldy Butte 12-2-17-	41.47333	-107.73167
Barrel Springs State	41.26692	-107.8668
Lookout wash 30-17	41.18154	-107.883746
CRESTON SOUTHEAST 5	41.646297	-107.600038
Amoco CHAMPLIN 276 E	41.64749	-107.781538
Amoco CHAMPLIN 276 D	41.61878	-107.713902
East Echo Springs 14	41.58952	-107.73205
Soco Husky 1B-28	41.42277	-107.77181
Duck Lake 1-1	41.475279	-107.82831

Home Federal 1C-5-14	41.20944	-107.77764
Soco 40-10-14-92	41.199398	-107.726438
FIVE MILE GULCH Unit	41.81709	-107.94528
FIVE MILE GULCH 6	41.773889	-107.908243
Echo Springs 2-2	41.654892	-107.84815
FOUR MILE GULCH 5	41.744744	-107.906464
SIBERIA 3-2	41.28453	-108.012207
Siberia Ridge Unit 6	41.803193	-108.041303
UPRR 4-21 6	41.773875	-108.041754
Baldy Butte 7-10-17-	41.46556	-107.74389
SOC FEDERAL 3-22	41.78077	-108.012153
C G Road Unit 25-1	41.7515	-107.9836
UPRR 4-31 FEE 2	41.744951	-108.080476
CHAMPLIN 446A MOCO-A	41.87472	-107.55761
Seminole Unit 1-25	42.01619	-106.81161
BOG FIELD WI UNIT 1	41.90401	-107.67321
FEDERAL 3-12	41.889837	-107.751129
FEDERAL W-16488 3-24	41.860349	-107.751178
MONUMENT LAKE UNIT	41.845952	-107.828612
CHAMPLIN536 AMOCO-B	41.83139	-107.77056
CHAMPLIN 533 AMOCO B	41.90365	-107.90651
CHAMPLIN533AMOCO-A1	41.87479	-107.86791

FUKAZAKI-FEDERAL	41.87527	-107.96487
FEDERAL 1-30	41.852705	-107.96368
MONUMENT LAKE 5	41.831477	-107.886594
STATE OF WYOMING	41.84051	-107.855843
NGC AMOCO UPRR Paten	41.904156	-108.061085
FEDERAL NGC-3	41.88937	-107.98368
CHAMPLIN 263 AMOCO H	41.874913	-107.983448
CHAMPLIN 452 amocoI1	41.874958	-108.061283
CHAMPLIN 452AMOCO C1	41.86045	-108.003115
CHAMPLIN263AMOCO-B	41.84639	-108.02291
CHAMPLIN 452 AMOCO K	41.847898	-108.059329
GLOVER HORSESHOE 1	41.91161	-108.18621
STOCK POND WI Unit1	41.891894	-108.11115
CHAMPLIN 448 AMOCO-A	41.882722	-108.09908
SIBERIA RIDGE W11490	41.850328	-108.152328
TABLE ROCK UNIT 6	41.55497	-108.43127
DELANEY RIM #9	41.55628	-108.371
TABLE ROCK NO2	41.5848	-108.384244
WAMSUTTER UNIT 6A	41.76113	-108.05391
Barrel Springs Unit	41.37119	-107.8199
Barrel Springs Unit	41.34583	-107.84611
Windmill Draw 1	41.27089	-107.943362

Ruger 24-32	41.22473	-108.006113
Dripping Rock 2	41.19624	-108.02665
Cepo 44-9	41.19537	-108.092091
Desert Rose 1	41.18426	-108.154466
Polar Bar Unit 2	41.14374	-108.176547
Cige 4-6-13-96	41.12377	-108.246841
Barrel Springs state	41.40377	-107.825583
Federal BH 43-320	41.580075	-107.900972
Federal 1-8	41.37975	-107.99547
Bitter Creek 15-1	41.35772	-108.530264
East Echo Springs 1-	41.61134	-107.742
Desert Springs Unit	41.804095	-108.438014
Unit Patented 23	41.741317	-108.469482
Table Rock Unit 16	41.56378	-108.41993
Table Rock 17	41.54626	-108.4245
Playa Unit 1-22	41.69399	-108.54833
Champlin 273 Amoco A	41.32783	-108.454
Hay Reservoir W30398	42.026788	-108.351951
Wamsutter 1-6	41.73741	-108.03261
Unit 4	41.542249	-108.39029
Higgins 18-98 8N-13-	41.507504	-108.442514
Table Rock Unit 25	41.589281	-108.366167

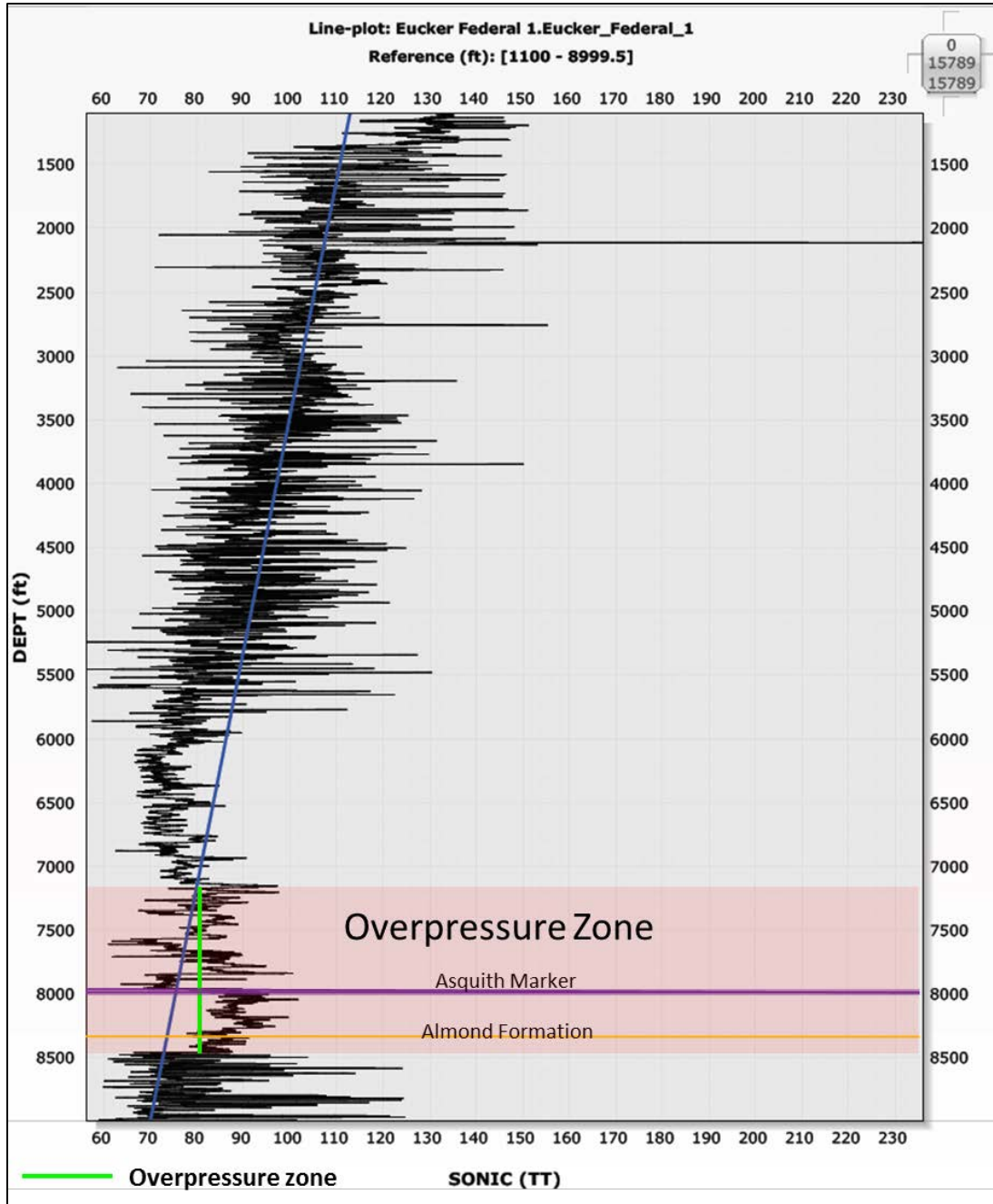


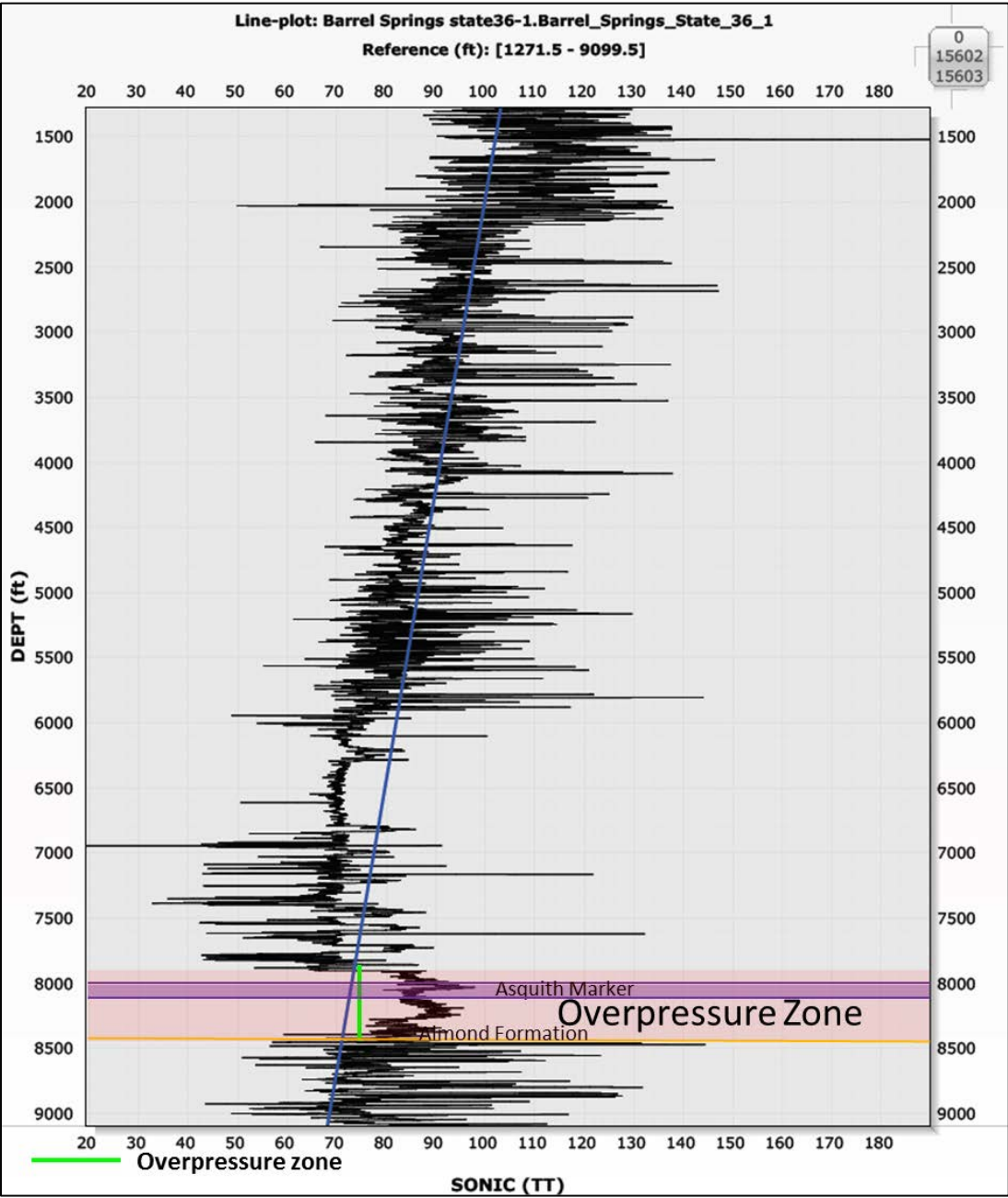
Hay Reservoir W30398	42.041269	-108.351948
Strang 1	41.91861	-108.06121
Delaney Rim Unit 8	41.549471	-108.380277
Hay Reservoir W30397	42.05575	-108.351935
Creston Unit 1	41.55577	-107.7014
Horseshoe Creek Unit	41.02391	-108.73231
Desert Springs 19	41.78052	-108.42122
Monument Lake Unit 2	41.80284	-107.8089
Coal Bank 1-3	41.56882	-107.70548
Fillmore Fed State 1	41.58269	-107.71364
Eucker Federal 1	41.603333	-107.713889
UPRR 31-22 1	41.527082	-108.548732
Long Draw Unit Fee1	41.42644	-108.48154
Trail Unit 1B-21D	41.087426	-108.666415
Kinney Unit 7	41.055679	-108.594097
Federal 1-13	41.0052	-107.93009
Legend Federal 1	41.263333	-108.531944
Seminole W369581-30	42.016235	-106.797647
Semonie Reservoir 1	41.960135	-106.900436
Champlin 535 Amoco A	41.356717	-108.348962
Laney Wash 15-1	41.44589	-108.32491
North Barrel Springs	41.51828	-108.194096

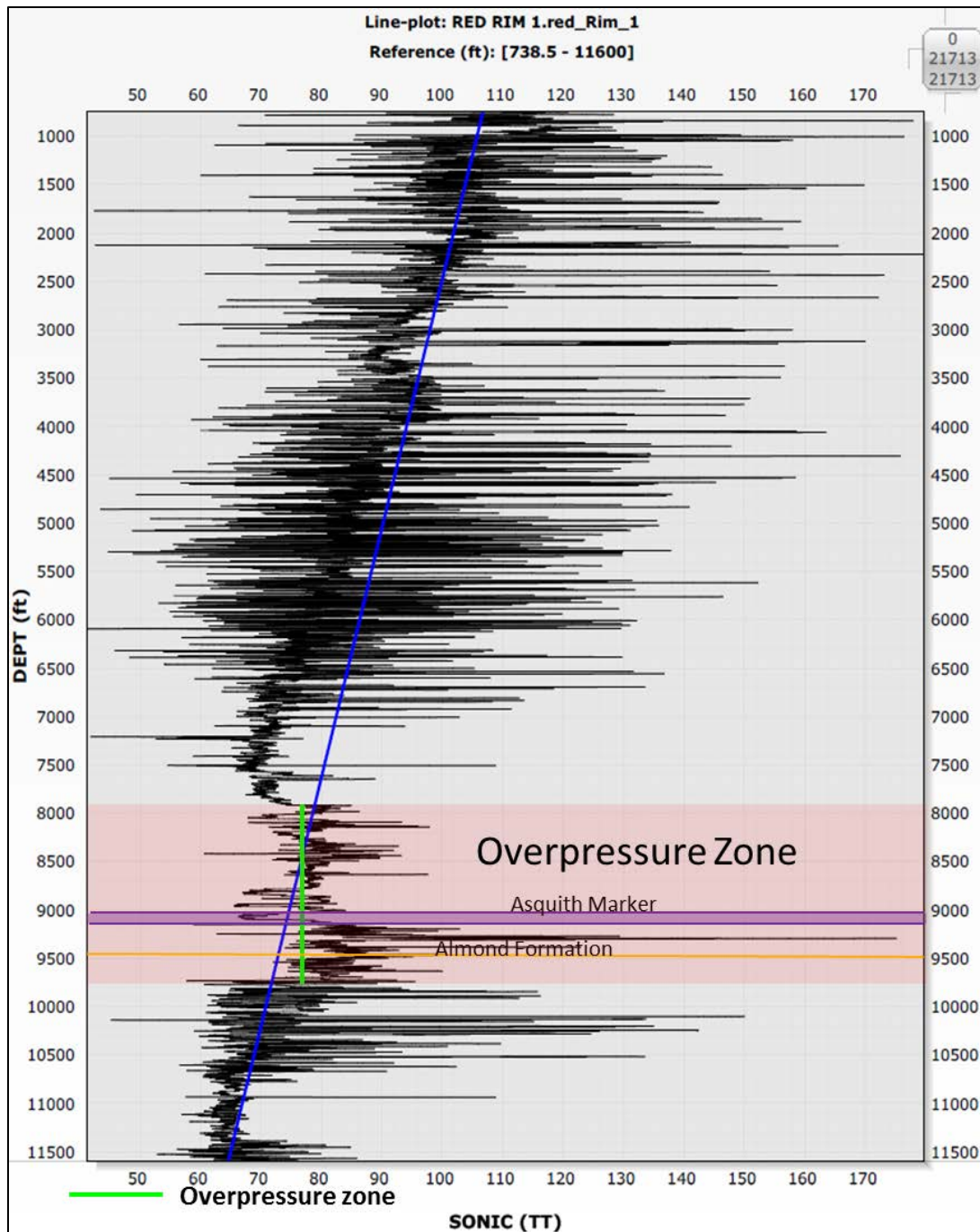
North Barrel Springs	41.561025	-108.164667
CHAMPLIN 293 AMOCO A	41.495977	-108.04019
Frewen 23-70	41.610353	-108.07292
Powder Mountain 1-18	41.01711	-108.3646
Desert Springs Unit	41.780566	-108.440438
Desert Springs Unit	41.74637	-108.457164
May 1-36 State	41.746191	-108.447679
Desert Springs Unit	41.7969	-108.44745
Lanier 1	41.509821	-108.57778
Wallace Federal 1	41.51711	-108.59701
Federal 1-30A	41.504423	-108.613917
State 1-36	41.497134	-108.623092
Champlin 135 Amoco B	41.445882	-108.622574
Welch Federal 1	41.348421	-108.64686
Blue Unit II 3-6-14-	41.211892	-107.795082
RED RIM 1	41.689887	-107.571449
Champlin 528 Amoco A	41.773329	-107.616088
Stage Stop Unit 2	41.506141	-108.539241
JEWELL 1	41.497646	-108.545721
Stage Stop 11	41.517001	-108.534801
Creston Nose 13-34	41.48885	-107.74198
Federal 1-30	41.503259	-107.808898

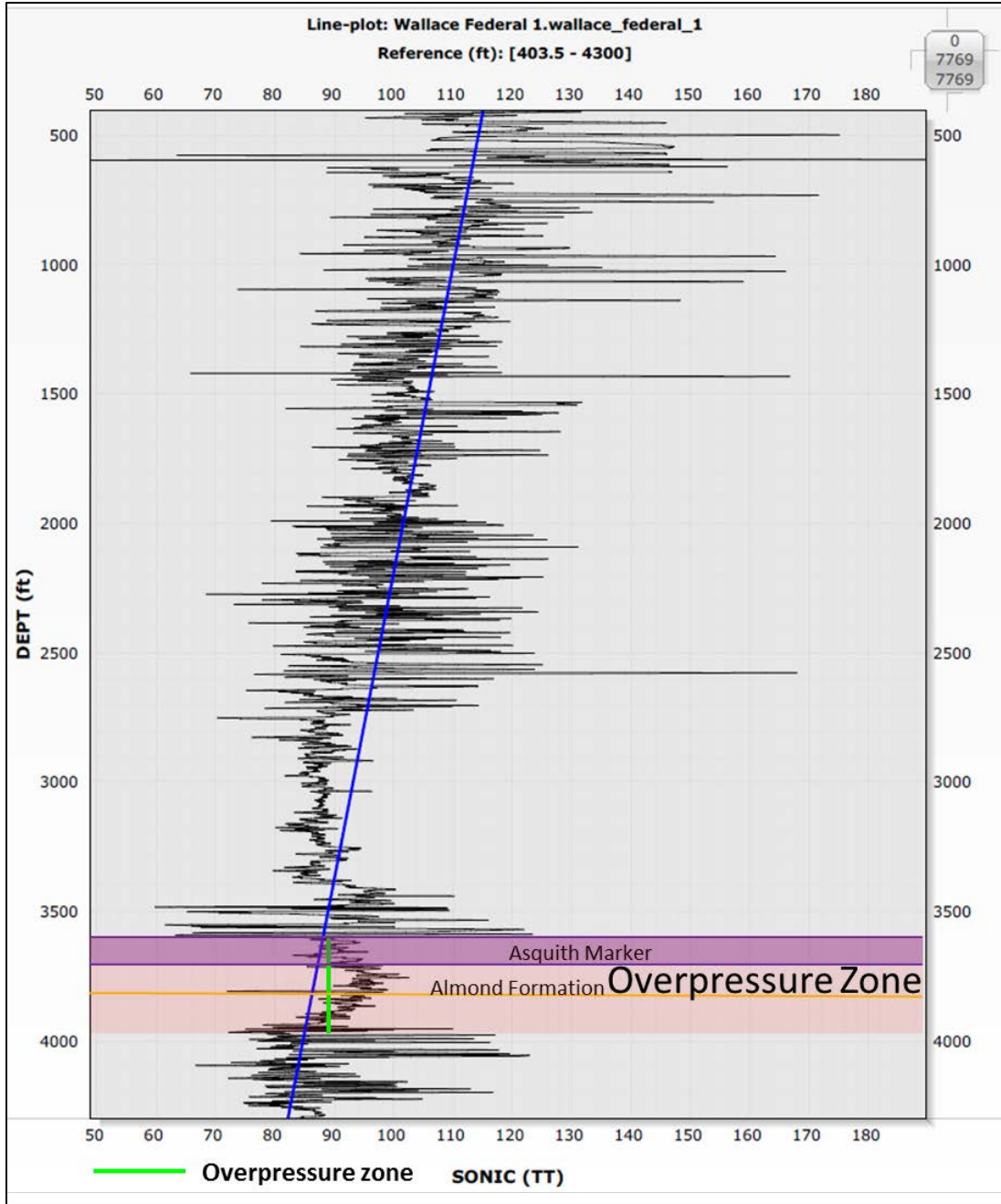
Barrel Springs Unit	41.35568	-107.90238
High Point 13-1	41.619361	-107.703768
Wamsutter 9-A	41.744574	-108.041843

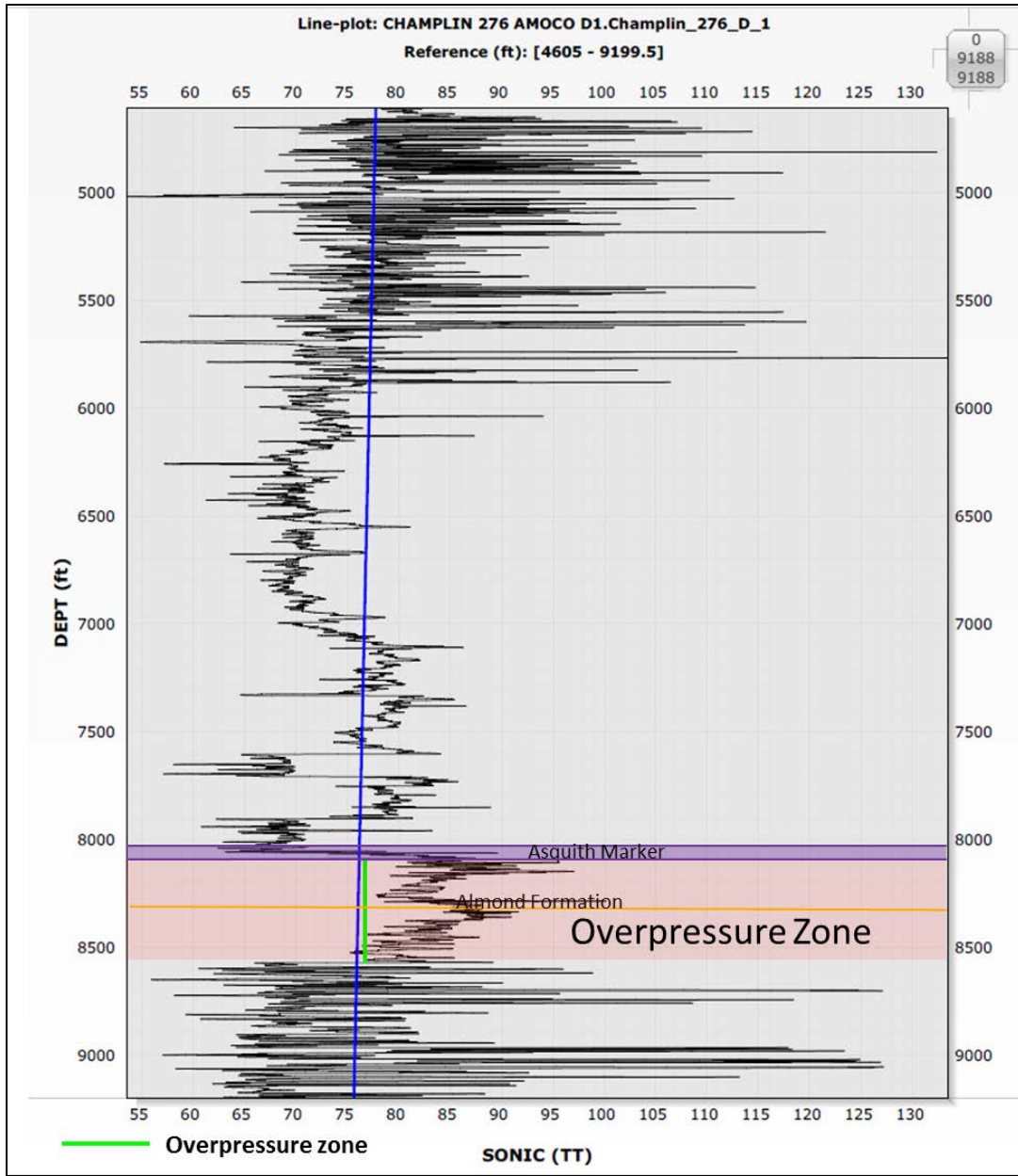
## Appendix 2: Overpressure Analysis



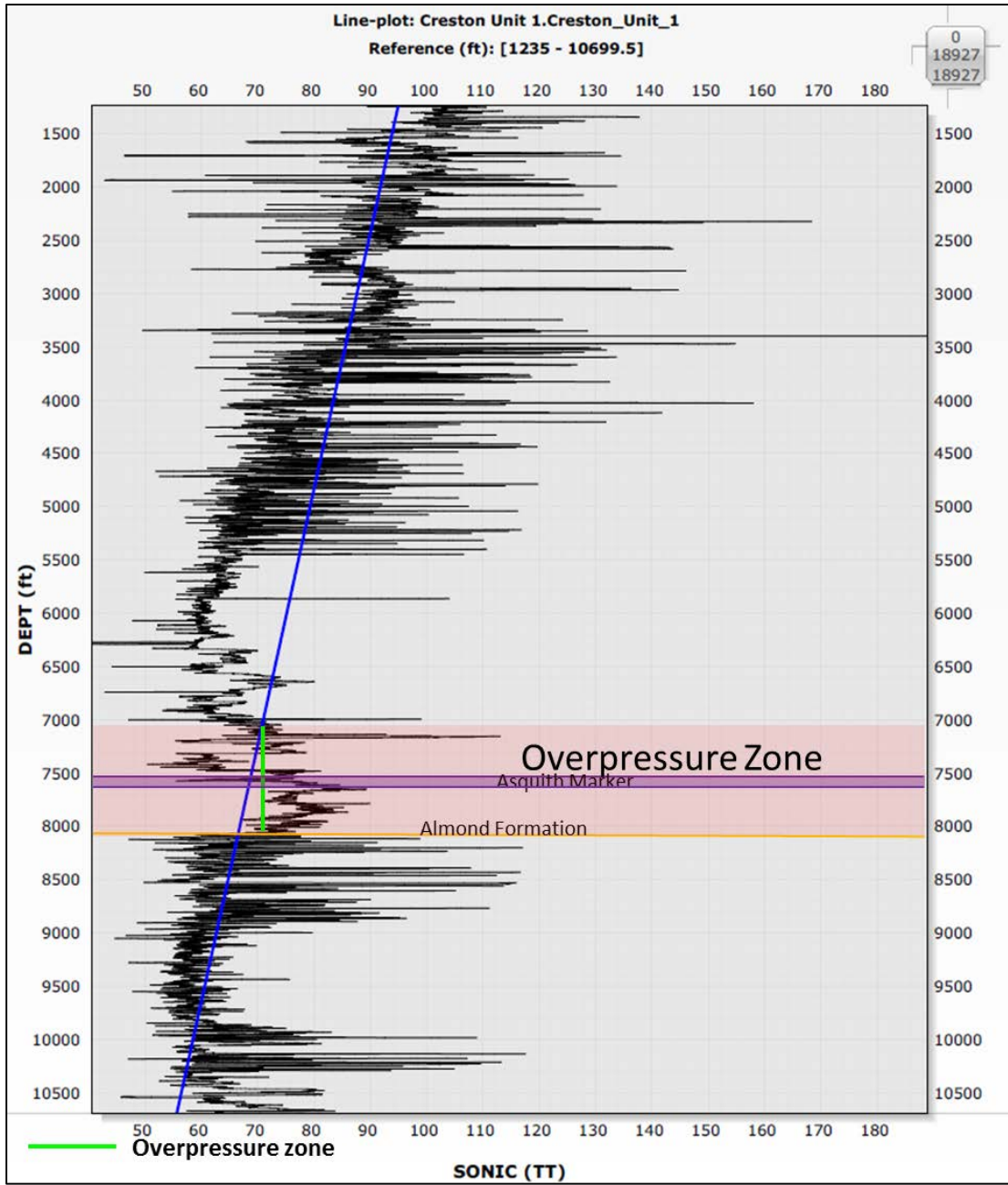


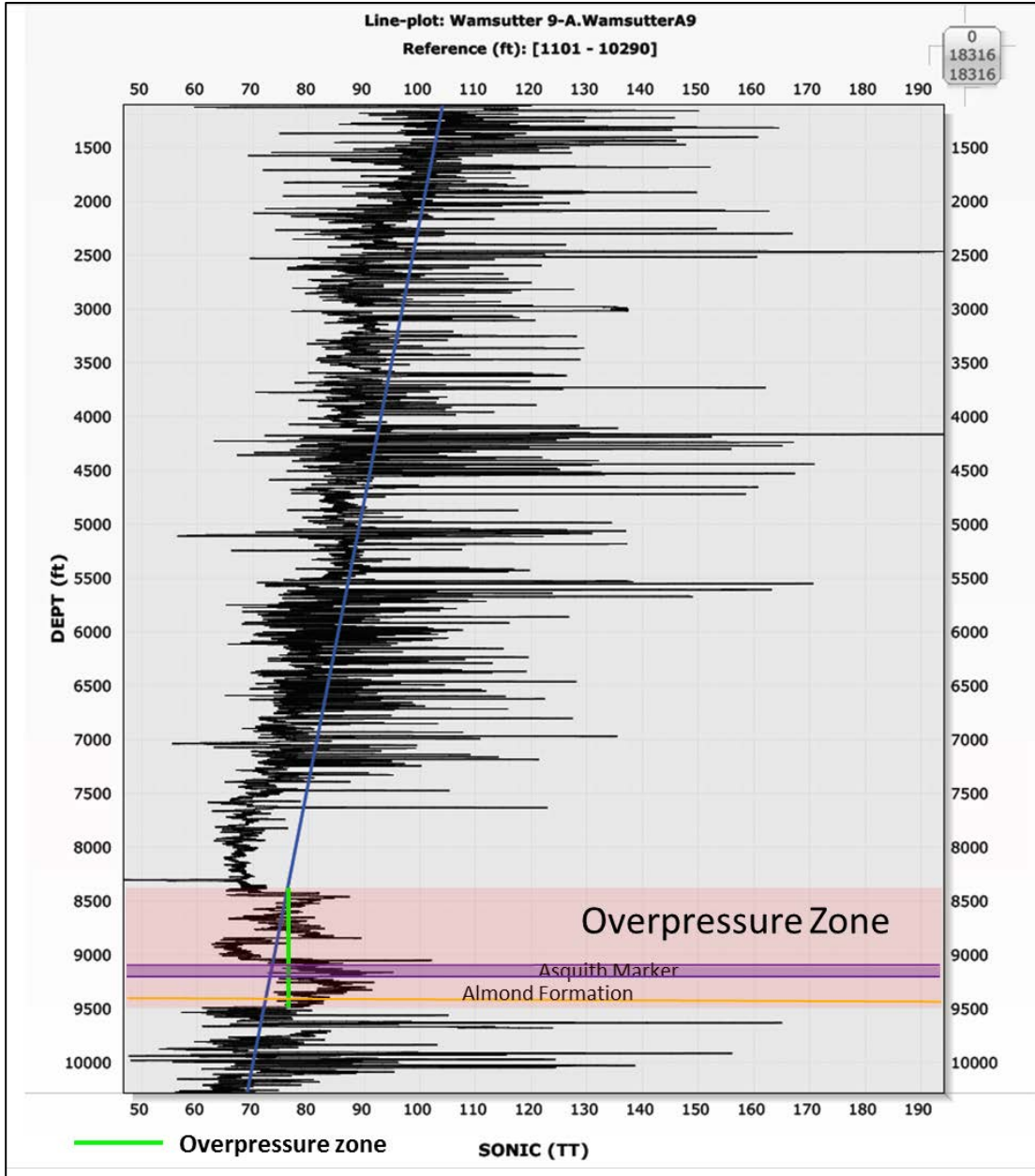




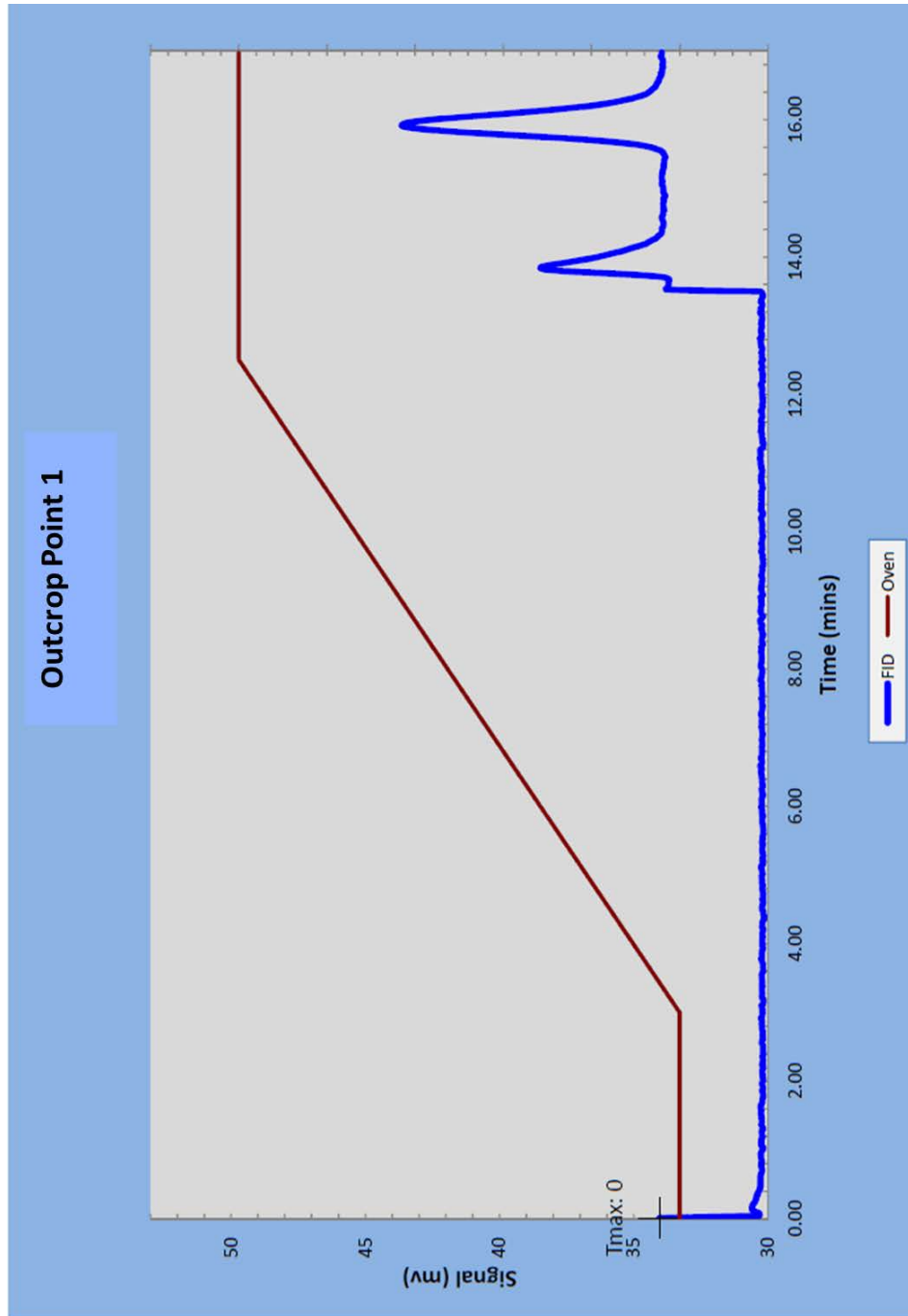








### Appendix 3: Pyrograms



### Outcrop Point 3



### Outcrop Point 4



### Outcrop Point 5



### Outcrop Point 6



### Outcrop Point 7





### Outcrop Point 8



8

INOVII 1 100001 0001

Horseshoe Creek 4937



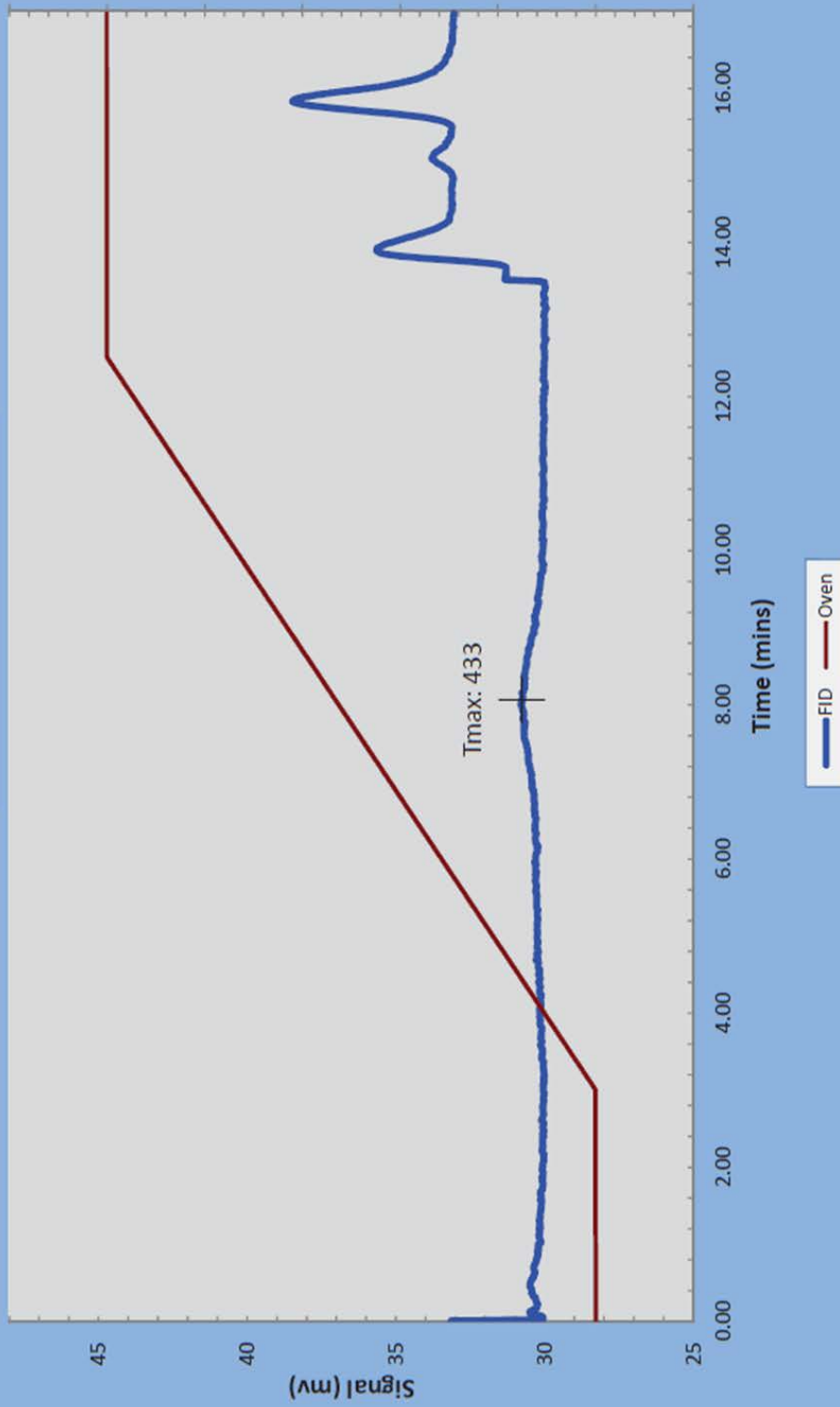
Stage Stop  
5380 - 5390 ft. (ROKU-150805-001)



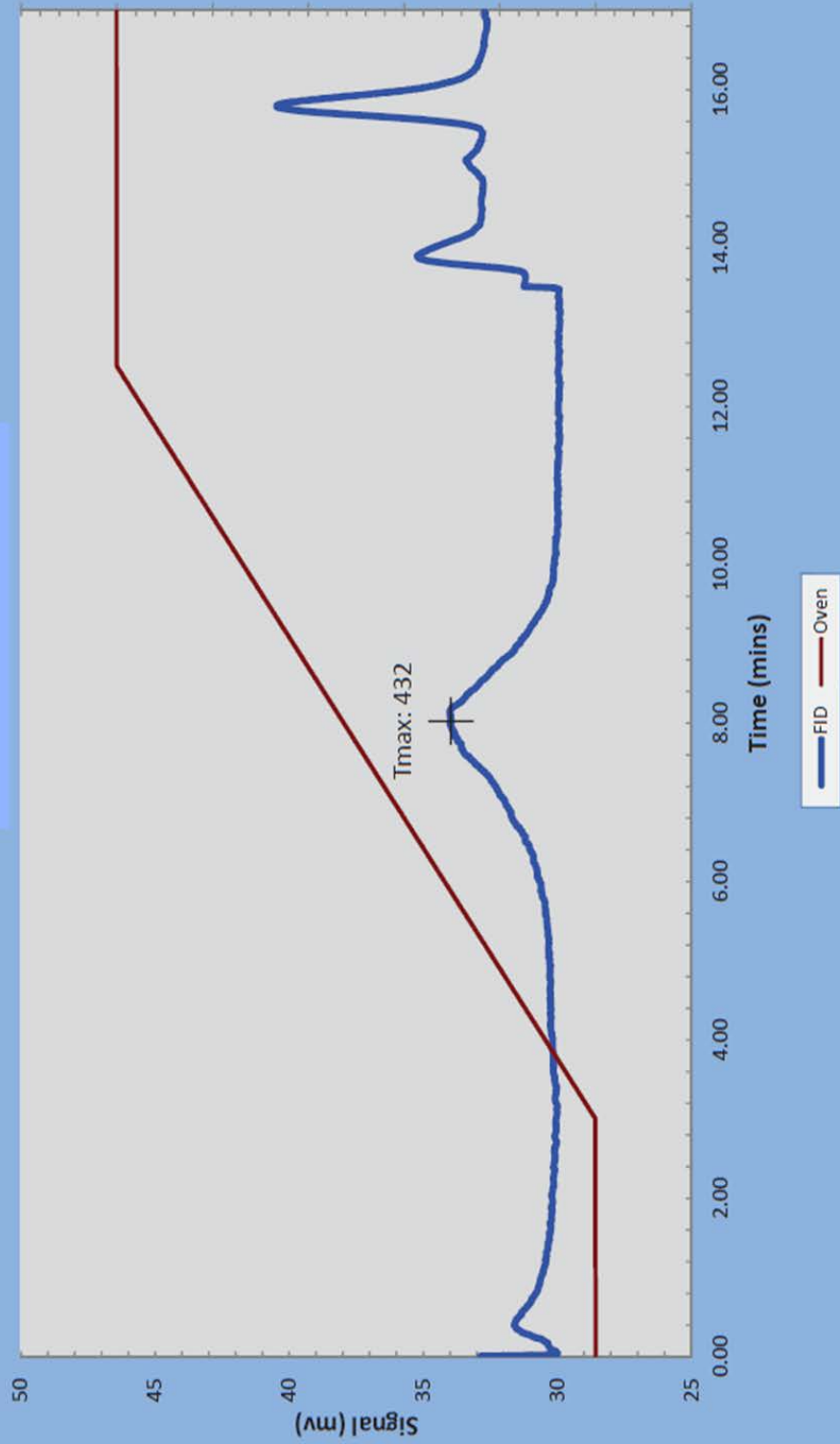
Stage Stop  
5400 - 5410 ft. (ROKU-150805-002)  
Low Temp S2 Shoulder



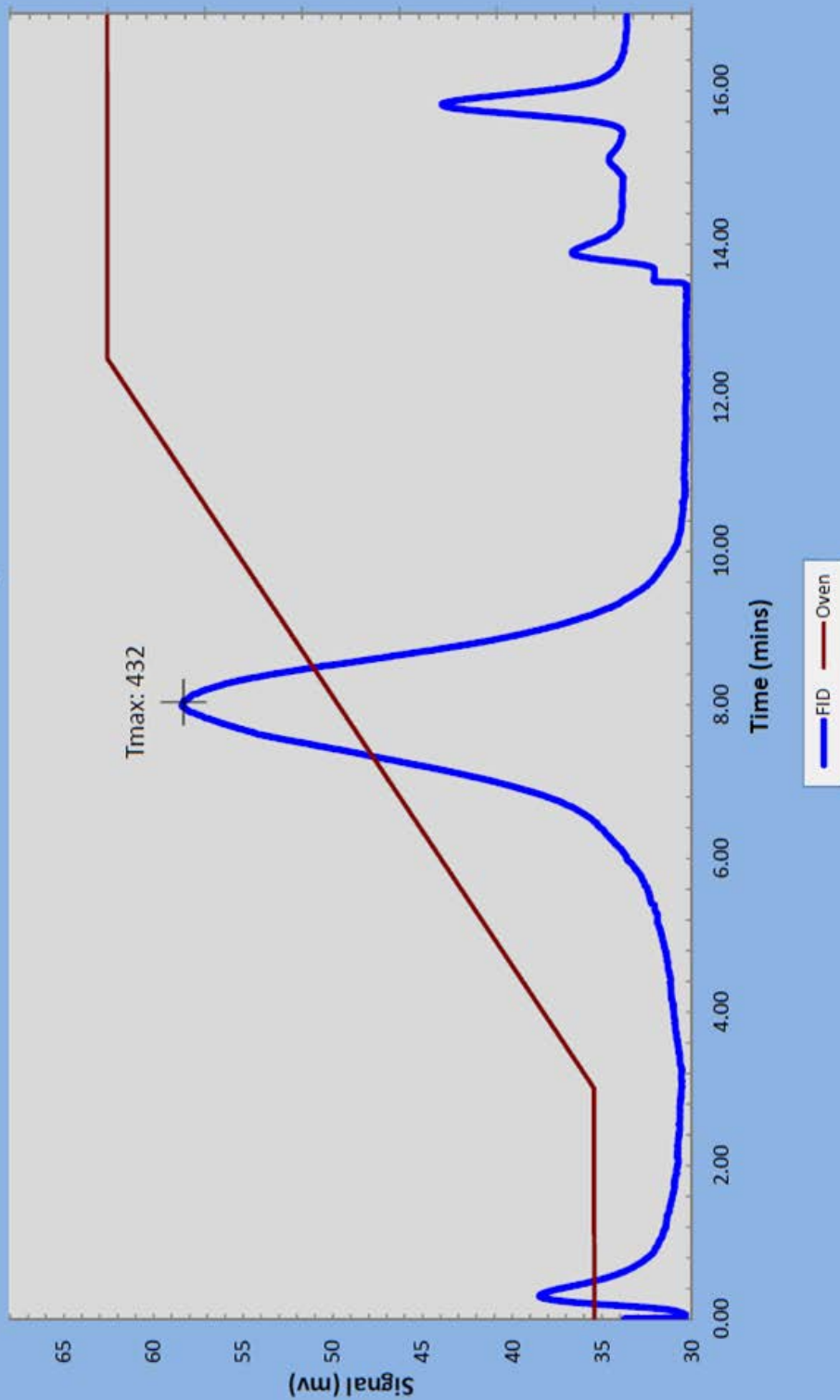
**Desert Springs Unit 19  
5946**



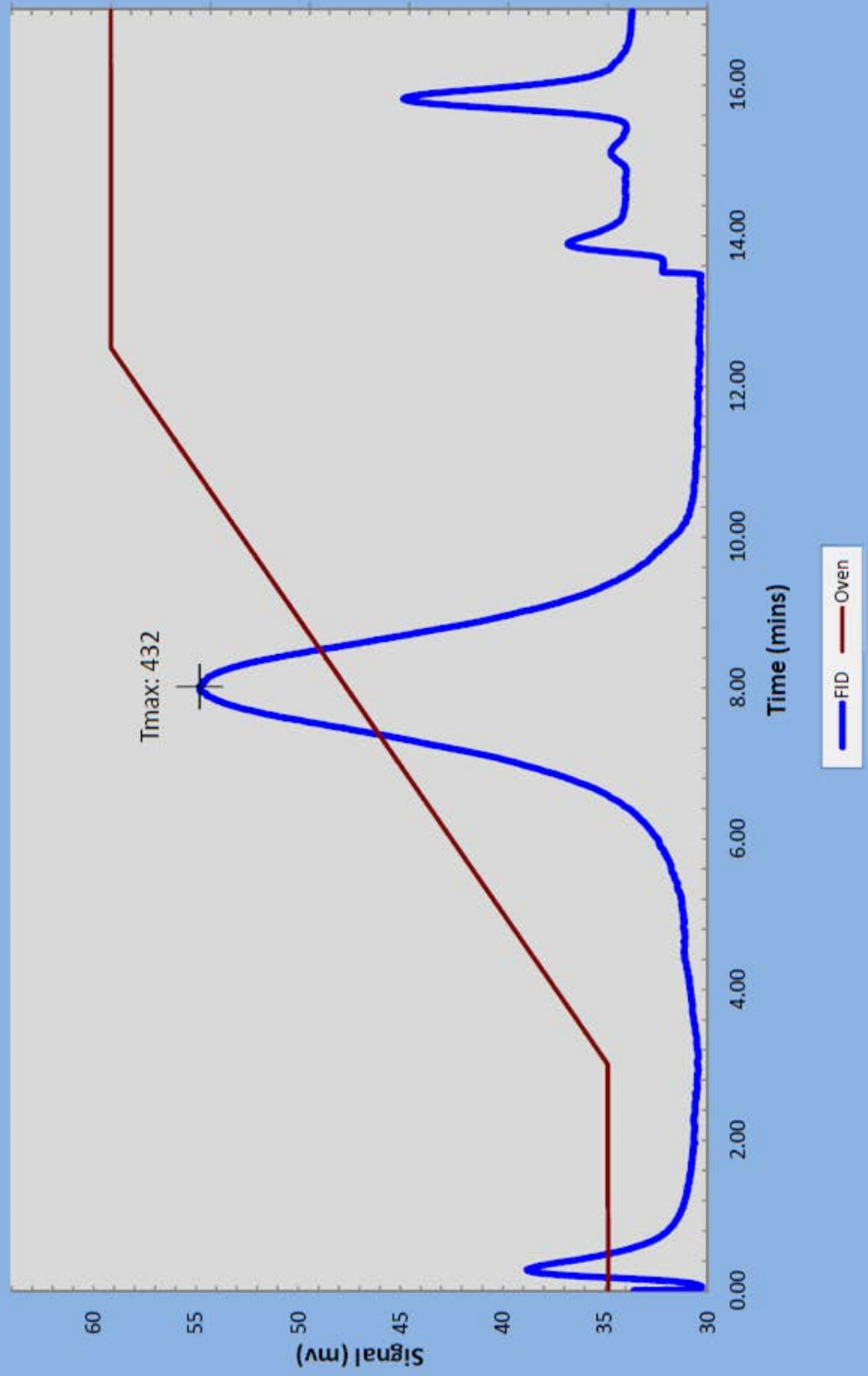
**Creston Unit 1  
7482**



276 D-1  
8138 ft. (ROKU-140402-001)  
Low Temp S2 Shoulder

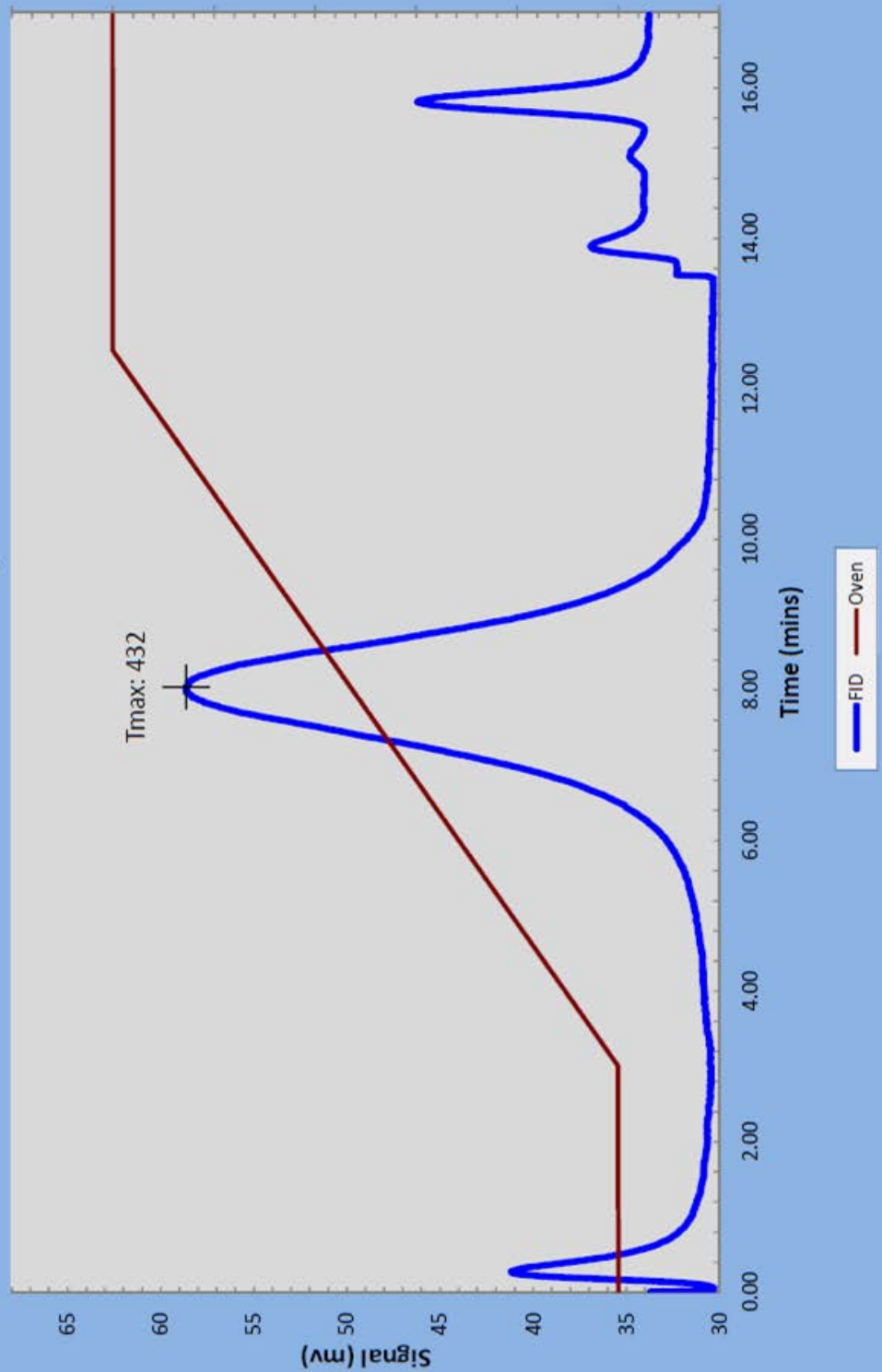


276 D-1  
8151 ft. (ROKU-140402-002)  
Low Temp S2 Shoulder

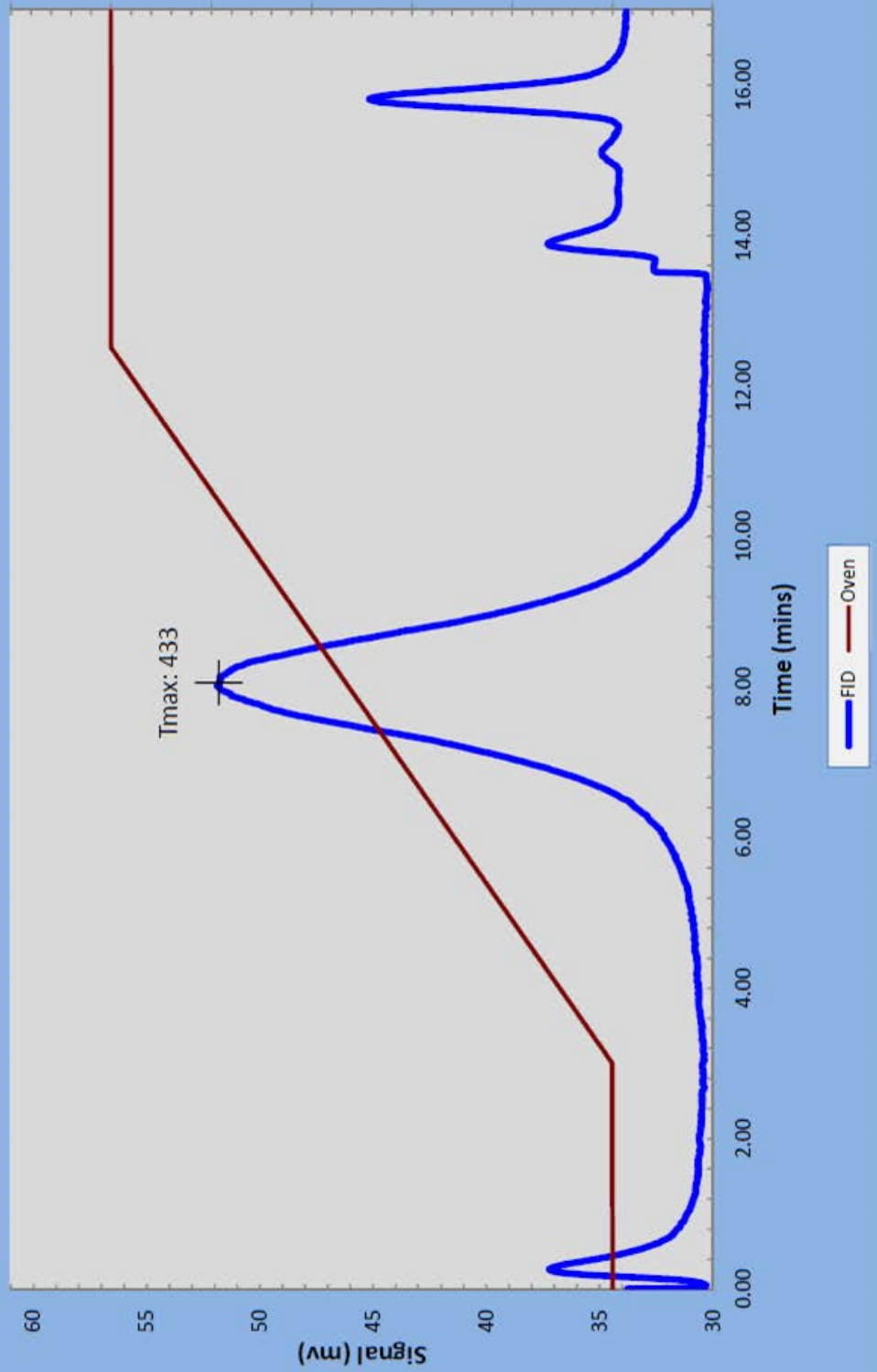




276 D-1  
8152 ft. (ROKU-140402-003)  
Low Temp S2 Shoulder



276 D-1  
8153 ft. (ROKU-140402-004)



276 D-1  
8154 ft. (ROKU-140402-005)



Champlin 276  
8970 - 9000 ft. (ROKU-150803-001)



Champlin 448  
10560 - 10570 ft. (ROKU-150804-001)



Chorney  
11370 - 11380 ft. (ROKU-150802-001)  
Low Temp S2 Shoulder



Chorney  
11390 - 11400 ft. (ROKU-150802-002)  
Low Temp S2 Shoulder



**2 monument Lake  
11430**





**2 monument Lake  
11447**



2 monument Lake  
11467



**Amoco Bog**  
**13320 - 13330 ft. (ROKU-150806-001)**



**Amoco Bog**  
**13320 - 13330 ft. (ROKU-150806-001)**



**Amoco Bog**  
13330 - 13340 ft. (ROKU-150806-002)



Champlin 446  
14195



**Champlin 446  
14205**



**Champlin 446  
14224**





## Appendix 4: XRD Analyses for other intervals.

### Horseshoe Creek Unit1 (4937 ft. depth)

Phase ID (7)	Chemical Formula	Wt% (esd)
Illite	$K(Al_4Si_2O_9(OH)_3)$	38.4 (2.2)
Quartz	$SiO_2$	30.0 (1.3)
Dolomite	$CaMg(CO_3)_2$	17.1 (1.5)
Microcline, ordered	$KAlSi_3O_8$	10.5 (3.1)
Kaolinite-1A	$Al_2Si_2O_5(OH)_4$	2.0 (0.5)
Pyrite	$FeS_2$	1.7 (0.2)
Albite, ordered	$NaAlSi_3O_8$	0.4 (0.1)

### Desert Springs Unit 19 (5946 ft. depth)

Phase ID (7)	Chemical Formula	Wt% (esd)
Quartz	$SiO_2$	37.8 (8.6)
Illite	$K(Al_4Si_2O_9(OH)_3)$	23.7 (5.7)
Dolomite	$CaMg(CO_3)_2$	19.3 (20.8)
Albite, ordered	$NaAlSi_3O_8$	9.2 (3.6)
Microcline, ordered	$KAlSi_3O_8$	7.6 (3.5)
Kaolinite-1A	$Al_2Si_2O_5(OH)_4$	1.5 (0.5)
Pyrite	$FeS_2$	0.9 (0.5)

### Creston Unit 1 (7482ft. depth)

Phase ID (7)	Chemical Formula	Wt% (esd)
Illite	$K(Al_4Si_2O_9(OH)_3)$	42.3 (2.8)
Quartz	$SiO_2$	31.9 (1.7)
Albite, ordered	$NaAlSi_3O_8$	8.2 (3.2)
Dolomite	$CaMg(CO_3)_2$	6.5 (2.5)
Microcline, ordered	$KAlSi_3O_8$	6.2 (1.7)
Kaolinite-1A	$Al_2Si_2O_5(OH)_4$	2.9 (1.7)
Pyrite	$FeS_2$	2.0 (0.2)

### Creston Unit 1 (7482ft. depth)

Phase ID (7)	Chemical Formula	Wt% (esd)
Illite	$K(Al_4Si_2O_9(OH)_3)$	40.4 (4.4)
Quartz	$SiO_2$	28.4 (2.8)
Microcline, ordered	$KAlSi_3O_8$	9.6 (2.9)
Dolomite	$CaMg(CO_3)_2$	7.6 (3.5)
Kaolinite-1A	$Al_2Si_2O_5(OH)_4$	6.6 (7.8)
Albite, ordered	$NaAlSi_3O_8$	5.2 (1.7)
Pyrite	$FeS_2$	2.1 (0.3)